UNIVERSITY OF CALIFORNIA,
IRVINE

Desymmetrization Strategies: Efforts Towards Salvileucalin B and Emetine

THESIS

submitted in partial satisfaction of the requirements
for the degree of

MASTER OF SCIENCES

in Organic Chemistry

by

Franco Alfonso Llamas

Thesis Committee:
Professor Christopher Vanderwal, Chair
Professor Vy Dong
Professor Scott Rychnovsky

2023

DEDICATION

To

my family and friends

in recognition of their worth

an apology

A feeling bears on itself the scars of its birth; it recollects as a subjective
emotion its struggle for existence;
it retains the impress of what might have been, but is not.

(Alfred North Whitehead
Process and Reality)

and hope

If the fool would persist in his folly he would become wise.

William Blake
Proverbs of Hell

TABLE OF CONTENTS

LIST OF FIGURES

LIST OF SCHEMES

LIST OF TABLES

ACKNOWLEDGEMENTS

I would like to express the deepest appreciation to my committee chair, Professor Christopher Vanderwal, for all the mentorship and support that he gave as both a PI and orals committee member. I am glad to have someone that supports and advocates for everyone in the group. I am grateful for the time that I had in the Vanderwal lab, and I look forward to whatever comes next.

I would like to thank my committee members, Professor Vy Dong and Scott Rychnovsky for their encouragement and guidance – especially with the job search. Their advice helped me look at the big picture and keep up the search even through tough times. Thank you as well to Professor Sergey Pronin for taking me in at first and giving me a start at UCI.

Thank you to Professor Tehshik Yoon and Dr. Wesley Swords for taking me under their wing at UW Madison and laying the groundwork for me in graduate school. Thank you to Dr. Shea Ramey from the Chemistry Learning Center for kindling and igniting my passion for organic chemistry. I am very lucky to have had an environment early on that allowed me to realize my passion. They were integral to my coming to UCI and am immensely grateful for it.

I also want to acknowledge the Pronin, Rychnovsky, Jarvo, Dong, and other labs and the very cool people in them. It was great to get to know and spend time with some awesome scientists and people and it helped a lot to keep me sane when things got rough. Thank you to Dr. Eric Touney, Dr. Nick Foy, and Dr. Will Thomas for the help and advice, as well as Brandon and Riley for being there when things got extra rough. The hang outs with Partho, Jake, Esteban, Ethan, Hannah, Brian, Andrew, Amy, Matt (5^{th} and 4^{th} floors!), Roman, Bryant, Ari, Brandon, and Dawid will be missed. Tacos, churros, and boba taste a lot better with good company and the memories will be held close.

I also send many thanks to the Vanderwal group. Big thanks to (soon to be) Dr. Joe Capani for mentoring me and laying the groundwork for me – especially with emetine, as well as Griffin and Lucas for showing me the ropes and giving me much encouragement and candid advice during my time here. It was a pleasure to be bay mates with Dr. Bonnie Pak, Jane, Julian, Jon, and Mira. Thank you for dealing with me blasting metal and my horrible puns. It was also great working alongside Jon and Bonnie Park in the mad scramble for the linker – that was a good character-building exercise. It was also a pleasure to be able to work alongside Dr. Scott Niman, Hanh, Phil, Brandon, Matt, Amber, and Sebastian. Thank you for your advice, help with reagents/reactions, and food recommendations. I would also like to thank Dr. Ryan Barrett, Dr. Nick Magann, and Dr. Ibo Çelik for help with the job search and general advice and wisdom. Shoutout to Josh for being a kind, enthusiastic, and energetic learner. It was a pleasure to mentor you (even if briefly) and I look forward to your development and wish you good luck in graduate school and beyond. I am very thankful for the privilege of working alongside such kind, patient, and thoughtful coworkers and very much look forward to whatever is in store for them.

Finally, I would like to send my many and deepest gratitude to my family and Emily for their undying support for me. I cannot express in words how thankful and happy I am to be supported by them and how they help bring out the best in me. Thank you for sticking with me and for comforting me when things got extra rough. Thank you for believing in me – especially during the times when I did not believe in myself. Thank you.

ABSTRACT OF THE THESIS

Desymmetrization Strategies: Efforts Towards Salvileucalin B and Emetine

by

Franco Alfonso Llamas

Master of Sciences in Organic Chemistry

University of California, Irvine, 2023

Professor Christopher Vanderwal, Chair

The thesis describes two desymmetrization approaches to two different natural products. The first chapter contains background on the salvileucalins and the Buchner reaction along with the work done towards the synthesis of salvileucalin B. This includes the synthesis of the diazo substrates for the Buchner reaction and the results of experimentation on a key Buchner reaction step in the sequence. The second chapter contains background on emetine and the work done towards its synthesis. This includes the synthesis of the dihydropyridine intermediate, the results of experimentation on the key step of acidic hydrolysis of the dihydropyridine to facilitate a double Pictet–Spengler reaction, exploration of an oxidative cleavage strategy, and the results on a model system to find conditions for a successful Pictet–Spengler reaction. Future directions of the project are also discussed, which include a Mukaiyama hydration strategy and modulation of the groups on the dihydropyridine nitrogen.

CHAPTER 1: Efforts Towards the Synthesis of Salvileucalin B via a Desymmetrization Approach

1.1 Introduction

Salvileucalins are part of a class of rearranged neoclerodane diterpenoids isolated by Izumi and co-workers from the *Salvia leucantha* plant (Figure 1.1). They all include a furan moiety along with interesting carbon frameworks – notably the fully substituted cyclopropane moiety in the norcaradiene core of salvileucalin B (**1.2**) and the cyclobutene moiety in salvileucalin C (**1.3**). The former is hypothesized to be directly biosynthetically related to salvileucalin A (**1.1**), while the latter is hypothesized to be directly biosynthetically related to salvileucalin D (**1.4**). Izumi and co-workers propose that salvileucalin A is converted to salvileucalin B via oxidation and an enzymatic intramolecular Diels-Alder reaction and posit that salvileucalin D is converted to salvileucalin C via a bicyclization to form the fused cyclobutene-cyclopentane system. [1,2]

Figure 1.1: Salvileucalins A-D

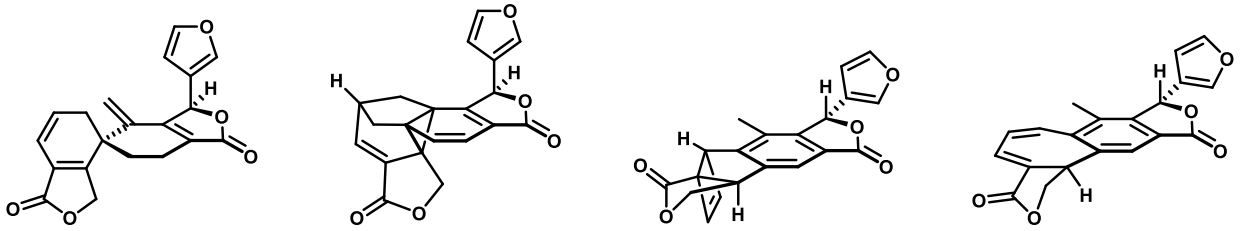

Salvileucalin A (1.1) Salvileucalin B (1.2) Salvileucalin C (1.3) Salvileucalin D (1.4)

While, to our knowledge, the bioactivity for salvileucalins A, C, and D have not been demonstrated, salvileucalin B exhibits cytotoxic activity against A549 and HT-29 cells with IC_{50} values of 5.23 μg/mL and 1.88 μg/mL, respectively.[1] This anti-cancer activity at low concentrations is of interest, especially since the mode of action is unknown. This bioactivity and desire to elucidate the mode of action provided a strong motivation to access ample quantities of salvileucalin B and analogues to enable pharmacophore studies.

1.2 Buchner reaction

Scheme 1.1: Buchner reaction from seminal publication

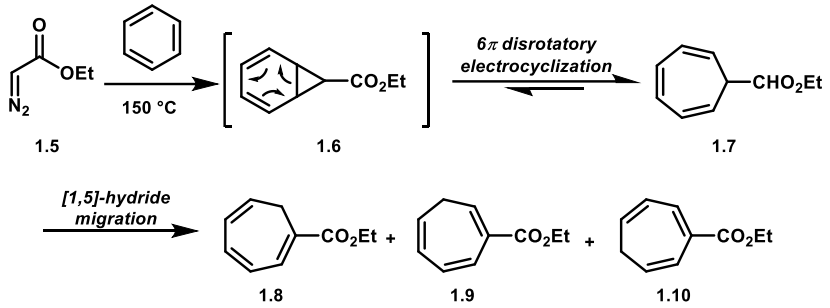

First reported by Buchner and Curtius in 1896, Buchner reactions have been utilized to synthesize norcaradienes (NCD) and cycloheptatrienes (CHT). In the seminal publication (Scheme 1.1),[3] the reaction between ethyl diazoacetate (**1.5**) and benzene produced a mixture of cycloheptatrienes (**1.8-1.10**) after the formed NCD (**1.6**) underwent reversible 6π disrotatory electrocyclic ring opening and [1,5]-hydride shifts from kinetic product CHT **1.7**.[4] Both non-catalyzed and metal-mediated variants of this reaction exist, but metal catalysts have been utilized mostly due to milder conditions. This generally leads to improved yields and suppresses formation of isomeric CHT products.[5] This reaction is unique in that it may provide access to highly substituted cyclopropane cores via dearomatization of an arene ring.[6]

1.2.1 Buchner reactions utilized in total synthesis

One example of the use of transition-metal mediated Buchner reactions is shown in Mander and co-workers' synthesis of gibberellin GA_{103} (Scheme 1.2).[7] Diazo decomposition of compound **1.11** and Buchner cycloaddition was performed with $Cu(acac)_2$, followed by in-*situ* addition of maleic anhydride **1.13** to furnish compound **1.14** via a Diels-Alder reaction. Intermediate **1.14** was then elaborated to GA_{103} (**1.15**) in four additional steps. The system was designed to have the diazo

fragment poised geometrically to attack the arene ring, and geometrical constraints were expected to suppress formation of the CHT product and benzylic C–H insertion.

Scheme 1.2: Mander and co-workers' synthesis of gibberellin GA_{103}

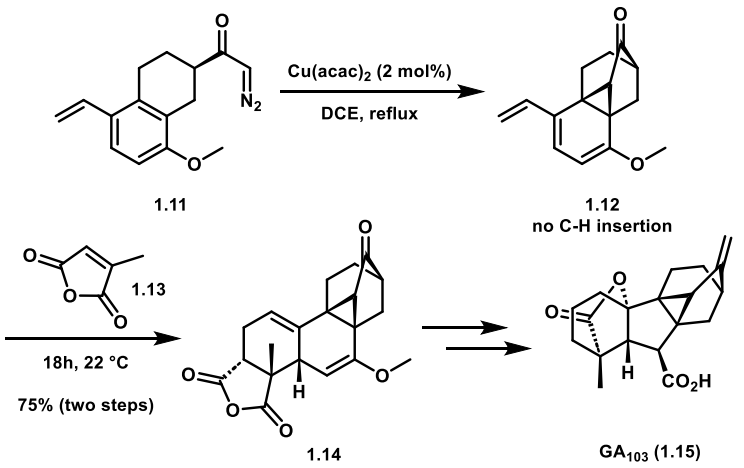

Scheme 1.3: Reisman and co-workers' synthesis of (+)–salvileucalin B

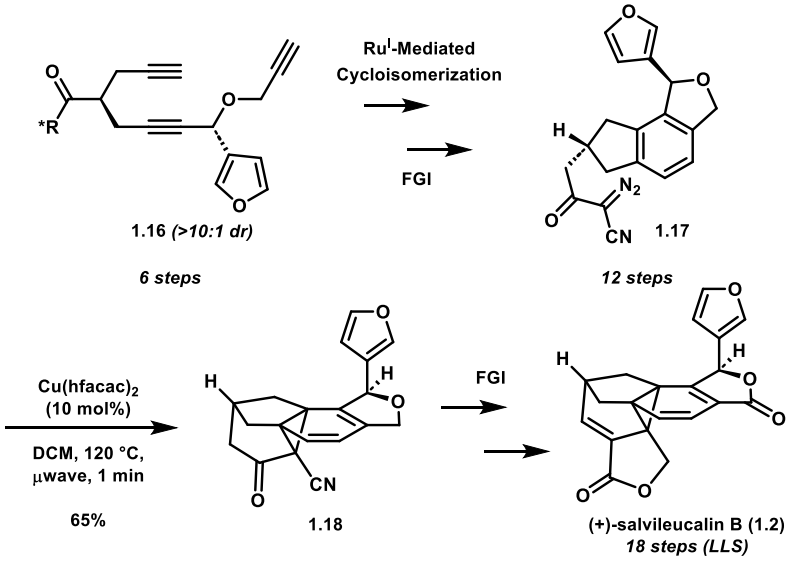

Another example is from Reisman and coworkers' synthesis of (+)–salvileucalin B (Scheme 1.3).[8] Metal-mediated cycloisomerization of enantiomerically enriched triyne **1.16** followed by functional group interconversions led to α-diazo-β-ketonitrile **1.17**. Diazo

decomposition of **1.17** led to the formation of the fully substituted cyclopropane in **1.18**. After a series of functional group interconversions and regioselective benzylic oxidation, (+)–salvileucalin B was obtained in an 18-step sequence (*LLS*). A previous study from Reisman and co-workers on metal-mediated Buchner reactions using α-diazo-β-ketonitriles showed that copper-mediated arene cyclopropanation was uniquely effective in giving the desired norcaradiene with minimal C–H insertion product.[6]

1.2.2 Norcaradiene and cycloheptatriene tautomer equilibrium

Scheme 1.4: Equilibrium between norcaradiene and cycloheptatriene tautomers

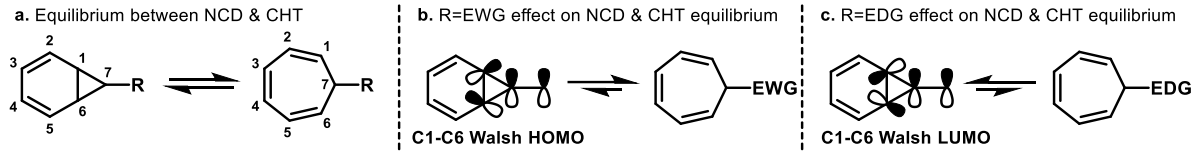

The conversion between the NCD and CHT tautomers can be affected by the sterics and electronics of the substituents on the cyclopropane in the NCD (Scheme 1.4a).[9] For example, large, bulky substituents on C1 and C6 may shift the equilibrium towards the NCD due to the steric destabilization of the CHT. The presence of electron-withdrawing or electron-donating groups on C7 may also affect the equilibrium due to the orbital interactions with Walsh cyclopropane molecular orbitals. The orbital overlap of the HOMO of π-electron withdrawing groups and the HOMO of the Walsh orbitals allow for the shortening of the C1-C6 bond, which can be equated to a higher bond strength, and thus may shift the equilibrium towards the NCD tautomer (Scheme 1.4b). With π-electron donating substituents, the orbital overlap of the LUMO of the substituent and the HOMO of the Walsh orbitals leads to increased antibonding character and destabilizes the NCD tautomer. This may shift the equilibrium towards the CHT tautomer (Scheme 1.4c). In the synthesis of salvileucalin B, Reisman and co-workers only observed the NCD tautomer after the key Buchner reaction step. This could be due to the presence of the tricyclo[3.2.1.0]octane

substructure, which would greatly destabilize the CHT tautomer if 6π electrocyclic ring-opening occurred.

1.3 Summary

The Buchner reaction is a well-established method to synthesize highly substituted cyclopropanes. We felt that a simplified version of the Reisman system may give salvileucalin B in a shorter sequence to synthesize the natural product and analogues. We hypothesized that the furan ring is a vestige of the biogenesis of **1.2** and that perhaps another functional group (or the absence of the furan) may influence the bioactivity. A concise route could facilitate pharmacophore studies to study its mode of action and probe the origins of its bioactivity.

1.4 Efforts towards synthesis of salvileucalin B

1.4.1 Introduction

Scheme 1.5: Retrosynthesis of salvileucalin B

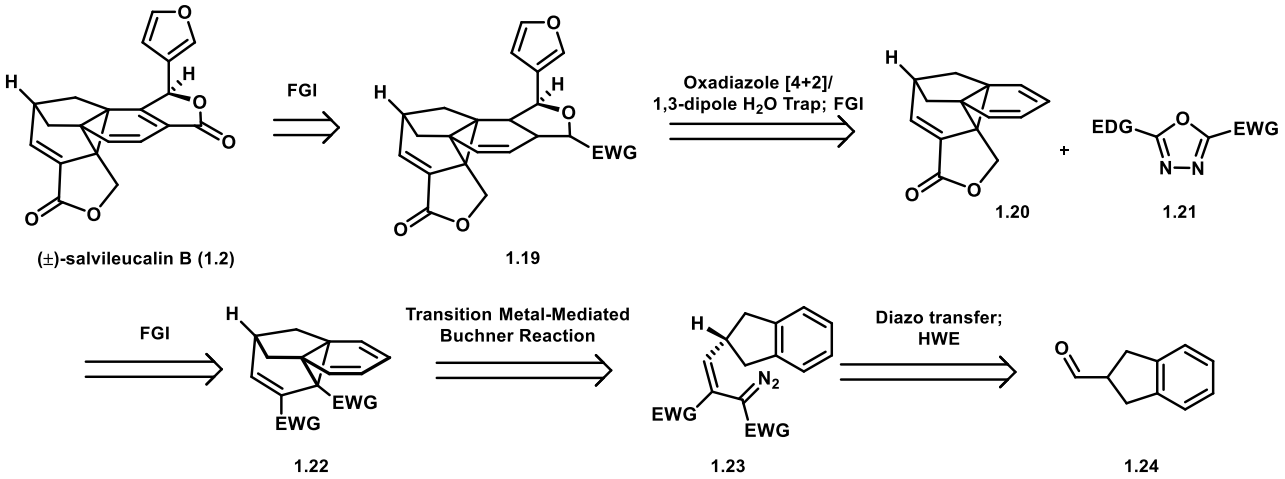

We hoped to access a symmetric norcaradiene core **1.20** after performing functional group interconversions on the Buchner reaction norcaradiene product **1.22**.[8,10] We planned to desymmetrize norcaradiene **1.20** with a [4+2] cycloaddition of 1,3,4-oxadiazole **1.21**,[11] and trap the resulting 1,3-dipole with an equivalent of water. Functional group interconversions and

oxidation manipulations would then lead to salvileucalin B. In retrospect, there was lack of precedent for the trapping of the 1,3-dipole with water after [4+2] cycloaddition. However, another selective de-symmetrization of the diene could be a possibility. Extensive experimentation may have been required for a successful transformation. Nonetheless, we thought that the Buchner reaction precursor, diazo **1.23**, could be accessed rapidly from aldehyde **1.24** (one step from commercial material) and could be modified with different electron-withdrawing groups to explore the reactivity of the Buchner reaction step. While we acknowledged that benzylic C-H insertion was a very plausible side-reaction, we thought that the chemoselectivity could be modulated through changing the catalyst and substituents near the diazo moiety.[10]

1.4.2 Synthesis of Buchner reaction substrate

Scheme 1.6: Synthesis of diazo transfer precursors

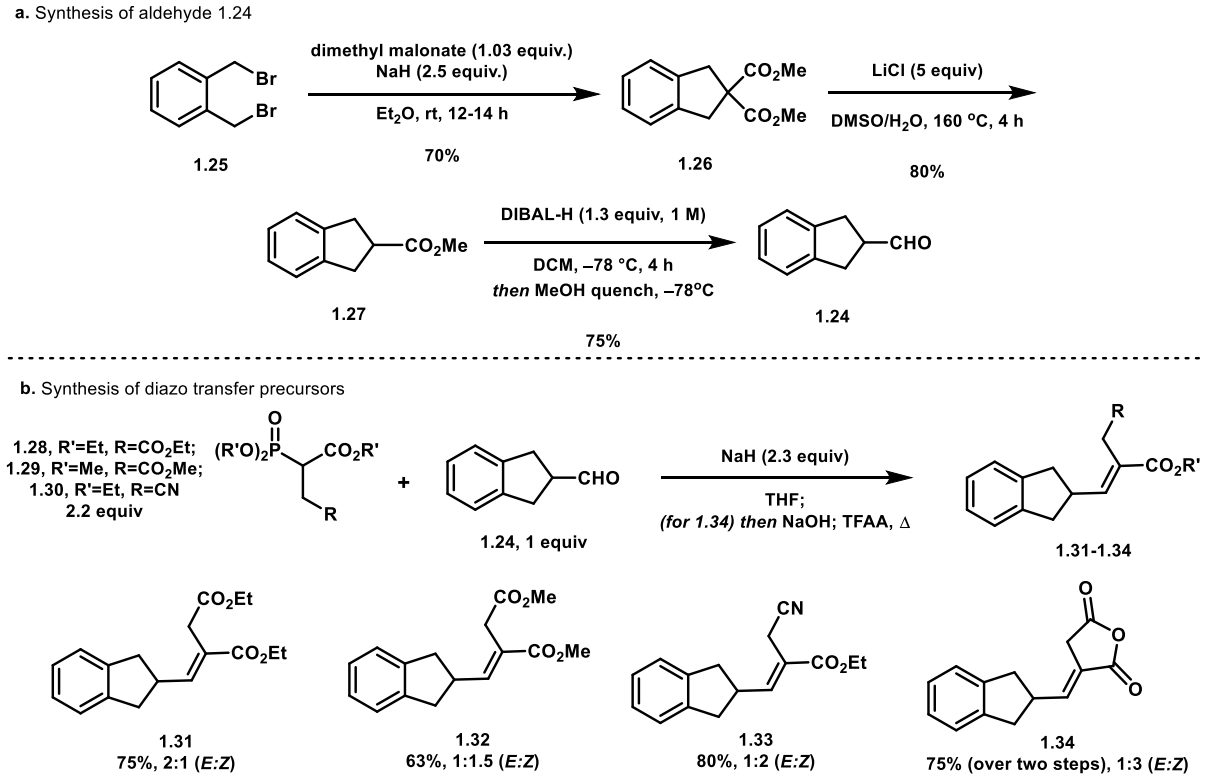

Our synthetic efforts started with alkylation of *o*-bromoxylene **1.25** with dimethyl malonate (Scheme 1.6a).[12] While aldehyde **1.24** could be accessed via reduction of the corresponding commercially available carboxylic acid,[13] we wanted to start the synthesis without the need to wait for the chemical to arrive. The alkylation proceeded smoothly and the corresponding diester **1.26** was subjected to Krapcho decarboxylation.[14] This ester was readily reduced to aldehyde **1.24** with DIBAL–H and a cold quench with methanol;[15] a HWE reaction to furnished the diester **1.31** (Scheme 1.6b).[16] Using this general protocol, we then synthesized other precursors **1.32-1.34** for the diazo-transfer reaction with different phosphonates **1.29-1.30** synthesized through an alkylation reaction.[16]

Scheme 1.7: Synthesis of cyano phosphonate

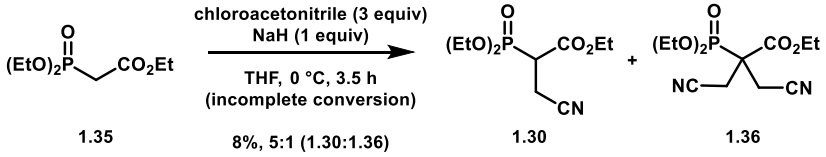

While diazo-transfer precursors **1.31, 1.32, and 1.34** were synthesized through readily synthesizable phosphonates **1.28-1.29**, initial attempts to purify phosphonate **1.30** were challenging due to the formation of significant amounts of the dialkylated phosphonate **1.36** (Scheme 1.7), which had similar polarity to **1.30**. We hypothesized that due to the lowered electrophilicity of chloroacetonitrile, it was consumed at a rate slow enough that it allowed significant amounts of deprotonation of the desired phosphonate **1.30** by the conjugate base of the starting material and therefore promoted the formation of dialkylated phosphonate **1.36**. We then experimented with the order of addition of reagents, equivalents of electrophile, and temperature to suppress formation of **1.36**, but the attempts were unsuccessful. An attempt to use bromoacetonitrile led to a similar outcome as using chloroacetonitrile. Attempts to distill **1.30** off

from **1.36** were also unsuccessful and led largely to decomposition. We later observed that quenching the reaction at partial conversion led to minimal formation of **1.36**. After scaling up the reaction and purification by silica gel chromatography, ample amounts of **1.30** were obtained to perform the HWE reaction and synthesize substrate **1.33**.

Table 1.1: Trials to effect diazo transfer on **1.31**

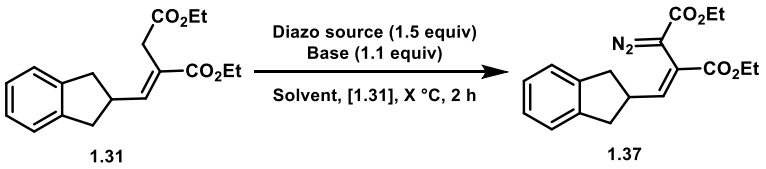

1.31 1.37

Entry	Diazo Source	Base	Solvent	[1.31] (molar)	Temp (°C)	Result
1	*p*-ABSA	DBU	MeCN	0.1	0 → rt → 40	SM
2	*p*-ABSA	DBU	MeCN	1	0 → rt → 40	SM
3	*p*-ABSA	LDA	THF	0.1	–78 → rt	SM
4	Ts-N_3	DBU	MeCN	1	0 → rt → 40	Trace
5	Ts-N_3	LDA	THF	1	–78 → rt	40%

We decided to then focus on effecting the diazo-transfer reaction on one substrate in hope that it would be generalizable to the others. Substrate **1.31** was then subjected to diazo-transfer reaction conditions (Table 1.1). Initial attempts to effect the transformation with *p*-ABSA and DBU led to recovered starting material. Experiments with a higher concentration of **1.31** also led to similar results. Utilizing LDA with *p*-ABSA also led to recovered starting material. Experiments with tosyl azide and DBU[8] led to trace product formation. However, the combination of LDA and tosyl azide led to ample formation of the desired diazo compound **1.37**. While the pKa of the α-protons of the ester is lowered only slightly by the unsaturation on the adjacent carbons due to stabilization of the anion via resonance, we hypothesize that this effect is not strong enough to allow for a comparatively weaker base like DBU to produce the enolate. Furthermore, we also hypothesize that tosyl azide could be a more competent electrophile due to the lower electron-

donating effect of the methyl group compared to the electron-donating effect of the acetamide group in *p*-ABSA. The acetamide group comparatively increases electron density in the conjugated aromatic and sulfonyl azide system, making the azide less electrophilic due to the increased partial negative charge on the sulfonyl group.

Scheme 1.8: Synthesis of diazo compounds for Buchner reaction

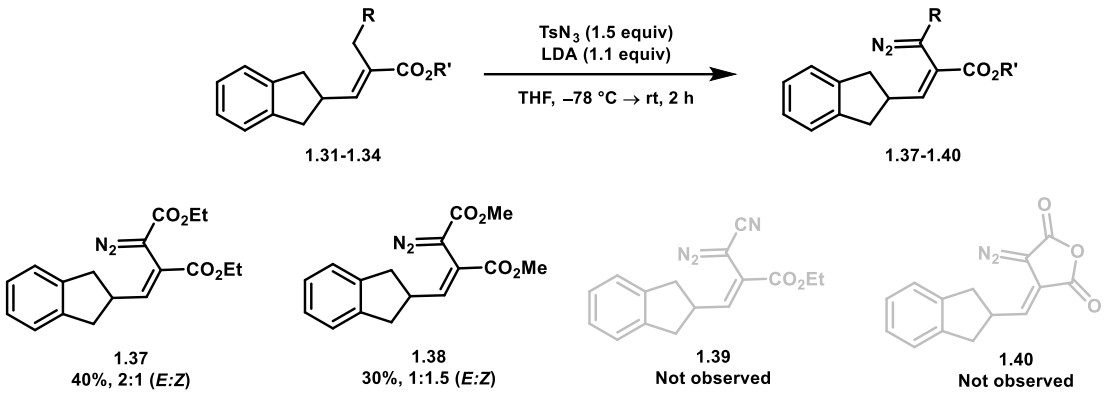

While these conditions worked with the methyl ester substrate **1.32**, they were not applicable to the cyano substrate **1.33** or the succinic anhydride substrate **1.34** (Scheme 1.8). Deuterium quenching experiments showed that both substrates **1.33** and **1.34** decomposed in strongly basic conditions rather than undergoing deuterium incorporation. While other conditions with weaker bases were tried at room temperature, elevated temperatures, and higher molarity, those experiments led to either recovered starting material or decomposition of starting material. At this point, we thought that it would be prudent to move on and explore the reactivity in the key Buchner reaction step.

1.4.3 Buchner reaction trials

Buchner substrate **1.37** was then subjected to a screen of electron deficient Cu^{II} and dirhodium^{II} complexes in an effort to form and isolate **1.41** (Table 1.2).[8,10] Unfortunately, benzylic C–H insertion product **1.42** was the major product with OH activation product **1.43** as a side

product; desired product **1.41** or its corresponding cycloheptatriene was never observed. A similar reactivity pattern was observed with the methyl ester substrate **1.38** as well (Table 1.3, structures tentative). While these experiments did not produce the desired product in observable amounts, they did show that the diazo compound likely formed a carbenoid when exposed to catalytic amounts of the metal complexes used.

Table 1.2: Buchner reaction trials for substrate **1.37**

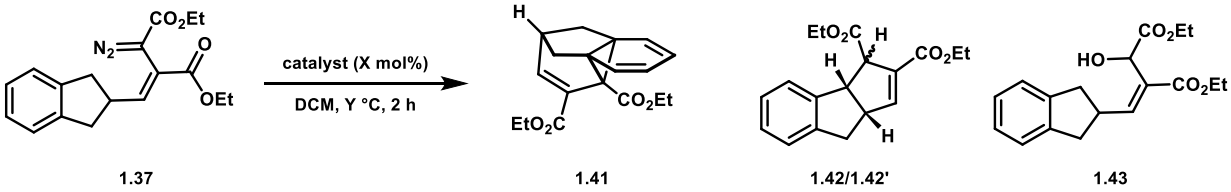

1.37 1.41 1.42/1.42' 1.43

Entry	Catalyst	Temp (°C)	Yield	Product ratio (1.41:1.42:1.42':1.43)
1[a]	$Cu(hfacac)_2$ (10 mol%)	120 (μwave)	N/A	Complex mixture
2[a]	$Cu(hfacac)_2$ (10 mol%)	rt	N/A	Complex mixture
3	$Rh_2(OAc)_4$ (2 mol%)	rt	N/A	0:1:1.2:1.2
4	$Rh_2(tfa)_4$ (2 mol%)	rt	N/A	0:5:1:3
5	$Rh_2(esp)_2$ (2 mol%)	rt	50% (5a)	N/A

[a]5 m instead of 2 h

Table 1.3: Buchner reaction trials for substrate **1.38**

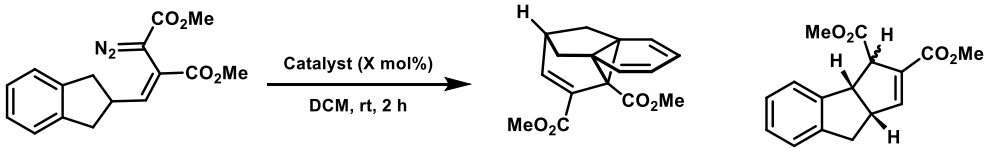

1.38 1.44 1.45/1.45'

Entry:	Catalyst:	Product ratio (1.44:1.45:1.45'):
1[a]	$Cu(hfacac)_2$ (10 mol%)	Complex mixture
2[a]	$Rh_2(OAc)_4$ (2 mol%)	0:1:1.2
3[a]	$Rh_2(tfa)_4$ (2 mol%)	0:5:1
4[a]	$Rh_2(esp)_2$ (2 mol%)	0:14:1

[a]Product ratios determined by crude NMR, structure tentative

1.5 Conclusion

The diazo compounds **1.37** and **1.38** were synthesized and we tested the key Buchner reaction step with these substrates. Unfortunately, benzylic C–H insertion was the dominant reaction course and no desired norcaradiene or its corresponding cycloheptatriene was observed. We hypothesize that this is because the HOMO–LUMO gap of the benzylic Csp^3–H σ-bond and the carbenoid π* antibonding orbital being smaller than the HOMO–LUMO gap of the C–C π-bond and the carbenoid π* antibonding orbital. With this hypothesis in mind, we looked towards changing the aromatic ring to be more electron rich to make the C–C π-bond in the aromatic ring more nucleophilic, thereby raising the energy of the indicated bond to reduce the HOMO–LUMO gap to promote the desired Buchner reaction. However, the strategy strayed close to Reisman and co-workers' previous enantioselective synthesis due to the similar substitution on the arene ring in the Buchner reaction and the type of transformations employed.[8] Because of this, we decided to shift focus to another natural product.

1.6 Experimental Procedures

Unless otherwise noted, all reactions were performed under an atmosphere of argon using flame-dried or oven-dried glassware and Teflon® coated stir bars. Anhydrous solvents were prepared by passage through columns of activated alumina. All amine bases were distilled from calcium hydride prior to use. Anhydrous solvents were prepared by passage through a column of activated alumina and a column packed with Q5 reactant, a supported copper catalyst for scavenging oxygen, under a positive pressure of argon. All other reagents were used as received or prepared according to literature procedures, unless otherwise noted. Unless otherwise specified, reaction progress was monitored by thin-layer chromatography (TLC) performed on Merck silica gel 60 F254 glass-backed TLC plates visualized with UV (254 nm) and potassium permanganate ($KMnO_4$)/heat or p-anisaldehyde/heat as developing agents. Column chromatography was performed using EMD Millipore 60 Å (0.040–0.063 mm) mesh silica gel (SiO_2), and eluent systems are reported as %v/v. All microwave reactions were performed using a Monowave 300 (Software Version 3.00) from Anton Paar, Graz, Sweden.

^{1}H NMR spectra were recorded at 298 K on Bruker GN500 (499 MHz), Bruker CRYO500 (500 MHz), and Bruker AVANCE600 (600 MHz) spectrometers. ^{13}C NMR spectra were recorded at 298 K on Bruker CRYO500 (125 MHz) and Bruker AVANCE600 (151 MHz) spectrometers. Chemical shifts are reported in ppm, referenced from $CHCl_3$ residual peak at 7.26 ppm (^{1}H NMR) and $^{13}CDCl_3$ at 77.16 ppm (^{13}C NMR). Coupling constants (J) are reported in Hz. Peak multiplicities are reported as ap (apparent), s (singlet), d (doublet), t (triplet), q (quartet), m (multiplet), br (broad). High resolution mass spectra (HRMS) were recorded on a Waters LCT Premier spectrometer using ESI-TOF. Low resolution mass spectra (LRMS) were recorded on a Waters LCT Premier spectrometer using ESI-TOF.

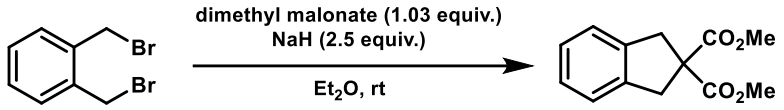

1.25 1.26

Dimethyl 1,3-dihydro-2*H*-indene-2,2-dicarboxylate 1.25. To a 500 mL three-necked flask equipped with a dropping funnel was added NaH (3.68 g, 92 mmol, 60% dispersion in mineral oil) and 80 mL of dry THF. The mixture was cooled to 0 °C, and diethyl malonate (4.75 mL, 41.3 mmol) was added portion-wise. Vigorous bubbling was observed. After complete addition of the malonate, the bubbling ceased after about 10 s. The ice bath was taken off and the mixture was stirred for 15 min. The dropping funnel was charged with **1.25** and 120 mL of dry THF. The solution of **1.25** was then added over 15 min. The reaction mixture started bubbling slowly. After complete addition of the **1.25** solution, the reaction mixture turned into a tan suspension. The reaction mixture was stirred at rt for 2 h. The reaction was then quenched by portion-wise addition of 1 M aqueous NaOH (100 mL). The mixture was diluted with Et_2O (100 mL), the layers were separated, and the aqueous layer was extracted with Et_2O (2 x 100 mL). The combined organic extracts were washed with brine, dried over $MgSO_4$, filtered, and concentrated under vacuum. The crude residue was purified by flash column chromatography (10% EtOAc in hexanes) to afford **1.26** as a fluffy, white powder (6.53 g, 70%). Spectral data of **1.26** matched those previously reported.[17]

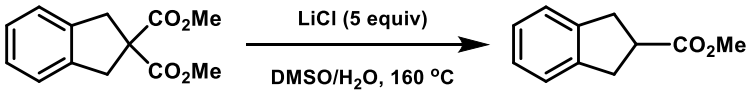

1.26 1.27

Methyl 2,3-dihydro-1*H*-indene-2-carboxylate 1.27. To a 100 mL round-bottomed flask open to air was added diester **1.26** (5.60 g, 23.9 mmol), LiCl (5.26 g, 124 mmol), and wet DMSO (80 mL). The flask was then placed in a pre-heated oil bath at 160 °C. The reaction mixture turned into a

clear, yellow solution at first, then turned into a gray suspension as the reaction progressed. The reaction mixture was stirred for 1 h at 160 °C, then cooled to rt. The brown solution was diluted with DI H_2O (500 mL), and the mixture was extracted with ethyl acetate (4 x 150 mL). The combined organic extracts were then washed with brine twice, dried with Na_2SO_4, filtered, and concentrated under vacuum. The crude residue was purified by flash column chromatography (5% EtOAc in hexanes) to afford **1.27** (3.37 g, 80%). Spectral data of **1.27** matched those previously reported.[18]

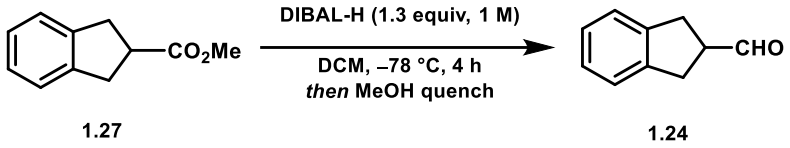

1.27 1.24

2,3-dihydro-1*H*-indene-2-carbaldehyde 1.24. To a 250 mL round-bottomed flask was added ester **1.27** (2.86 g, 16.2 mmol) and dry DCM (80 mL). The flask was then placed in a dry ice/acetone bath and the solution was cooled to –78 °C over 20 min. A solution of 1 M DIBAL-H in dry DCM (21.4 mL, 21.4 mmol) was added over 30 min dropwise via cannula, with a 2 mL cannula wash with dry DCM. The reaction mixture was stirred for 2 h at –78 °C. The reaction was then quenched at –78 °C with MeOH (2.6 mL, 65 mmol), and the mixture was stirred at –78 °C for 10 min. The mixture was warmed to 0 °C, and saturated aqueous $NaHCO_3$ solution (25 mL) was added. The solution was warmed to rt and stirred vigorously for 30 min, after which the mixture became an emulsion. The solution was diluted with DCM (20 mL) and saturated aqueous $NaHCO_3$ solution (20 mL) and stirred vigorously for 1 h, which led to a biphasic mixture. The layers were separated, and the aqueous layer was extracted with DCM (2 x 80 mL). The combined organic extracts were washed with brine, dried with Na_2SO_4, filtered, and concentrated under vacuum. The crude residue was purified by flash column chromatography (4% EtOAc in hexanes) to afford **1.24** (1.768 g, 75%). Spectral data of **1.24** matched those previously reported.[19]

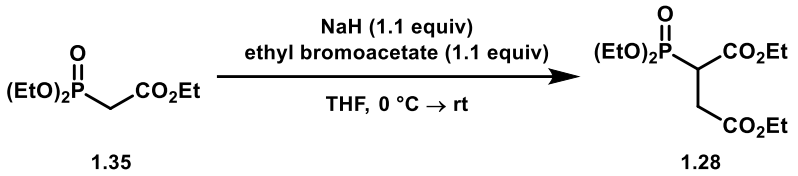

Diethyl 2-(diethoxyphosphoryl)succinate 1.28. To a 100 mL round-bottomed flask was added phosphonate **1.35** (2.18 mL, 11.0 mmol), dry THF (22 mL). The reaction mixture was then cooled to 0 °C, and NaH (440 mg, 11.0 mmol, 60% dispersion in mineral oil) was added portion-wise. The mixture was stirred for 10 min, after which ethyl bromoacetate was added dropwise. The formation of a white precipitate was observed upon addition of the bromoacetate. The reaction mixture was slowly warmed to rt and stirred for 2 h. The reaction was quenched by the addition of saturated aqueous NH_4Cl at rt. DI H_2O was added until the aqueous layer became clear. The layers were separated, and the aqueous layer was extracted with EtOAc (2 x 50 mL). The combined organic extracts were washed with brine, dried over Na_2SO_4, filtered, and concentrated under vacuum. The crude residue was purified by flash column chromatography (80% EtOAc in hexanes) to afford **1.28** (2.48 g, 90% purity (w/w%), 80% yield) with an impurity tentatively assigned as the dialkylated product (9:1, **1.28**:dialkylated product). Spectral data of **1.28** matched those previously reported.[20]

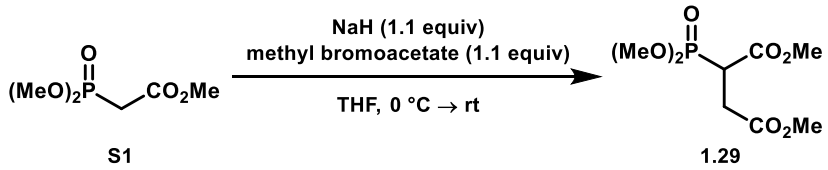

Dimethyl 2-(dimethoxyphosphoryl)succinate 1.29. The procedure for **1.28** was followed, with the following deviations: **S1** (1.62 mL, 10.0 mmol) as the starting phosphonate, methyl bromoacetate (1.0 mL, 11 mmol) as the bromoacetate, stirred mixture of **S1** and NaH for 30 min instead of 10 min, and stirred reaction mixture with all reagents added for 16 h. The crude residue was purified by flash column chromatography (80% EtOAc in hexanes) to afford **1.29** (2.05 g,

90% purity (w/w%), 73%) with the impurity being tentatively assigned as dialkylated product (9:1, **1.29**:dialkylated product). Spectral data of **1.29** matched those previously reported.[21]

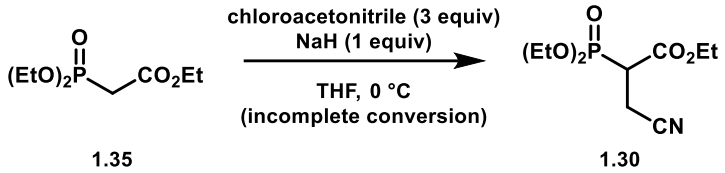

1.35 1.30

Ethyl 3-cyano-2-(diethoxyphosphoryl)propanoate 1.30. To a 250 mL round-bottomed flask was added NaH (1.21 g, 30.2 mmol, 60% dispersion in mineral oil) and dry THF (95 mL), and the mixture was cooled to 0 °C. **1.35** (6.78 g, 6.00 mL, 30.2 mmol) was then slowly added dropwise, and the mixture was stirred at 0 °C. The mixture turned into a clear, yellow solution. In a separate 250 mL round-bottomed flask equipped with an addition funnel was added chloroacetonitrile (5.80 mL, 91.4 mmol) and dry THF (40 mL), and the solution was cooled to 0 °C. The deprotonated phosphonate solution was then added via cannula to the addition funnel above the chloroacetonitrile solution. The deprotonated phosphonate solution was then added dropwise to the chloroacetonitrile solution over 45 min at 0 °C. The reaction mixture was stirred at 0 °C for 2.5 h, at which time the formation of the dialkylated side product was observed to form. The reaction was quenched with saturated aqueous NH_4Cl solution and DI H_2O was added until the bottom layer was clear. The layers were separated, and the aqueous layer was extracted with EtOAc (2 x 40 mL). The combined organic extracts were washed with brine, dried over Na_2SO_4, filtered, and concentrated under vacuum. The crude residue was purified by flash column chromatography (10% acetone in DCM to 15% acetone in DCM gradient) to afford **1.30** (792 mg, 80% purity (w/w%), 8%) with the impurity tentatively assigned as the dialkylated product (4:1 **1.30**:dialkylated product). Spectral data of **1.30** matched those previously reported.[22]

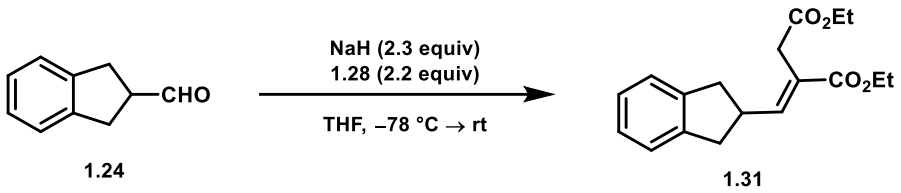

1.24 1.31

Diethyl 2-((2,3-dihydro-1*H*-inden-2-yl)methylene)succinate 1.31. To a 25 mL round-bottomed flask was added phosphonate **1.28** (250 mg, 90% purity, 0.80 mmol) and dry THF (3.2 mL) and the mixture was cooled to 0 °C. NaH (20 mg, 0.83 mmol, 60% dispersion in mineral oil) was added portion-wise to the phosphonate solution and the mixture was stirred for at 0 °C for 20 min, then cooled to –78 °C with an acetone/dry ice bath. In a separate 10 mL round-bottomed flask, a solution of aldehyde **1.24** (53 mg, 0.36 mmol) in dry THF (0.72 mL) was prepared and was added to the deprotonated phosphonate solution via cannula (followed with a 0.3 mL dry THF cannula wash). The reaction mixture was stirred for 3 h. The acetone/dry ice bath was removed, and the reaction was quenched with saturated aqueous NH_4Cl solution. DI H_2O was added until the bottom layer was clear. The layers were separated, and the aqueous layer was extracted with EtOAc (2 x 10 mL). The combined organic extracts were washed with brine, dried over Na_2SO_4, filtered, and concentrated under vacuum. The crude residue was purified by flash column chromatography (10% EtOAc in hexanes) to afford **1.32** (83 mg, 76%) as a mixture of diastereomers (2:1 *E*:*Z* ratio). The diastereomers were separated via flash column chromatography (10% EtOAc in hexanes) for characterization. The isomers were identified by the ^{1}H NOESY correlation between the 6.13 ppm signal and the 3.26 ppm signal in the *Z* isomer. **E isomer:** ^{1}H NMR (500 MHz, $CDCl_3$) δ 7.23 – 7.19 (m, 2 H), 7.18 – 7.14 (m, 2H), 7.06, (d, *J* = 10.1 Hz, 1H), 4.20 (q, *J* = 7.3 Hz, 2H), 4.16 (q, *J* = 7.3 Hz, 2H), 3.41 (s, 2 H), 3.36 (ddd, *J* = 8.1, 8.3, 9.4 Hz, 1H), 3.14 (dd, *J* = 8.0, 15.8 Hz, 2H), 2.86 (dd, *J* = 8.0, 15.6 Hz, 2H), 1.32 – 1.24 (m, 6H); ^{13}C NMR (151 MHz, CDCl3) δ 170.95, 167.08, 148.69, 142.30, 126.58, 125.38, 124.46, 60.95, 39.63, 39.24, 32.64, 14.26, 14.24. HRMS

(ESI) *m / z* calcd for $C_{18}H_{22}O_4Na$ $[M+Na]^+$ 325.1416, found 325.1330. **Z isomer:** ^1H NMR (500 MHz, $CDCl_3$) δ 7.22-7.18 (m, 2H), 7.17-7.12 (m, 2H), 6.13 (d, *J* = 9.6 Hz, 1H), 4.25-4.19 (q, *J* = 7.1 Hz, 2H), 4.17-4.10 (m, 3H), 3.29-3.19 (m, 4H), 2.80-2.74 (dd, *J* = 7.5, 15.8 Hz, 2H), 1.31-1.27, (t, *J* = 7.3 Hz, 3H), 1.27-1.23 (t, *J* = 7.0 Hz, 3H); ^{13}C NMR (125 MHz, $CDCl_3$) δ 171.42, 167.06, 150.43, 142.68, 126.40, 125.39, 124.97, 124.49, 60.77, 60.56, 40.33, 39.87, 39.62, 39.41, 14.23, 14.21. HRMS (ESI) *m / z* calcd for $C_{18}H_{22}O_4Na$ $[M+Na]^+$ 325.1416, found 325.1405.

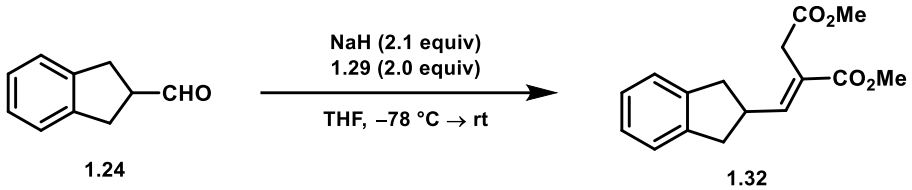

1.24 1.32

Dimethyl 2-((2,3-dihydro-1*H*-inden-2-yl)methylene)succinate 1.32. The procedure for **1.28** was followed, with the following deviations: phosphonate **1.29** (1.55 g, 90% purity, 5.51 mmol) was used as a starting material, NaH (139 mg, 5.79 mmol, 60% dispersion in mineral oil), aldehyde **1.24** (400 mg, 2.74 mmol) was used, and the reaction mixture was stirred for 3.5 h before quenching. The workup was scaled up by 7.5x to account for the increased scale. The crude residue was purified by flash column chromatography (10% EtOAc in hexanes) to afford **1.32** (473 mg, 63%) as a mixture of diastereomers (1.5:1 *E*:*Z* ratio). The diastereomers were separated via flash column chromatography (10% EtOAc in hexanes) for characterization. **E isomer (3:1 ratio with Z isomer):** ^1H NMR (500 MHz, $CDCl_3$) δ 7.24 – 7.19 (m, 2H), 7.19 – 7.14 (m, 2H), 7.08 (d, *J* = 10.1 Hz, 1H), 3.76 (s, 3H), 3.71 (s, 3H), 3.44 (s, 2H), 3.41 – 3.31 (m, 1H), 3.15 (dd, *J* = 7.8, 15.6 Hz), 2.86 (dd, *J* = 7.8, 15.6 Hz); ^{13}C NMR (125 MHz, $CDCl_3$) δ 171.84, 171.33, 167.46, 167.06, 150.90, 149.22, 142.63, 142.20, 126.62, 126.44, 124.91, 124.50, 124.48, 52.14, 52.08, 52.00, 51.70, 39.99, 39.81, 39.65, 39.53, 39.20, 32.32. **Z isomer:** ^1H NMR (500 MHz, $CDCl_3$) δ 7.24 – 7.19 (m, 2H), 7.19 – 7.13 (m, 2H), 6.16 (d, *J* = 9.8 Hz, 1H), 4.20 – 4.18 (m, 1H), 3.77 (s, 3H), 3.70 (s, 3H), 3.29 (s, 2H), 3.24 (dd, *J* = 8.1, 15.2 Hz, 2H), 2.78 (dd, *J* = 8.1, 15.2 Hz, 2H); ^{13}C NMR (125 MHz,

$CDCl_3$) δ 171.84, 167.06, 150.91, 142.63, 126.45, 124.52, 124.50, 51.99, 51.70, 39.99, 39.82, 39.54.

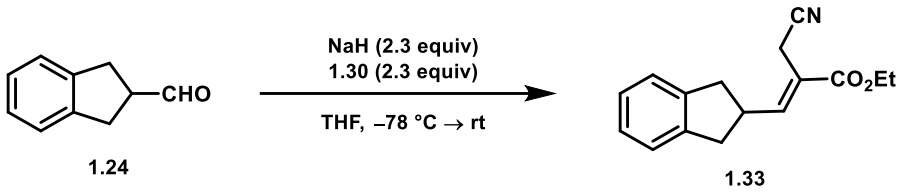

1.24 1.33

Ethyl 2-(cyanomethyl)-3-(2,3-dihydro-1*H*-inden-2-yl)acrylate 1.33. The procedure for **1.28** was followed, with the following deviations: phosphonate **1.30** (990 mg, 80% purity, 2.69 mmol) was used as a starting material, NaH (66 mg, 2.80 mmol, 60% dispersion in mineral oil), aldehyde **1.24** (192 mg, 1.18 mmol) was used, and the reaction mixture was stirred for 13.5 h before quenching. The workup was scaled up by 3x to account for the increased scale. The crude residue was purified by flash column chromatography (10% EtOAc in hexanes) to afford **1.33** (243 mg, 80.5%) as a mixture of diastereomers (1:2 *E*:*Z* ratio). The diastereomers were separated via flash column chromatography (10% EtOAc in hexanes) for characterization. **E isomer:** ^{1}H NMR (500 MHz, $CDCl_3$) δ 7.25 – 7.21 (m, 2H), 7.21 – 7.16 (m, 2H), 7.14 (d, *J* = 10.5 Hz, 1H) 4.27 (q, *J* = 7.1 Hz, 2H), 3.5 – 3.39 (m, 3H), 3.25 (dd, *J* = 7.9, 15.6 Hz, 2H), 2.89 (dd, *J* = 7.4, 15.6 Hz, 2H), 1.33 (t, *J* = 7.1 Hz, 3H); ^{13}C NMR (126 MHz, $CDCl_3$) δ 165.46, 150.90, 141.77, 126.83, 124.57, 121.90, 117.46, 61.68, 39.67, 39.65, 38.96, 15.33, 14.29. HRMS (ESI) *m / z* calcd for $C_{16}H_{17}NO_2Na$ $[M+Na]^+$ 278.1157, found 278.1157. **Z isomer:** ^{1}H NMR (500 MHz, $CDCl_3$) δ 7.24 – 7.19 (m, 2H), 7.19 – 7.12 (m, 2H), 6.49 (dt, *J* = 9.6, 1.5 Hz, 1H), 4.29 (q, *J* = 7.2 Hz, 2H), 4.19 (dd, *J* = 7.6, 15.5 Hz, 1H), 3.36 (s, 2H), 3.23 (dd, *J* = 7.9, 15.6 Hz, 2H), 2.79 (dd, *J* = 7.5, 15.6 Hz, 2H), 1.34 (t, *J* = 7.1 Hz, 3H); ^{13}C NMR 126 MHz, $CDCl_3$) δ 165.00, 151.69, 142.32, 126.64, 124.56, 121.16, 117.45, 61.35, 39.68, 39.55, 22.80, 14.27. HRMS (ESI) *m / z* calcd for $C_{16}H_{17}NO_2Na$ $[M+Na]^+$ 278.1157, found 278.1152.

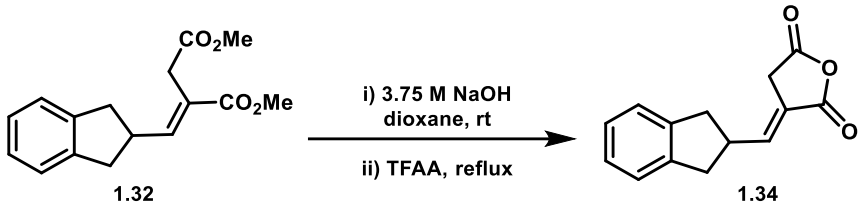

3-((2,3-dihydro-1*H*-inden-2-yl)methylene)dihydrofuran-2,5-dione 1.34. i) To a 1-dram vial was added diester **1.32** (150 mg, 0.547 mmol, 2.5:1 *E*:*Z* ratio), dioxane (1 mL), and 3.75 M aqueous NaOH (1.25 mL, 8.5 mmol). Electrical tape was wrapped around the mouth of the vial and the vial was placed in a pre-heated oil bath at 87 °C. The solution was headed at reflux for 2 h, then cooled to rt. The reaction was quenched with 3 M aqueous HCl, and the HCl solution was added until pH was about 1 as determined by pH paper. The suspension was extracted with EtOAc (2 x 1 mL), and the combined organic extracts were passed through a Na_2SO_4 filter followed by concentration under vacuum. The white residue (115 mg, 92% assuming full saponification) was then taken crude to the next step.

ii) To a 1 mL vial was added the white residue (115 mg, 0.467 mmol) from i) and TFAA (1.45 mL, 10.3 mmol). The reaction mixture was heated in an oil bath set to 45 °C and then to reflux for 1 h. The reaction mixture was then cooled to rt and concentrated under vacuum to afford **1.34** (93 mg, 87%, 1:3.5 *E*:*Z* ratio). The residue was dry loaded onto celite and purified further by flash column chromatography (20% EtOAc in hexanes) for characterization and subsequent reactions. (Note: Product may decompose back to the diacid on untreated silica gel.) Diagnostic peaks for ratio were δ 2.94 – 2.86 (m, 4H, *E*), 2.82 – 2.76 (dd, *J* = 6.8, 15.6 Hz, 2H, *Z*). **E and Z isomers combined (3.5:1 ratio):** ^{1}H NMR (600 MHz, $CDCl_3$) δ 7.25 – 7.17 (m, 8H, *E/Z*), 7.17 – 7.13 (m, 1H, *Z*) 4.52

– 4.43 (m, 1H, *Z*), 3.59 – 3.54 (m, 4H, *E/Z*), 3.28 (dd, *J* = 8.2, 15.6 Hz, 2H, *Z*), 3.26 – 3.18 (m, 5H, *E/Z*), 2.94 – 2.86 (m, 4H, *E*), 2.79 (dd, *J* = 6.8, 15.6 Hz, 2H, *Z*).

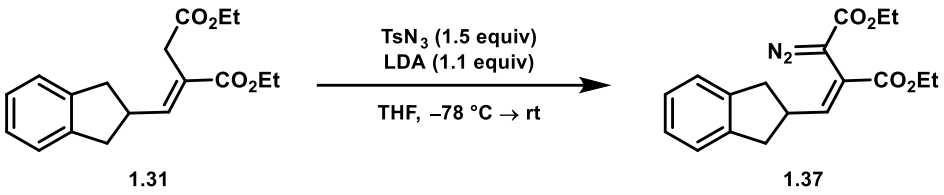

1.31 1.37

diethyl (*E*)-2-diazo-3-((2,3-dihydro-1*H*-inden-2-yl)methylene)succinate 1.37. To a 1-dram vial with a septum was added diisopropylamine (10 µL) and dry THF (0.33 mL). The solution was cooled to –78 °C with an acetone/dry ice bath. *n*-BuLi (2.3 M solution in hexanes, 40 µL, 0.1 mmol) was added dropwise to the vial. Into a separate 1 dram vial was added diester **1.31** (20 mg, 0.066 mmol, 1:1.5 *E*:*Z* isomer) and dry THF (0.13 mL), and the solution was added to the LDA solution dropwise via cannula. The solution was stirred for 20 min, after which TsN_3 (24 mg, 20 µL, 90% purity, 0.12 mmol) was added dropwise to the solution. The solution turned orange and bubble formation was observed after addition of the azide. The reaction mixture was stirred at –78 °C for 2.5 hours. The acetone/dry ice bath was removed and replaced with an ice bath, and the reaction was quenched with saturated aqueous $NaHCO_3$. The layers were separated, and the aqueous layer was extracted with EtOAc (3 x 1 mL). The combined organic extracts were washed with brine, dried over Na_2SO_4, filtered, and concentrated under vacuum. The crude residue was purified by flash column chromatography (5% EtOAc in hexanes to 10% EtOAc in hexanes) to afford **1.37** (8 mg, 40%, 2:1 *E*:*Z* ratio) as a yellow oil. The diastereomers were separated by flash column chromatography (2-5-10% Et_2O in hexanes gradient) for characterization. **E isomer:** ^{1}H NMR (500 MHz, $CDCl_3$) δ 7.24 – 7.11, (m, 5H), 4.27 – 4.21 (m, 4H), 3.35 (dp, *J* = 2.5, 7.6 Hz, 1H), 3.20 (dd, *J* = 7.7, 15.6 Hz, 2H), 2.88 (dd, *J* = 7.2, 15.8 Hz, 2H), 1.30 (q, *J* = 7.2 Hz, 6H); Z **isomer:** ^{1}H NMR (500 MHz, $CDCl_3$) δ **E and Z isomers:** ^{13}C NMR (151 MHz, $CDCl_3$) δ 165.40, 164.97, 153.36, 146.73, 142.44, 142.12, 126.64, 126.59, 126.57, 126.51, 126.41, 124.53, 124.48,

118.31, 117.80, 61.58, 61.42, 61.26, 61.21, 41.06, 40.24, 39.92, 38.65, 14.53, 14.48, 14.27, 14.22. IR (thin film): 2981, 2959, 2936, 2906, 2843, 2099, 1701 cm^{-1}.

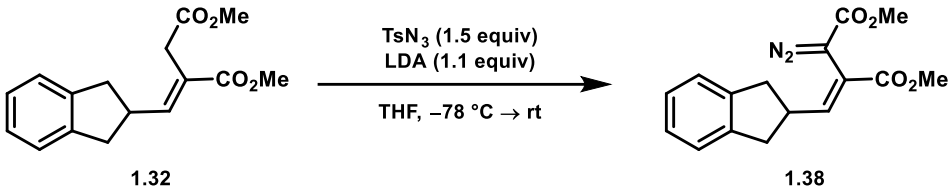

1.32 1.38

dimethyl (*E*)-2-diazo-3-((2,3-dihydro-1*H*-inden-2-yl)methylene)succinate 1.38. The procedure for **1.37** was followed, with the following deviations: diester **1.32** (20 mg, 0.073 mmol, 1:1.5 *E*:*Z* ratio) was used as a starting material. The crude residue was purified by flash column chromatography (5% EtOAc in hexanes to 10% EtOAc in hexanes) to afford **1.38** (7 mg, 30%, 1:1.5 *E*:*Z* ratio) as a yellow oil. Diagnostic peaks for ratio were 6.34 (d, *J* = 10.2 Hz, 1H, *E*), 6.23 (dd, *J* = 9.5, 13.7, 1H, *Z*). **E and Z isomers (1:1.5 ratio):** ^{1}H NMR (500 MHz, $CDCl_3$) δ 7.24–7.09 (m, 9H, *E*/*Z*), 6.34 (d, *J* = 10.2 Hz, 1H, *E*), 6.23 (dd, *J* = 9.5, 13.7, 1H, *Z*), 3.81 – 3.67 (m, 14H, *E*/*Z*), 3.27 – 3.16 (m, 4H, *E*/*Z*), 2.93 – 2.76 (m, 4H, *E*/*Z*); ^{13}C NMR (126 MHz, $CDCl_3$) δ 165.82, 165.44, 154.06, 147.47, 142.39, 142.05, 141.96, 141.85, 135.21, 126.68, 126.64, 126.62, 126.57, 126.54, 124.66, 124.56, 124.49, 124.47, 124.45, 117.98, 117.43, 63.26, 53.53, 52.79, 52.55, 52.29, 52.23, 52.15, 42.20, 41.13, 40.30, 39.86, 39.61, 38.61, 37.39, 35.84.

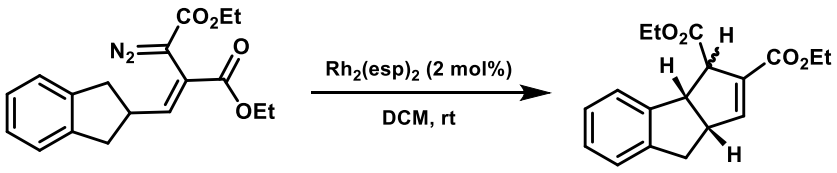

1.37 1.42/1.42'

diethyl (3α*S*,8α*S*)-3,3α,8,8α-tetrahydrocyclopenta[α]indene-2,3-dicarboxylate 1.42/1.42'. A stock solution of $Rh_2(esp)_2$ (2 mg) in dry, degassed DCM (1 mL) was prepared by sonication. To

a 1-dram vial with a septum was added diazo **1.37** (5 mg, 0.02 mmol), followed by 0.10 mL of the prepared stock solution. The reaction mixture was stirred at rt for 21 h. The solvent was evaporated, and the reaction mixture was run through a silica gel plug with 50% EtOAc in hexanes as the eluent. The crude residue was concentrated under vacuum and was purified by preparatory TLC (20% EtOAc in hexanes) to afford **1.42** (2.3 mg, 50%, stereochemistry unassigned). ^{1}H NMR (500 MHz, $CDCl_3$) δ 7.19 – 7.10, (m, 4H), 6.98 (t, *J* = 2.2 Hz, 1H), 4.36 (t, *J* = 9.3 Hz, 1H), 4.24 – 4.10 (m, 3H), 3.85 – 3.78 (m, 1H), 3.74 (qd, *J* = 7.1, 4.9 Hz, 1H), 3.21 (dd, *J* = 16.3, 10.3 Hz, 1H), 2.97 (dd, *J* = 16.3, 5.7 Hz, 1H), 1.35 – 1.14 (m, 3H), 0.92 (t, J = 7.1 Hz, 3H). HRMS (ESI) *m / z* calcd for $C_{18}H_{20}O_4Na$ $[M+Na]^+$ 323.1259, found 323.1243.

1.7 References

1. Aoyagi, Y.; Yamazaki, A.; Nakatsugawa, C.; Fukaya, H.; Takeya, K.; Kawauchi, S.; Izumi, H. Salvileucalin B, A Novel Diterpenoid with an Unprecedented Rearranged Neoclerodane Skeleton from *Salvia leucantha* Cav. *Org. Lett.* **2008**, *10*, 4429.

2. Aoyagi, Y.; Yamazaki, A.; Kato, R.; Tobe, F.; Fukaya, H.; Nishikawa, T.; Nakahashi, A.; Miura, N.; Monde, K.; Takeya, Koichi. Salvileucalin C, a Novel Rearranged Neoclerodane Diterpene from *Salvia leucantha*. *Tet. Lett.* **2011**, *52*, 1851.

3. Buchner, E.; Curtius, T. Ueber Pseudophenylessigsäure. *Chem. Ber.* **1896**, *29*, 106.

4. Doering, W. V. E.; Laber, G.; Vonderwahl, R.; Chamberlain, N. F.; Williams, R.

B. The Structure of the Buchner Acids. *J. Am. Chem. Soc.* **1956**, *78*, 5448.

5. Ye, T.; Mckervey, M. A. Organic Synthesis with α-Diazo Carbonyl Compounds. *Chem. Rev.* **1994**, *94*, 1091.

6. Levin, S.; Nani, R. R.; Reisman, S. E. Rapid Assembly of the Salvileucalin B Norcaradiene Core. *Org. Lett.* **2010**, *12*, 780.

7. King, G. R.; Mander, L. N.; Monck, N. J. T.; Morris, J. C.; Zhang, H. B. A New and Efficient Strategy for the Total Synthesis of Polycyclic Diterpenoids: The Preparation of Gibberellins (±)-GA_{103} and (±)-GA_{73}. *J. Am. Chem. Soc.* **1997**, *119*, 3828.

8. Levin, S.; Nani, R. R.; Reisman, S. E. Enantioselective Total Synthesis of (+)-Salvileucalin B. *J. Am. Chem. Soc.* **2011**, *133*, 774.

9. McNamara, O. A.; Maguire, A. R. The Norcaradiene–Cycloheptatriene Equilibrium. *Tetrahedron*, **2011**, *67*, 9.

10. Davies, H. M. L.; Beckwith, R. E. J. Catalytic Enantioselective C−H Activation by Means of Metal−Carbenoid-Induced C−H Insertion. *Chem. Rev.* **2003**, *103*, 2861.

11. Eliot, G. I.; Fuchs, J. R.; Blagg, B. S. J.; Ishikawa, H.; Tao, H.; Yuan, Z.-Q.; Boger, D. L. Intramolecular Diels−Alder/1,3-Dipolar Cycloaddition Cascade of 1,3,4-Oxadiazoles. *J. Am. Chem. Soc.* **2006**, *128*, 10589.

12. Carlson, G. L. B.; Quina, F. H.; Zarnegar, B. M.; Whitten, D. G. Excited State Interactions and Decay Routes in Bichromophoric Systems. Nonconjugated Phenyl Ketones. *J. Am. Chem. Soc.* **1975**, *97*, 347.

13. Zhang, Y.; Ji, P.; Dong, Y.; Wei, Y.; Wang, W. Deuteration of Formyl Groups via a Catalytic Radical H/D Exchange Approach. *ACS Catal.* **2020**, *10*, 2226.

14. Carson, C. A.; Kerr, M. A. Total Synthesis of (+)-Phyllantidine. *Angew. Chem. Int. Ed.* **2006**, *45*, 6560.

15. Ziegler, K.; Martin, H.; Krupp, F. Metallorganische Verbindungen, XXVII Aluminiumtrialkyle und Dialkyl-Aluminiumhydride Aus Aluminiumisobutyl-Verbindungen. *Liebig. Ann. Chem.* **1960**, *629*, 14.

16. Snyder, S. A.; Sherwood, T. C.; Ross, A. G. Total Syntheses of Dalesconol A and B. *Angew. Chem. Int. Ed.* **2010**, *49*, 5146.

17. Hoshino, D.; Mori, Keiji. Divergent Access to Seven/Five-Membered Rings Based on [1,6]-Hydride Shift/Cyclization Process. *Org. Lett.* **2021**, *23*, 9403.

18. Qin, H.; Cai, W.; Wang, S.; Guo, T.; Li, G.; Lu, H. N-Atom Deletion in Nitrogen Heterocycles. *Angew. Chem. Int. Ed.* **2021**, *60*, 20678.

19. Zhang, M.; Yuan, X.-A.; Zhu, C.; Xie, Jin. Deoxygenative Deuteration of Carboxylic Acids with D_2O. *Angew. Chem. Int. Ed.* **2019**, *58*, 312.

20. Caesar, J. C.; Griffiths, D. V.; Griffiths, P. A.; Tebby, J. C. Reactions of Ylides Formed from Trialkyl Phosphites with Dialkyl Acetylenedicarboxylates in the Presence of Carbon Dioxide. *J. Chem. Soc. Perkin Trans.* **1990**, *1*, 2329.

21. Trost, B. M.; Melvin, L. S. Bromomalonates as Synthetic Reagents. Transfer Alkylations. *J. Am. Chem. Soc.* **1976**, *98*, 1204.

22. Toumi, B.; Samarat, A.; Harizi, A.; Amri, H. An Efficient Approach to the Synthesis of Ethyl α-Cyanoalkyl β-Substituted Acrylates by the HWE Olefination of Ethyl 2-(Diethoxyphosphoryl) Cyanoalkanoates. *Phosphorus, Sulfur, and Silicon and the Related Elements* **2010**, *3*, 652.

CHAPTER 2: Efforts Towards the Synthesis of Emetine via a Desymmetrization Approach

2.1 Introduction

(–)-Emetine (**2.1**) is part of the class of ipecac alkaloids isolated from the root of *Psychotria ipecacuanha* that possess a benzoquinolizidine structural motif. While it has been used as an emetic and expectorant in traditional medicine,[1] its role in inhibition of protein synthesis has led to it being investigated as an antiviral agent – specifically for COVID-19. Kumar and co-workers have demonstrated with *in vitro* studies on Vero cells that emetine acts on the translation initiator eIF4E and therefore inhibits the replication of the virus.[2] (–)-Emetine was also shown to be effective against pulmonary arterial hypertension (PAH) in rat models due to its ability to inhibit the proliferation of pulmonary artery smooth muscle cells (PASMC) without significant toxic effects in normal cells. It provides inhibitory effects on the levels of CyPA and its receptor Bsg, both of which assist in the proliferation of PASMC cells. This bioactivity has generated interest in (–)-emetine's use as an alternative to vasodilator drugs for the treatment of PAH.[3]

The biosynthesis of (–)-emetine is proposed to start from tyrosine (**2.2**) and loganin (**2.5**) (Scheme 2.1). The former is transformed into dopamine (**2.4**) through an oxidase and tyrosine decarboxylase and the latter transformed into secologanin (**2.6**) by cytochrome P450 CYP72A1. Dopamine and secologanin are then converted to (*S*)-*N*-deacetylisoipecoside (**2.7**) via a Pictet–Spengler-like transformation by deacetylisoipecoside synthase. (*S*)-*N*-deacetylisoipecoside is then converted into protoemetine (**2.8**) by a series of *O*-methyltransferases and glycosidases. Finally, protoemetine is converted to (–)-emetine via condensation of another equivalent of dopamine followed by modification by other *O*-methyltransferases.[4]

Scheme 2.1: Proposed biosynthesis of (–)-emetine

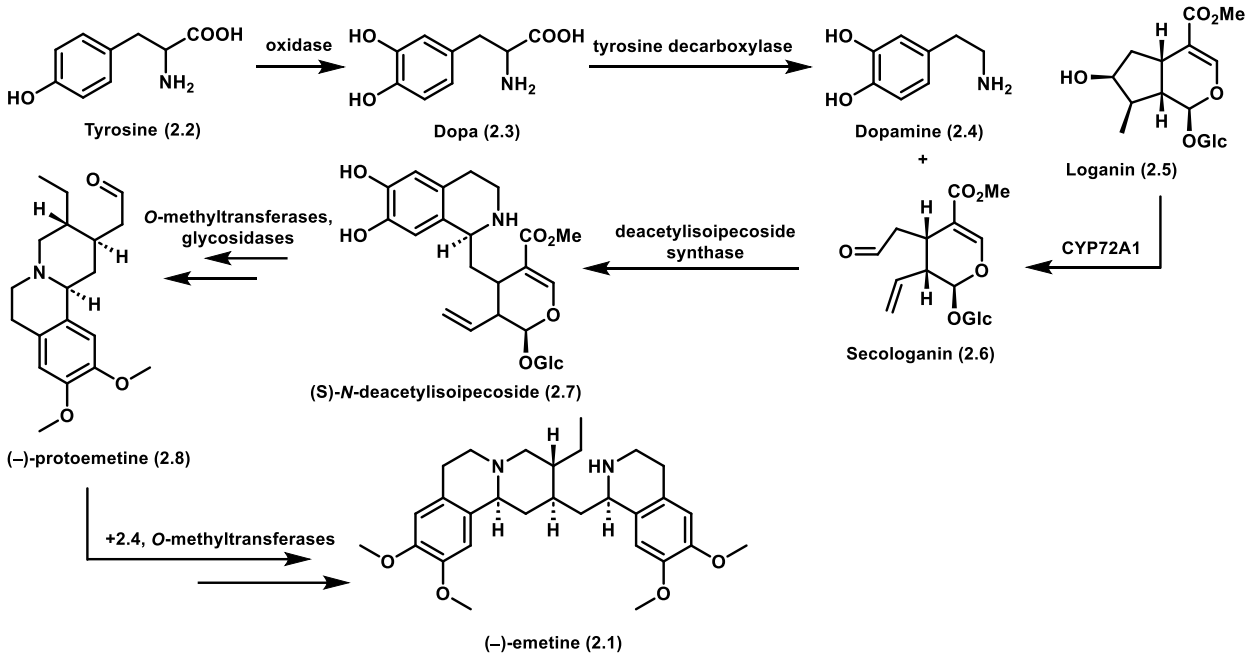

2.2 Previous approaches to (–)-emetine

There have been several approaches towards (–)-emetine. For example, Tietze and co-workers synthesized (–)-emetine via utilization of asymmetric reductions of imines synthesized via the Bischler–Napieralski reaction (Scheme 2.2a).[5] Furthermore, Itoh and co-workers have utilized an asymmetric Cu^{I}-mediated allylation of imine **2.13** followed by a diastereoselective recrystallization to obtain enantiomerically enriched tetrahydroisoquinoline **2.14** (Scheme 2.2 b).[6] The synthesis was completed via the same method as Tietze and co-workers. In terms of organocatalytic methods, Córdova and co-workers[7] as well as Franzén and co-workers[8] utilized proline-derived catalysts for one-pot formation of the benzoquinolizidine moiety; the strategies are very similar (Scheme 2.2c). There is also a process-scale synthesis by Tokuyama and co-workers that utilized strategies from the previously mentioned syntheses to obtain 237 g of (–)-emetine (Scheme 2.3).[9] They synthesized the same benzoquinolizidine **2.14** via a similar strategy to Itoh and coworkers' synthesis. The elaboration to intermediate **2.21** was also strategically similar.

Finally, they utilized Tietze and co-workers' strategy of a Bischler–Napieralski reaction followed by asymmetric hydrogenation to synthesize (–)-emetine with an overall yield of 12% over 13 steps.

Scheme 2.2: Previous approaches towards (–)-emetine

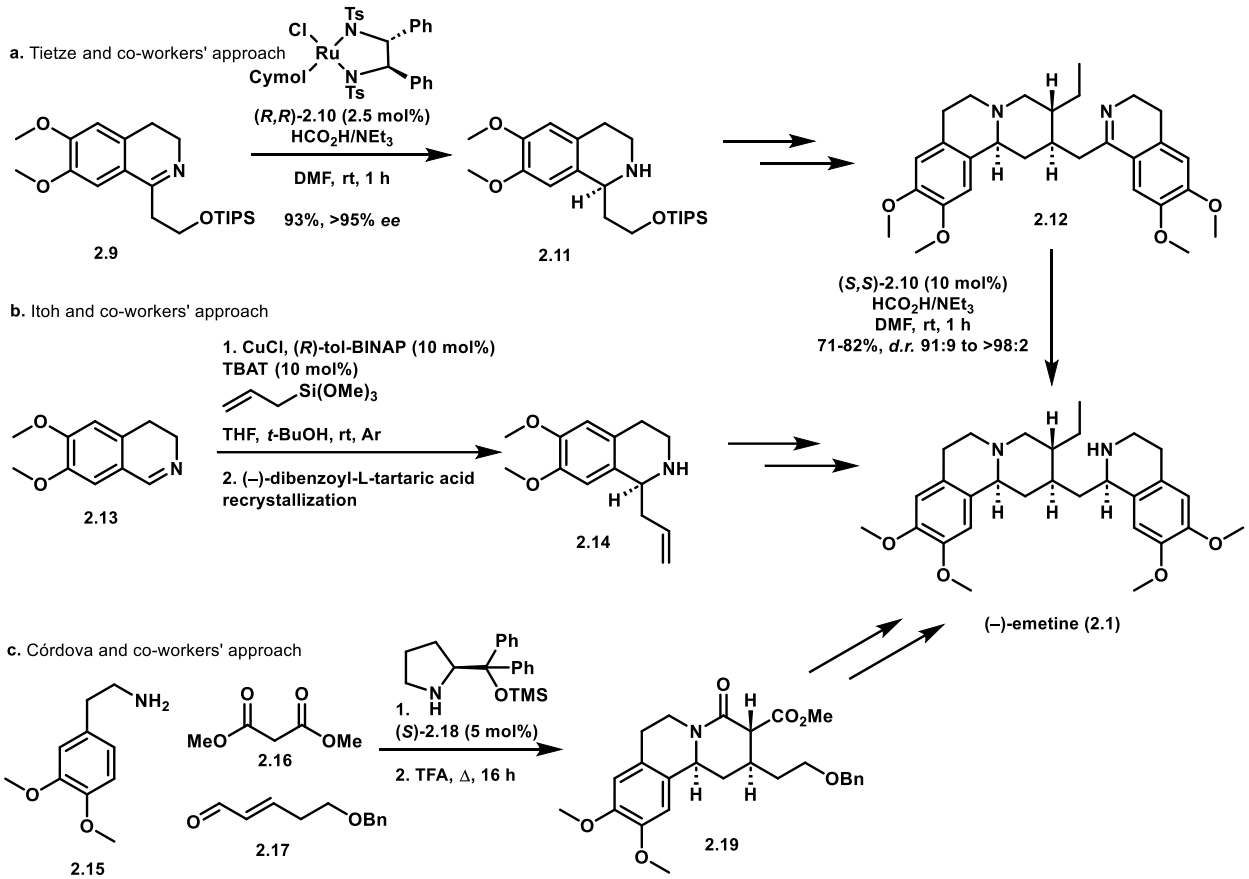

Scheme 2.3: Process-scale synthesis of (–)-emetine

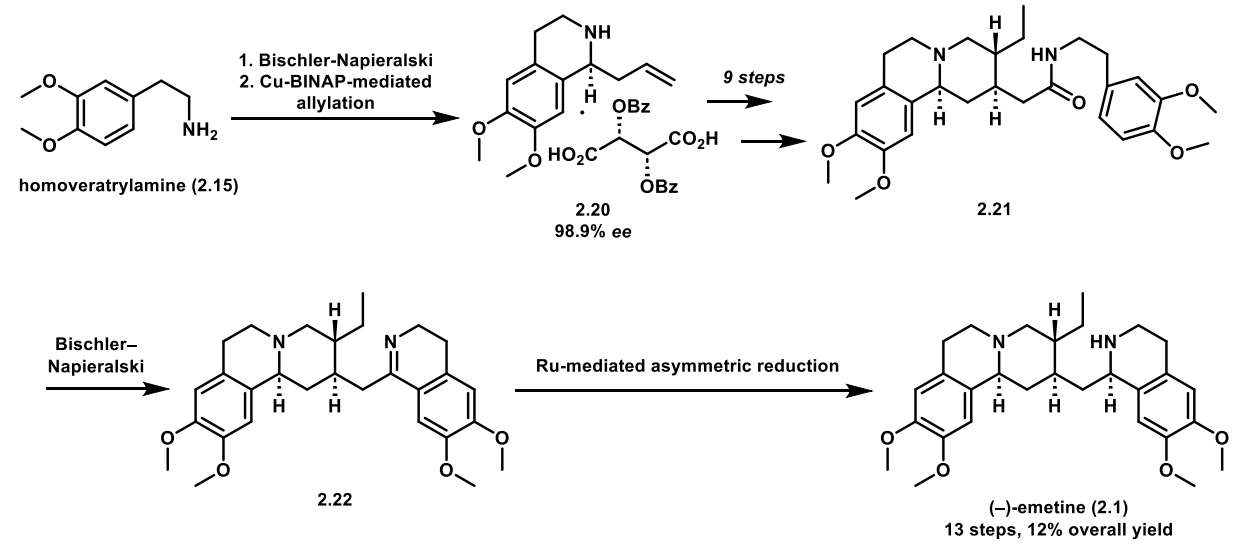

2.3 Summary

The overarching theme between the previously mentioned syntheses is the stepwise formation of both nitrogen-containing rings. A strategy where both nitrogen-containing rings are formed in one step to form a symmetrical intermediate followed by a desymmetrization could allow for more direct access to (–)-emetine and analogues. While a process-scale synthesis does exist for (–)-emetine, a significantly shorter synthesis with good average yield per step may lead to another sequence that could compete with the one produced by Tokuyama and co-workers.

2.4 Efforts towards the synthesis of emetine

2.4.1 Introduction

Scheme 2.4: Retrosynthetic analysis of emetine

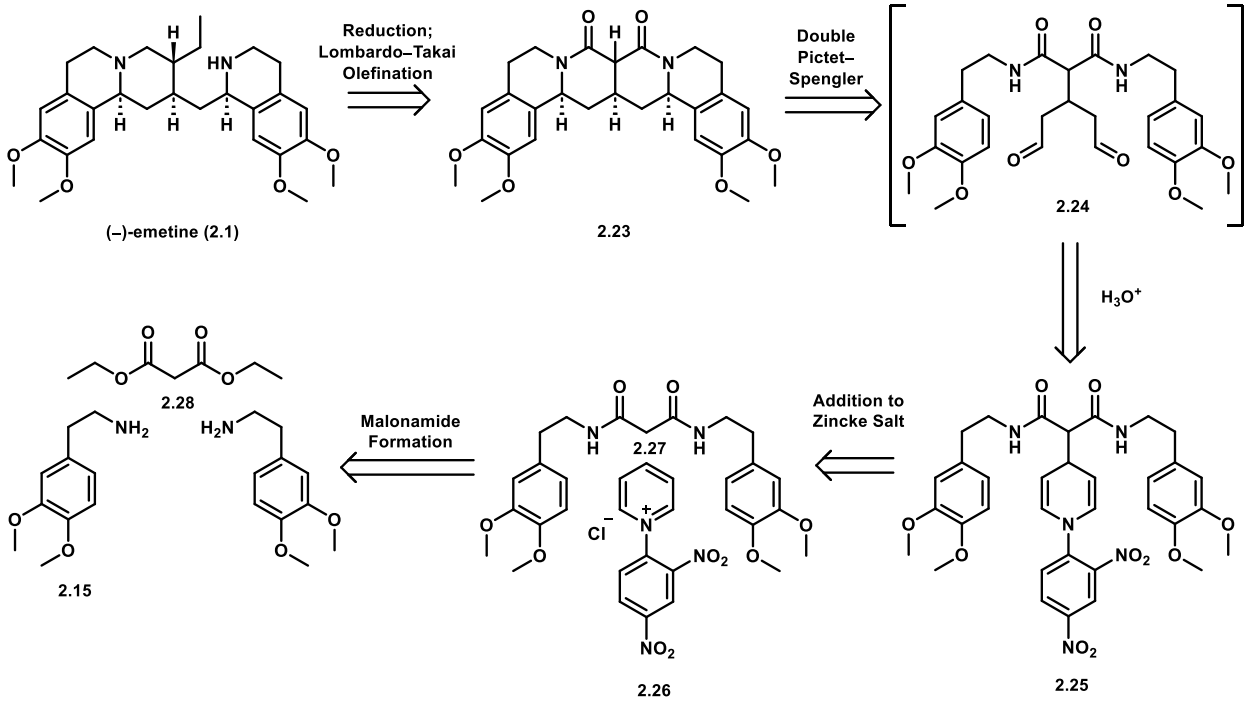

To achieve a concise sequence, my colleague Joseph Capani helped propose a route towards symmetrical hexacycle **2.23**. He proposed accessing hexacycle **2.23** via the acid-mediated unmasking of a dihydropyridine **2.25** to produce dialdehyde intermediate **2.24**, followed by a

double Pictet–Spengler reaction. Dihydropyridine **2.25** could be accessed via addition of malonamide **2.27** into Zincke salt **2.26**.[10] Finally, malonamide **2.27** could be accessed by double condensation of homoveratrylamine (**2.15**) with diethyl malonate (**2.28**).[11,12] In terms of elaborating hexacycle **2.23** to emetine, I proposed a Lombardo–Takai olefination[13,14] to both add a carbon to the skeleton and provide a possibility to break the C-N bond. Emetine might then be accessed via global reduction. While the latter half of the synthesis could face challenges like over-methylenation or a recalcitrant hemiaminal opening, we felt that access to hexacycle **2.23** could be rapid enough to test the downstream chemistry of the sequence. This could then provide an opportunity to experiment with how to deliver one carbon to the symmetrical diamide in an enantioselective manner.

2.4.2 Efforts towards synthesis of key hexacycle

Our synthetic efforts were initiated by my colleague Joseph Capani, who synthesized malonamide **2.27** by irradiating neat homoveratrylamine and diethyl malonate with microwave radiation. After experimentation with different solvents heated to reflux with microwave radiation, I found that *m*-xylene gave the highest yields and mediated faster conversion to product.

Scheme 2.5: Synthesis of dihydropyridine

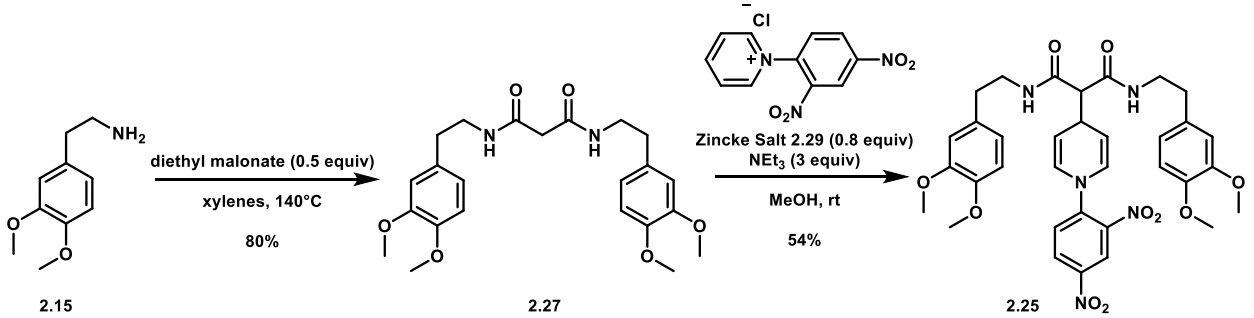

Dihydropyridine **2.25** was synthesized from malonamide **2.27** through exposure of the latter to Zincke salt **2.29** and triethylamine in methanol. The product was an insoluble red powder

that precipitated out of solution when it formed. The product was sensitive to untreated and neutralized silica gel. To circumvent this, Zincke salt **2.29** was used as the limiting reagent, which allowed a simple purification via filtration followed by washing with cold methanol to cleanly yield grams of the desired dihydropyridine **2.25**.

Table 2.1: Attempts towards acid hydrolysis and the double Pictet–Spengler reaction

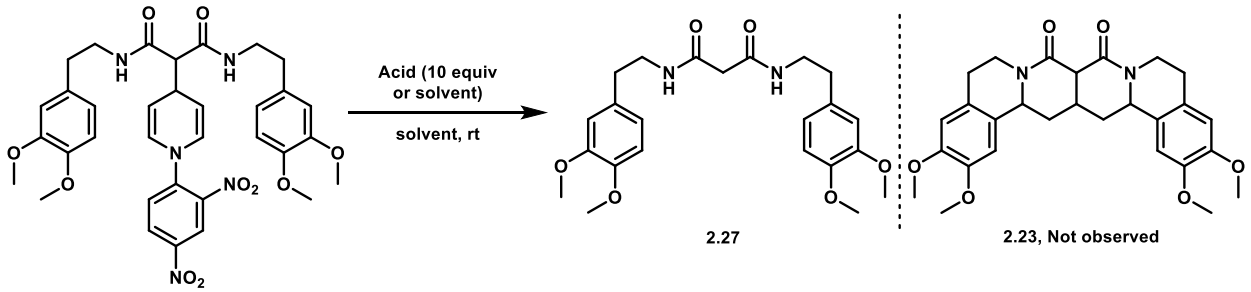

Entry	Solvent	Acid	Entry	Solvent	Acid
1	DME	H_3PO_4	5	TFA	N/A
2	DMF	H_3PO_4	6	MeCN/H_2O (1:1)	TFA
3	Me_2CO	H_3PO_4	7	DCM	TFA
4	Dioxane	H_3PO_4	8	$CDCl_3$	TFA

Other Brønsted and Lewis acids tried: HCl, MsOH, HBF_4, HCO_2H, AcOH, PPTS, 100x w/w SiO_2, BF_3•Et_2O (1.1 equiv)
Miscellaneous trials: 1:1 MeCN/H_2O, HFIP with 10 equiv H_2O (wrt 2.25)

Table 2.2: pH and temperature studies

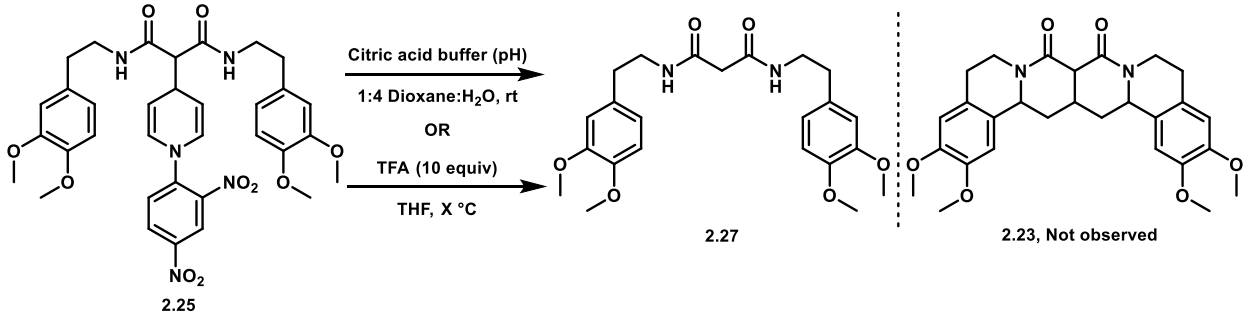

Entry	pH	Result (2.25:2.27 ratio)	Entry	Temp (°C)	Result
1	3	4:1	1	rt	2.27 only
2	4	1:7.2	2	0	2.27 only
3	5	1:11	3	–20	2.27 only
4	6	1:7.9	4	–78	1:1 (2.25:2.27)

Dihydropyridine **2.25** was then exposed to various Brønsted and Lewis acids in efforts to transform it into the desired hexacycle **2.23** (Table 2.1). Unfortunately, all that was observed was

formation of malonamide **2.27** in all the trials run. Variations in pH and temperature in efforts to suppress the formation of **2.27** also led to formation of malonamide **2.27** (Table 2.2). We hypothesize that exposure of the dihydropyridine **2.25** to any Brønsted or Lewis acid primes the malonamide fragment to be ejected as a leaving group which promotes aromatization of the dihydropyridine back to a Zincke salt. With these results, I then thought to access the hexacycle via an alternative route with the intent to probe the downstream chemistry.

Scheme 2.6: Oxidative cleavage strategy towards the hexacycle

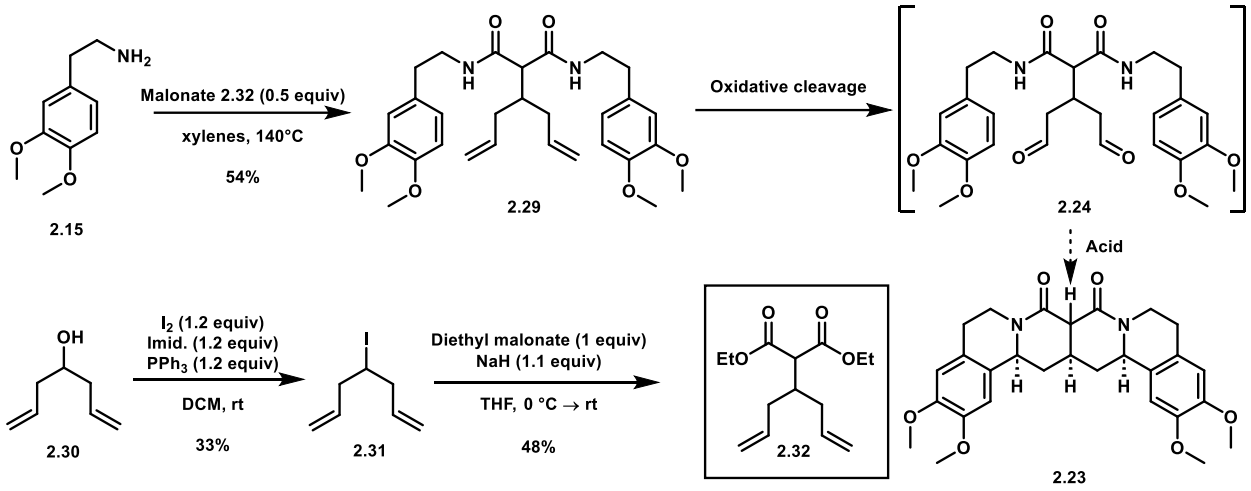

We thought that the dialdehyde **2.24** could be accessed oxidative cleavage of a diene moiety (Scheme 2.6).[15] We hypothesized that ozonolysis conditions would be deleterious to the electron rich ring and moved forward with osmium-mediated oxidative cleavage. To this end, we synthesized substrate **2.29** in three steps. Alkyl iodide **2.31** was synthesized from commercial alcohol **2.30** via an Appel reaction. Alkylation of diethyl malonate with **2.31** proceeded smoothly.[15] The malonate **2.32** was then subjected to the same microwave conditions used in the formation of the original malonamide **2.27** to furnish the oxidative cleavage substrate **2.29**. Exposure of substrate **2.29** to several Os^{VIII} sources resulted in complex mixtures (Table 2.3a).

Table 2.3: Oxidative cleavage conditions on substrates **2.29** and **2.33**

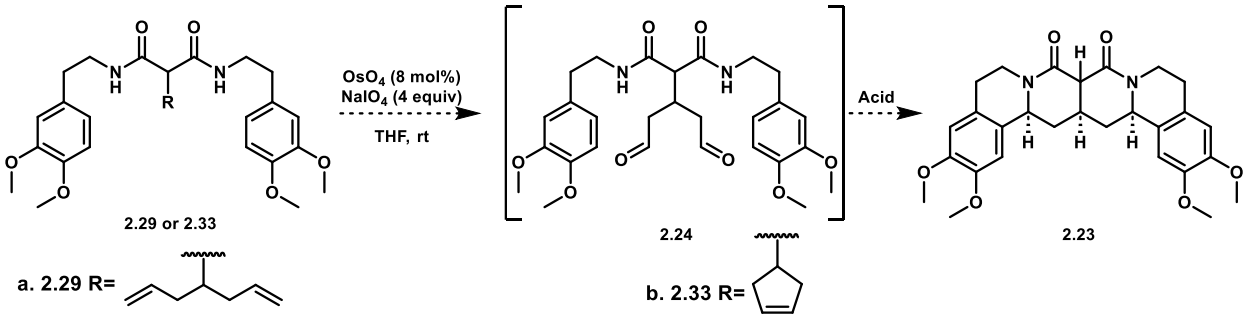

Entry	OsO_4 Source	Acid	Result
1	OsO_4 stock in *i*-PrOH	None	Complex mixture
2	OsO_4 stock in *i*-PrOH	H_3PO_4	Complex mixture
3	$K_2OsO_4•2H_2O$	None	Complex mixture
4	$K_2OsO_4•2H_2O$	TFA	Complex mixture

Entry	OsO_4 Source	Acid	Result
1	OsO_4 stock in *i*-PrOH	None	Complex mixture
2	OsO_4 stock in *i*-PrOH	H_3PO_4	Complex mixture
3	$K_2OsO_4•2H_2O$	None	Complex mixture
4	$K_2OsO_4•2H_2O$	TFA	Complex mixture

Scheme 2.7: Variations of oxidative cleavage strategy

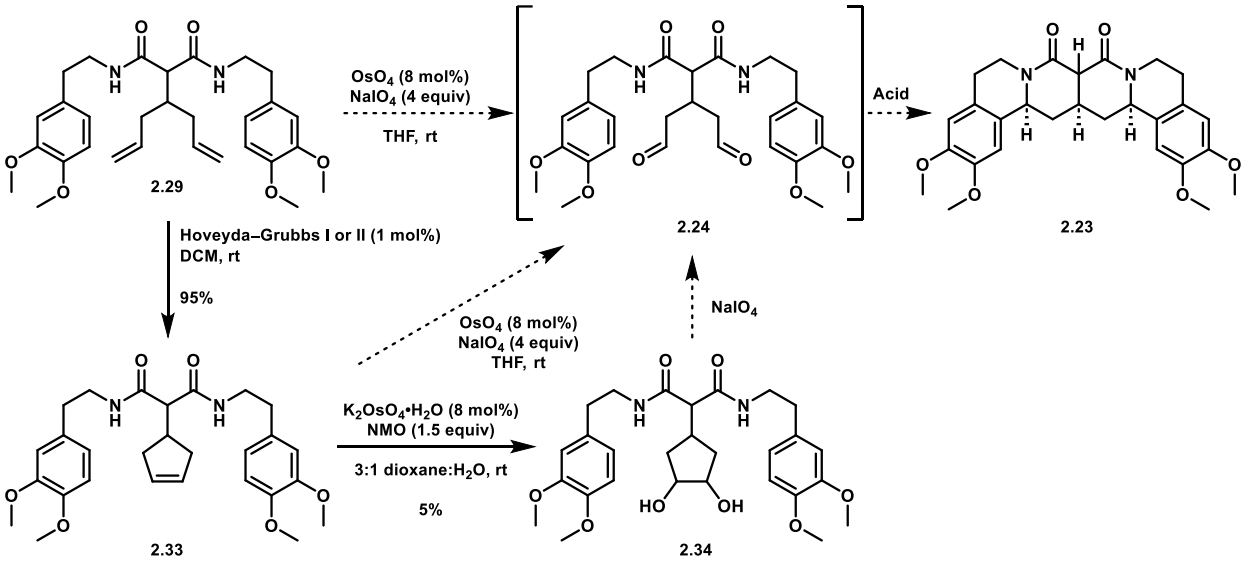

Taking inspiration from the literature, the diene moiety was converted to a cyclopentene via exposure of the diene **2.29** to the Hoveyda–Grubbs II catalyst (Scheme 2.7).[15] Exposure of the cyclopentene substrate **2.33** to various Os^{VIII} sources also led to complex mixtures (Table 2.3b). To circumvent this, I then thought to perform the transformation in a step-wise fashion. We planned to first form the diol **2.34** from the cyclopentene[16] then subsequently perform oxidative cleavage with sodium periodate.[17] While the diol **2.34** was observed and characterized, it was isolated in a low yield. We hypothesize that diol **2.34** is highly soluble in water, and that an aqueous workup

would not be amenable to isolation of the diol. Variations in workup, for example adding in solid sodium thiosulfate, followed by filtration, may allow for isolation of greater amounts of diol.

2.4.3 Model system for Pictet–Spengler

Scheme 2.8: Synthesis of model system for Pictet–Spengler

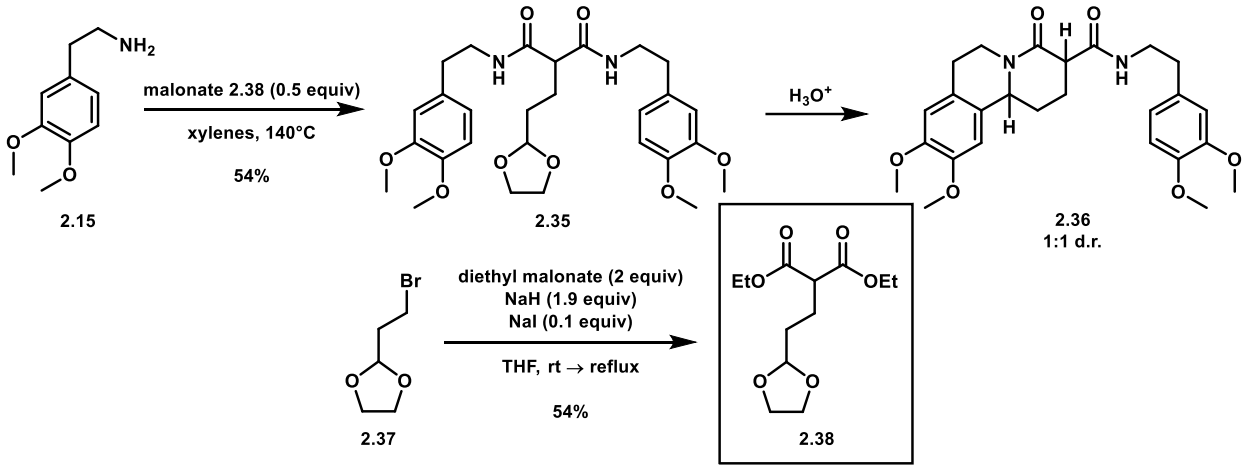

Table 2.4: Screen of conditions for model system

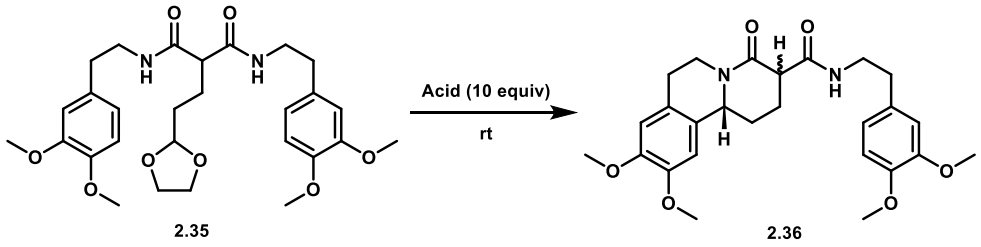

Entry	Acid	Result
1[a]	Silica gel	Complex mixture
2	AcOH	Mostly SM
3	H_3PO_4	Complex mixture
4	TFA	Complex mixture
5	$TsOH•H_2O$	Trace product
6	3:1 $HCO_2H:H_2O$	70% 2.36, 1:1 d.r.

[a]100 x w/w with respect to SM

Concurrently, we also explored the reactivity of a model system to probe the feasibility of the proposed Pictet–Spengler step.[18] The model system **2.35** was synthesized in a similar manner

to diene substrate **2.29** (Scheme 2.8). After exposure of dioxolane **2.35** to a screen of various Brønsted and Lewis acids, we discovered that using a 3:1 ratio of formic acid to water facilitated hydrolysis and a Pictet–Spengler to produce the corresponding product **2.36** with 1:1 d.r. (Table 2.4). **2.36** was isolated cleanly with a 3:1 d.r. These results show that the one-pot unmasking of an aldehyde followed by Pictet–Spengler strategy may be feasible. We hope that these conditions are generalizable to the dialdehyde system.

2.5 Conclusion

While the initial strategy of acid hydrolysis of the dihydropyridine did not proceed as planned, there are several possible avenues to move forward. One avenue would include accessing diol **2.34** followed by oxidative cleavage to access the key hexacycle **2.23** (Scheme 2.7). Other alternative strategies could be employed, one of which includes Mukaiyama hydration of the dihydropyridine to form the hemiaminal, which if formed may undergo hydrolysis to unmask the dialdehyde moiety and undergo the double Pictet–Spengler (Scheme 2.9a).[19] Other different electron deficient groups like carbamoyl or acyl groups on the nitrogen in the dihydropyridine may also be utilized (Scheme 2.9b).[20,21] We hypothesize that these groups may prevent the deleterious rearomatization pathway when the dihydropyridine is exposed to acid.

Scheme 2.9: Future directions

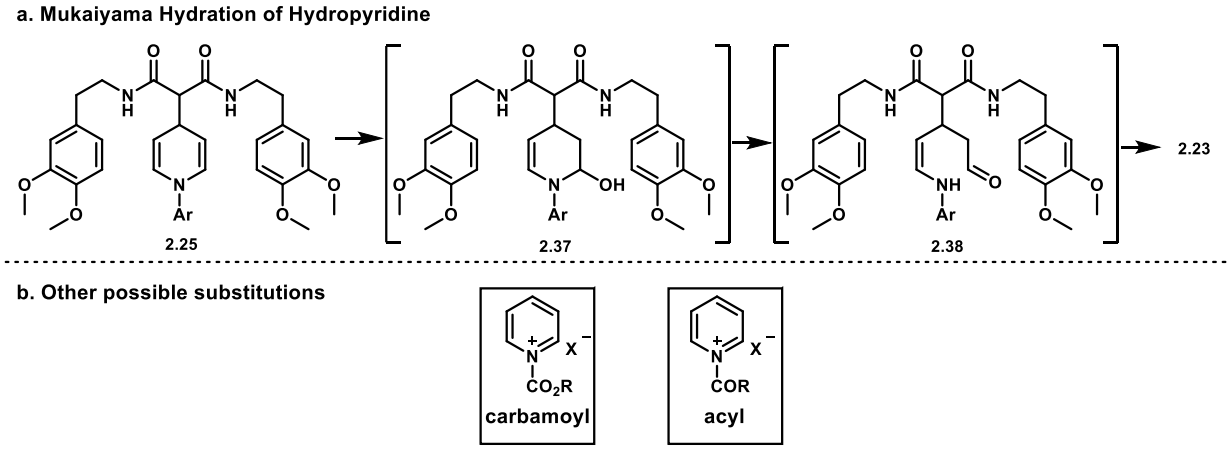

2.6 Experimental Procedures

See **Section 1.6**.

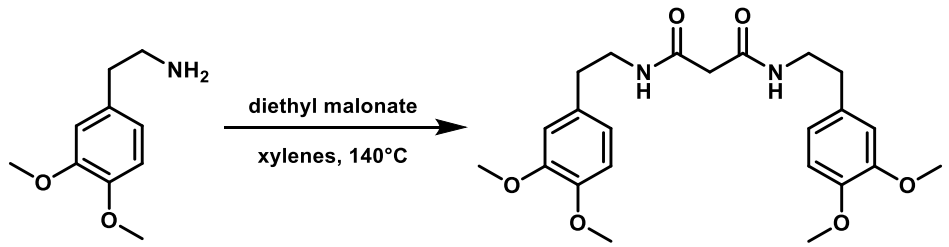

2.15 **2.27**

N[1],*N*[3]**-bis(3,4-dimethoxyphenethyl)malonamide 2.27**. To a microwave vial was added amine **2.15** (823 mg, 0.77 mL, 4.55 mmol), diethyl malonate (364 mg, 0.35 mL, 2.27 mmol), and xylenes (9 mL). The vial was capped and irradiated with microwave radiation at 140 °C for 1 h periods until all malonate was consumed and no mono-amide was observed, which typically required 3 cycles at this scale. The solvent was evaporated under vacuum with the water bath set to 50 °C, and the crude residue was purified by flash column chromatography (80% EtOAc in hexanes) to afford **2.27** (782 mg, 80%) as a yellow solid. Spectral data of **1.29** matched those previously reported.[10]

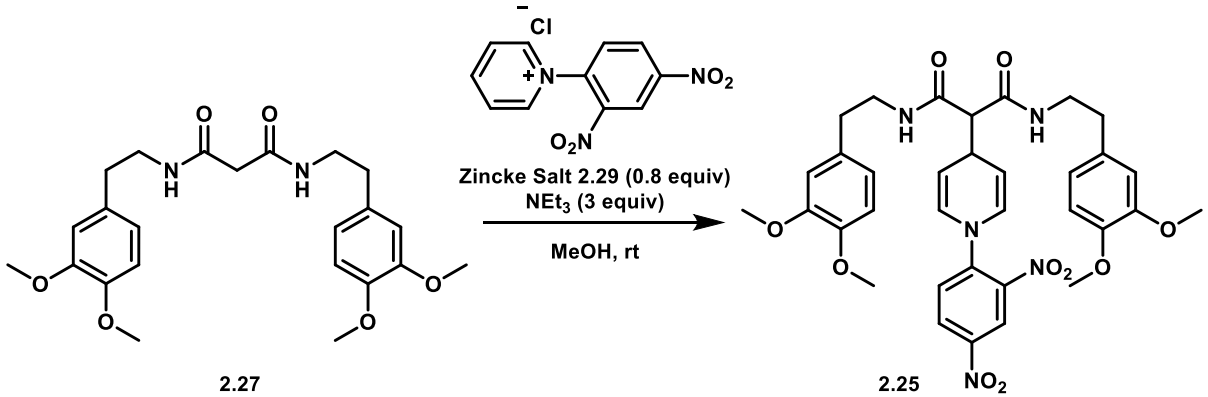

2.27 **2.25**

N[1],*N*[3]**-bis(3,4-dimethoxyphenethyl)-2-(1-(2,4-dinitrophenyl)-1,4-dihydropyridin-4-yl)malonamide 2.25**. To a 2-dram vial was added malonamide **2.27** (175 mg, 0.407 mmol), Zincke salt **2.29** (95 mg, 0.34 mmol), MeOH (3 mL), and lastly triethylamine (0.05 mL, 0.36 mmol). Upon addition of triethylamine, a red precipitate formed. The reaction mixture was stirred for 1 h at rt,

at which point the mixture was a red suspension. The mixture was filtered with a Buchner funnel and washed with cold MeOH (2 x 1 mL). The filtrate was dried under vacuum to afford **2.25** (153 mg, 67% yield) as a red powder. Scale up experiments (1.82 mmol of **2.29**) consistently gave around 40% yields. ^{1}H NMR (600 MHz, $CDCl_3$) δ 8.76 (d, J = 2.6 Hz, 1H), 8.36 (dd, J = 9.1, 2.6 Hz, 1H), 7.36 (d, J = 9.1 Hz, 1H), 6.80 (d, J = 7.9 Hz, 2H), 6.77 – 6.56 (m, 6H), 6.20 – 5.82 (m, 2H), 5.02 – 4.64 (m, 2H), 3.87 (s, 6H), 3.84 (s, 6H), 3.66 – 3.38 (m, 5H), 2.90 (d, J = 8.7 Hz, 1H), 2.77 (t, J = 7.1 Hz, 4H); ^{13}C NMR (151 MHz, CDCl3) δ 167.99, 149.08, 147.82, 142.10, 142.07, 140.16, 131.06, 128.33, 127.46, 123.18, 123.09, 120.75, 111.99, 111.42, 107.23, 63.04, 55.98, 55.95, 40.86, 36.29, 35.26. HRMS (ESI) *m / z* calcd for $C_{34}H_{38}N_5O_{10}$ $[M+H]^+$ 676.2618, found 676.2625.

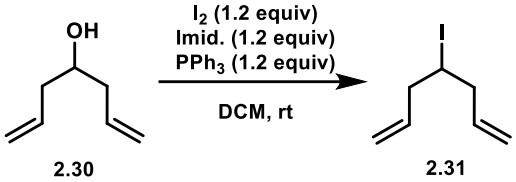

4-iodohepta-1,6-diene 2.31. To a 100 mL round-bottomed flask was added alcohol **2.30** (1.12 g, 1.30 mL, 10.0 mmol), imidazole (8.17 mg, 12.0 mmol), and PPh_3 (3.15 g, 12.0 mmol). The flask was cooled to 0 °C, and I_2 crystals (3.05 g, 12.0 mmol) were added slowly, portion-wise. The solution turned from yellow to brown as I_2 was added. The flask was covered with aluminum foil, and the reaction mixture was stirred for 2 h. The reaction mixture was then triturated with pentanes, and the solution was filtered through a celite plug. The trituration protocol was repeated once. The filtrate was then diluted with MeCN (150 mL) and the MeCN was extracted with pentanes (3 x 50 mL). The combined pentane layers were extracted with MeCN, then concentrated under vacuum at 600 mmHg for 10-15 min to afford **2.31** (778 mg, 94% purity (w/w%), 33%) as a clear oil, contaminated with pentanes. Note: The MeCN layer was again extracted with pentanes (3 x 200 mL), and the combined extracts were concentrated under vacuum at 500 mmHg with the water

bath set to 30 °C. Copper balls were then added to the solution collected in the roto-evaporator trap and then was further concentrated down via an air stream. This solution and the concentrated extracts were combined and purified by flash column chromatography (pentanes). The collected fractions were evaporated at 500 mmHg and afforded more **2.31** (1160 mg, 87% purity (w/w%), 52%) contaminated with pentanes. The iodide can be stored at ~4 °C with copper as an inhibitor to prevent decomposition/discoloration. Spectral data of **1.29** matched those previously reported.[15]

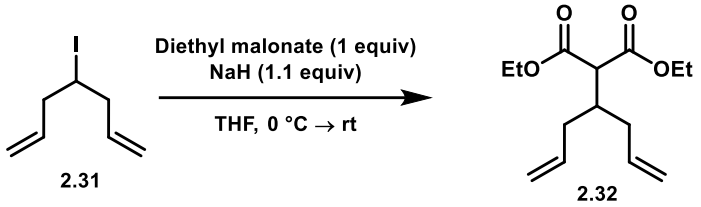

diethyl 2-(hepta-1,6-dien-4-yl)malonate 2.32. To a 25 mL two-necked round-bottomed flask was added diethyl malonate (240 g, 0.23 mL, 1.5 mmol) and dry DMF (3.3 mL). NaH (52 mg, 1.3 mmol, 60% suspension in mineral oil) was added in one portion at rt and the suspension was stirred for 15 min. Alkyl iodide **2.31** (250 mg, 87% in pentane, 1.0 mmol) was added in one portion and the flask was placed in a pre-heated oil bath set to 165 °C. The reaction mixture was heated at reflux for 1 h, then cooled to rt. DI H_2O (15 mL) was added to quench the reaction, and the aqueous layer was extracted with Et_2O (2 x 20 mL). The combined organic extracts were washed sequentially with 5 M aqueous NaOH (8 mL), brine, dried over $MgSO_4$, filtered, and concentrated under vacuum. The crude residue was purified by flash column chromatography (6% EtOAc in hexanes) to afford **2.32** (132 mg, 93% purity, 48%), contaminated with Et_2O (after Et_2O transfer). Spectral data of **1.32** matched those previously reported.[15]

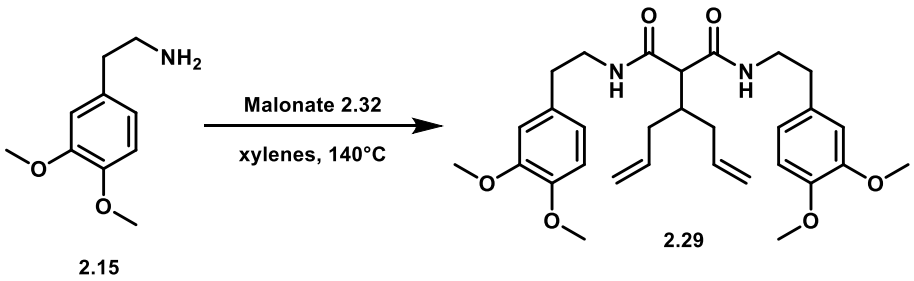

N^1,N^3-bis(3,4-dimethoxyphenethyl)-2-(hepta-1,6-dien-4-yl)malonamide 2.29. To a microwave vial was added amine **2.15** (186 mg, 0.173 mL, 1.02 mmol), malonate **2.32** (140 mg, 93% purity, 0.512 mmol), and toluene (0.43 mL). The vial was irradiated with microwave radiation at 160 °C for 1 h periods until no malonate was observed, which typically required 3 cycles at this scale. The mixture was concentrated under vacuum, and the crude residue was purified by flash column chromatography (10% acetone in DCM) to afford **2.29** (174 mg, 64.5%) as a yellow powder. ^{1}H NMR (600 MHz, $CDCl_3$) δ 6.92 (t, J = 5.8 Hz, 2H), 6.76 (d, J = 7.9 Hz, 2H), 6.70 (d, J = 7.7 Hz, 4H), 5.65 (ddt, J = 17.1, 10.3, 7.1 Hz, 2H), 5.02 – 4.91 (m, 4H), 3.84 (s, 6H), 3.82 (s, 6H), 3.46 (ddt, J = 26.5, 13.5, 6.5 Hz, 4H), 2.85 (d, J = 9.2 Hz, 1H), 2.74 (t, J = 7.2 Hz, 4H), 2.14 – 2.01 (m, 3H), 1.95 (dt, J = 14.6, 7.4 Hz, 2H); ^{13}C NMR (151 MHz, $CDCl_3$) δ 170.05, 149.07, 147.77, 135.32, 131.10, 120.64, 117.54, 111.87, 111.40, 58.20, 55.92, 55.87, 40.89, 40.24, 35.17, 34.39. HRMS (ESI) *m / z* calcd for $C_{30}H_{40}N_2O_6Na$ $[M+Na]^+$ 547.2784, found 547.2774.

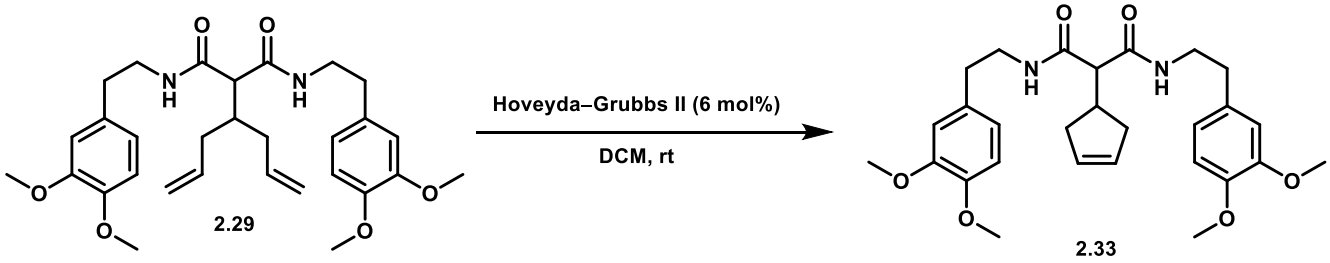

2-(cyclopent-3-en-1-yl)-N^1,N^3-bis(3,4-dimethoxyphenethyl)malonamide 2.33. To a 1-dram vial was added malonamide **2.29** (19.4 mg, 0.037 mmol), Hoveyda–Grubbs II catalyst (2 mg, 0.002 mmol), and DCM (7.4 mL). The solution turned tan, and light bubbling was observed. The reaction

was stirred for 10 min at rt. DMSO (0.016 mL, 50 equiv wrt catalyst) was then added and the reaction was stirred overnight. The reaction mixture was concentrated under vacuum and the crude residue was purified by flash column chromatography (12% acetone in DCM) to afford **2.33** (17 mg, 94%). ^{1}H NMR (500 MHz, $CDCl_3$) δ 6.85 (t, J = 5.8 Hz, 2H), 6.78 (d, J = 8.2 Hz, 2H), 6.71 (d, J = 6.8 Hz, 4H), 5.59 (s, 2H), 3.85 (s, 6H), 3.83 (s, 6H), 3.55-3.38 (m, 4H), 2.79 (d, J = 10.8 Hz, 1H), 2.76 – 2.63 (m, 5H), 2.31 (dd, J = 14.6, 8.2 Hz, 2H), 2.01 (dd, J = 14.8, 6.4 Hz, 2H); ^{13}C NMR (126 MHz, $CDCl_3$) δ 170.38, 149.06, 147.76, 131.19, 129.42, 120.69, 111.89, 111.38, 60.40, 55.96, 55.88, 40.99, 40.92, 36.49, 35.31. HRMS (ESI) *m / z* calcd for $C_{28}H_{36}N_2O_6Na$ $[M+Na]^+$ 519.2471, found 519.2470.

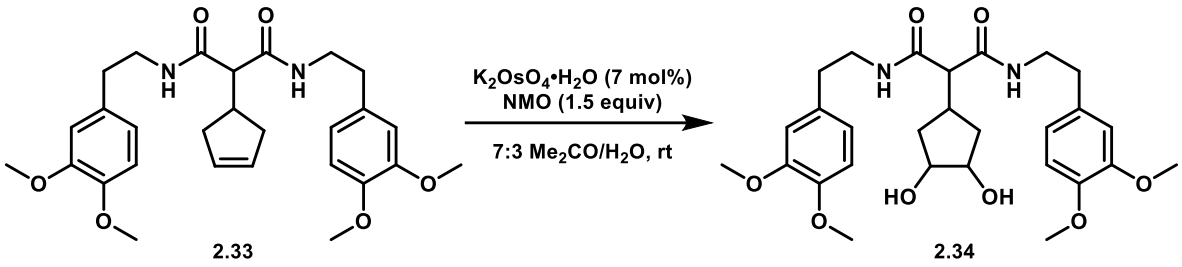

2.33 2.34

2-(3,4-dihydroxycyclopentyl)-*N*^{1},*N*^{3}-bis(3,4-dimethoxyphenethyl)malonamide 2.34. To a 1-dram vial was added malonamide **2.33** (46 mg, 0.092 mmol), NMO (16 mg, 0.14 mmol), 7:3 acetone/DI H_2O (1 mL), and lastly K_2OsO_4•$2H_2O$ (2.2 mg, 0.006 mmol). The solution was stirred at rt for 64.5 h. The reaction was quenched with saturated aqueous $Na_2S_2O_3$. The aqueous layer was extracted with EtOAc (2 x 3 mL). The combined organic extracts were filtered through a Na_2SO_4 filter and concentrated under vacuum. The crude residue was purified by flash column chromatography (1% NH_4OH, 9% MeOH, 90% DCM) to afford **2.34** (3 mg, 5%) as a white solid. ^{1}H NMR (400 MHz, $CDCl_3$) δ 6.86 – 6.66 (m, 2H), 6.75 – 6.67 (m, 2H), 6.54 (t, *J* = 4.9 Hz, 2H), 4.08 – 3.94 (m, 2H), 3.87 (s, 6H), 3.85 (s, 6H), 3.57 – 3.39 (m, 4H), 2.74 (ap t, J = 7.2 Hz, 5H), 2.56 (d, J = 10.4 Hz, 1H), 2.44 – 2.19 (br s, 2H), 1.76 – 1.40 (m, 4H). HRMS (ESI) *m / z* calcd for $C_{28}H_{38}N_2O_8Na$ $[M+Na]^+$ 553.2526, found 553.2506.

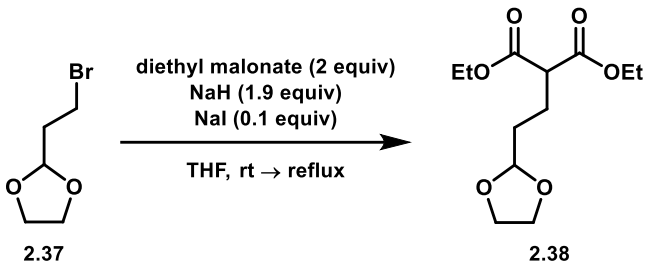

2.37 2.38

diethyl 2-(2-(1,3-dioxolan-2-yl)ethyl)malonate 2.38. To a 25 mL three-necked round-bottomed flask equipped with a condenser was added diethyl malonate (0.96 g, 0.92 mL, 6.0 mmol) and dry THF (10 mL). NaH (140 mg, 5.7 mmol, 60% dispersion in mineral oil) was added portion-wise at rt. Very vigorous bubbling was observed, and after 5 min the solution was clear. The malonate enolate solution was stirred for 5 min, after which the flask was placed in a pre-heated 90 °C oil bath. Dioxolane **2.37** was added dropwise as the enolate solution was heating up. A white precipitate was formed upon addition of the dioxolane. The reaction mixture was allowed to reflux for 16 h. The reaction mixture was then cooled to rt, and the reaction was quenched by the addition of saturated aqueous NH_4Cl. The aqueous layer was extracted with EtOAc (3 x 20 mL). The combined organic extracts were washed with brine, dried over Na_2SO_4, filtered, and concentrated under vacuum. The crude residue was purified by flash column chromatography (10% EtOAc in hexanes) to afford **2.38** (414 mg, 53%). Spectral data of **2.38** matched those previously reported.[23]

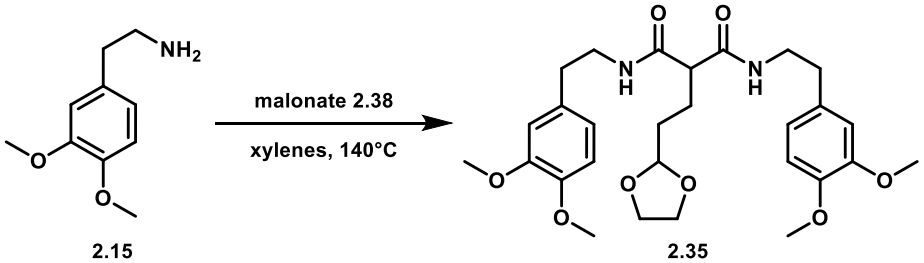

2.15 2.35

2-(2-(1,3-dioxolan-2-yl)ethyl)-*N*^{1},N^3-bis(3,4-dimethoxyphenethyl)malonamide 2.35. To a 1-dram vial was added amine **2.15** (324 mg, 0.30 mL, 1.79 mmol), malonate **2.38** (200 mg, 93% purity, 0.715 mmol), and *m*-xylene (0.72 mL). The vial was sealed with Teflon tape and the reaction

mixture was placed in a pre-heated oil bath set to 160 °C. The reaction mixture was heated to reflux for 30 min. The reaction mixture was cooled down to rt, at which point the mixture solidified. The reaction mixture was diluted with *m*-xylene and filtered with a Hirsch funnel. The solid on the funnel was washed with *m*-xylene (3 x 1 mL) and was dried on the filter to afford **2.35** (205 mg, 54%) as a light yellow powder. ^{1}H NMR (400 MHz, $CDCl_3$) δ 6.89 (t, J = 5.8 Hz, 2H), 6.78 (d, J = 8.6 Hz, 2H), 6.74 – 6.69 (m, 4H), 4.78 (t, J = 4.4 Hz, 1H), 3.86 (s, 6H), 3.83 (s, 6H), 3.80 – 3.75 (m, 2H), 3.55 – 3.35 (m, 2H), 2.99 (t, J = 7.7 Hz, 1H), 2.73 (t, J = 7.1 Hz, 4H), 1.90 (q, J = 7.6 Hz, 2H), 1.61 (td, J = 7.5, 4.4 Hz, 2H); ^{13}C NMR (101 MHz, $CDCl_3$) δ 170.87, 149.25, 147.94, 131.40, 120.85, 112.15, 111.63, 104.15, 65.03, 56.12, 56.06, 54.31, 41.06, 35.43, 31.13, 27.29. HRMS (ESI) *m / z* calcd for $C_{28}H_{38}N_2O_8Na$ $[M+Na]^+$ 553.2526, found 553.2524.

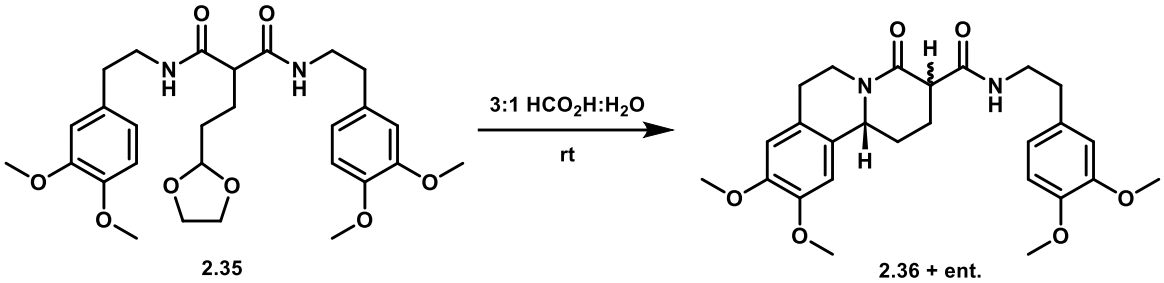

2.35 2.36 + ent.

(11β*R*)-*N*-(3,4-dimethoxyphenethyl)-9,10-dimethoxy-4-oxo-1,3,4,6,7,11β-hexahydro-2*H*-pyrido[2,1-*α*]isoquinoline-3-carboxamide 2.36. To a 1-dram vial was added dioxolane **2.35** (10 mg, 0.019 mmol), formic acid (0.28 mL), and DI H_2O (0.10 mL). The reaction was stirred for 52 h at rt. The reaction was diluted with DI H_2O (0.40 mL), and the reaction was quenched with 3.75 M aqueous NaOH. Vigorous heat evolution was observed. The mixture was stirred for 30 min, after which it turned into a white suspension. The aqueous solution was extracted with EtOAc (2 x 3 mL), filtered through a Na_2SO_4 plug, and concentrated under vacuum. The crude residue was purified by flash column chromatography (10% acetone in DCM to 20% acetone in DCM gradient) to afford **2.36** (6 mg, 70%) as a colorless oil. Note: The crude reaction mixture showed a 1:1 d.r., while the purified product showed a 3:1 d.r. Diagnostic peaks used were 4.80 – 4.73 (m, 1H, **minor**

diast.), 4.70 (dt, J = 12.8, 4.5 Hz, 1H, **major diast.**), 4.62 (d, J = 5.5 Hz, 1H, **minor diast.**), 4.58 (dd, J = 11.4, 4.7 Hz, 1H **major diast.**). **Mixture of major diast. and minor diast. (3:1):** ^{1}H NMR (600 MHz, $CDCl_3$) δ 7.96 (s, 1H, **minor diast.**), 7.55 (s, 1H, **major diast.**), 6.83 – 6.60 (m, 10H), 4.80 – 4.73 (m, 1H, **minor diast.**), 4.70 (dt, J = 12.8, 4.5 Hz, 1H, **major diast.**), 4.62 (d, J = 5.5 Hz, 1H, **minor diast.**), 4.58 (dd, J = 11.4, 4.7 Hz, 1H **major diast.**), 3.94 – 3.74 (m, 24H), 3.57 – 0.78 (m, 40H); ^{13}C NMR (151 MHz, $CDCl_3$) δ 168.24, 167.23, 148.94, 148.00, 147.91, 147.56, 131.57, 128.75, 126.75, 120.69, 120.59, 112.08, 111.92, 111.50, 111.34, 111.22, 108.10, 56.92, 56.88, 56.17, 56.13, 55.98, 55.95, 55.89, 55.82, 47.18, 46.68, 41.30, 41.27, 40.65, 35.40, 30.98, 29.62, 28.39, 27.97, 22.09, 20.53. HRMS (ESI) *m / z* calcd for $C_{26}H_{32}N_2O_6Na$ $[M+Na]^+$ 491.2158, found 491.2153.

2.7 References

1. Wiegrebe, W.; Kramer, W. J.; Shamma, M. The Emetine Alkaloids. *J. Nat. Prod.* **1984**, *47*, 397.

2. Kumar, R.; Afsar, M.; Khandelwal, N.; Chander, Y.; Riyesh, T.; Dedar, R.; Gulati, B. R.; Pal, Y.; Barua, S.; Tripathi, B. N.; Hussain, T.; Kumar, N. Emetine Suppresses SARS-CoV-2 Replication by Inhibiting Interaction of Viral mRNA with eIF4E. *Antiviral Res.* **2021**, *189*, 105056.

3. Siddique, M. A.; Satoh, K.; Kurosawa, R.; Kikuchi, N.; Elias-Al-Mamun, Md.; Omura, J.; Satoh, T.; Nogi, N.; Sunamura, S.; Miyata, S.; Ueda, H.; Tokuyama, H.; Shimokawa, H. Identification of Emetine as a Therapeutic Agent for Pulmonary Arterial Hypertension: Novel Effects of an Old Drug. *Arterioscler. Thromb. Vasc. Biol.* **2019**, *39*, 2367.

4. Cheong, B.E.; Takemura, T.; Yoshimatsu, K.; Sato, F. Molecular Cloning of an O-Methyltransferase from Adventitious Roots of *Carapichea ipecacuanha*. *Biosci., Biotechnol., Biochem.* **2011**, *1*, 107.

5. Tietze, L. F.; Rackelmann, N.; Sekar, G. Catalyst-Controlled Stereoselective Combinatorial Synthesis. *Angew. Chem., Int. Ed.* **2003**, *42*, 4254.

6. Itoh, T.; Miyazaki, M.; Fukuoka, H.; Nagata, K.; Ohsawa, A. Formal Total Synthesis of (−)-Emetine Using Catalytic Asymmetric Allylation of Cyclic Imines as a Key Step. *Org. Lett.* **2006**, *8*, 1295.

7. Lin, S.; Deiana, L.; Tseggai, A.; Córdova, A. Concise Total Synthesis of Dihydrocorynanthenol, Protoemetinol, Protoemetine, 3-*epi*-Protoemetinol and Emetine. *Eur. J. Org. Chem.* **2011**, *2012*, 398.

8. Zhang, W.; Bah, J.; Wohlfarth, A.; Franzén, J. A Stereodivergent Strategy for the Preparation of Corynantheine and Ipecac Alkaloids, Their Epimers, and Analogues: Efficient Total Synthesis of (−)-Dihydrocorynantheol, (−)-Corynantheol, (−)-Protoemetinol, (−)-Corynantheal, (−)-Protoemetine, and Related Natural and Nonnatural Compounds. *Chem. – Eur. J*. **2011**, *17*, 13814.

9. Yamada, M.; Azuma, K.; Takizawa, I.; Ejima, Y.; Yamano, M.; Satoh, K.; Doi, T.; Ueda, H.; Tokuyama, H. Efficient and Scalable Asymmetric Total Synthesis of (−)-Emetine with Pharmaceutical Grade Quality; First Multigram Scale Synthesis. *Org. Process Res. Dev.* **2023**, *27*, 343.

10. Yasumitsu, T.; Kunihiro, S.; Mitsuhiko, M.; Takehiko, M. Studies on Ring-Opening of Heterocyclic Compounds. V. The Reaction of N-(2,4-dinitrophenyl)pyridinium Chloride with Active Methylene Compounds. *Yakugaku Zasshi.* **1972**, *92*, 371.

11. Saidov, A. S.; Turgunov, K. K.; Levkovich, M. G.; Vinogradova, V. I. Synthesis of *bis*-Tetrahydroisoquinolines Based on Homoveratrylamine and Several Dibasic Acids. 4. Reaction with Malonic and Succinic Acids. *Chem. Nat. Compd.* **2015**, *51*, 316.

12. Yao, Q.-J.; Judeh, Z. M.-A. 1,1′ -Methylene-bis(1,1′ ,2,2′ ,3,3′ ,4,4′ -octahydroisoquinoline): Synthesis, Reaction, Resolution, and Application in Catalytic Enantioselective Transformations. *Tetrahedron*. **2011**, *67*, 4086.

13. Takai, K.; Fujimura, O.; Kataoka, Y.; Utimoto, K. Preparation of Alkenyl Sulfides and Enamines by Alkylidenation of Carboxylic Acid Derivatives. *Tet. Lett.* **1989**, *30*, 211.

14. Pine, S. H.; Pettit, R. J.; Geib, G. D.; Cruz, S. G.; Gallego, C. H.; Tijerina, T.; Pine, R. D. Carbonyl Methylenation Using a Titanium-Aluminum (Tebbe) Complex. *J. Org. Chem.* **1985**, *50*, 1212.

15. Parks, B. W.; Gilbertson, R. D.; Domaille, D. W.; Hutchinson, J. E. Convenient Synthesis of 6,6-Bicyclic Malonamides: A New Class of Conformationally Preorganized Ligands for f-Block Ion Binding. *J. Org. Chem.* **2006**, *71*, 9622.

16. VanRheenen, V.; Cha, D. Y.; Hartley, W. M. Catalytic Osmium Tetroxide Oxidation of Olefins: *cis*-1,2-cyclohexanediol. *Org. Synth.* **1978**, *58*, 43.

17. Trost, B. M.; Dong, G.; Vance, J. A. A Diosphenol-Based Strategy for the Total Synthesis of (−)-Terpestacin. *J. Am. Chem. Soc.* **2007**, *129*, 4540.

18. Tamelen, E.; Shamma, M.; Burgstahler, A.; Wolinsky, J.; Tamm, R.; Aldrich, P. The Total Synthesis of Yohimbine. *J. Am. Chem. Soc.* **1958**, *80*, 5006.

19. Crossley, S. W. M.; Obradors, C.; Martinez, R. M.; Shenvi, R. A. Mn-, Fe-, and Co-Catalyzed Radical Hydrofunctionalizations of Olefins. *Chem. Rev.* **2016**, *116*, 8912.

20. Comins, D. L.; Brown, J. D. Regioselective Addition of Titanium Enolates to 1-acylpyridinium Salts. A Convenient Synthesis of 4-(2-oxoalkyl)pyridines. *Tet. Lett.* **1984**, *25*, 3297.

21. Kinya, A.; Kobayashi, T.; Yamamoto, Y. Addition of Trimethylsilyl Enol Ethers to Quinolinium Salts: A Facile Synthesis of Methyl 2-(2-Oxoalkyl)-1,2-dihydroquinoline-1-carboxylates and Their Cyclization. *Heterocycles* **1984**, *22*, 1519.

22. Asskar, G.; Rivard, M.; Martens, T. Glutaconaldehyde as an Alternative Reagent to the Zincke Salt for the Transformation of Primary Amines into Pyridinium Salts. *J. Org. Chem.* **2020**, *85*, 1232.

23. Tian, M.-Q.; Shen, Z.-Y.; Zhao, X.; Walsh, P. J.; Hu, X.-H. Iron-Catalyzed Tertiary Alkylation of Terminal Alkynes with 1,3-Diesters via a Functionalized Alkyl Radical. *Angew. Chem. Int. Ed.* **2021**, *60*, 9706.

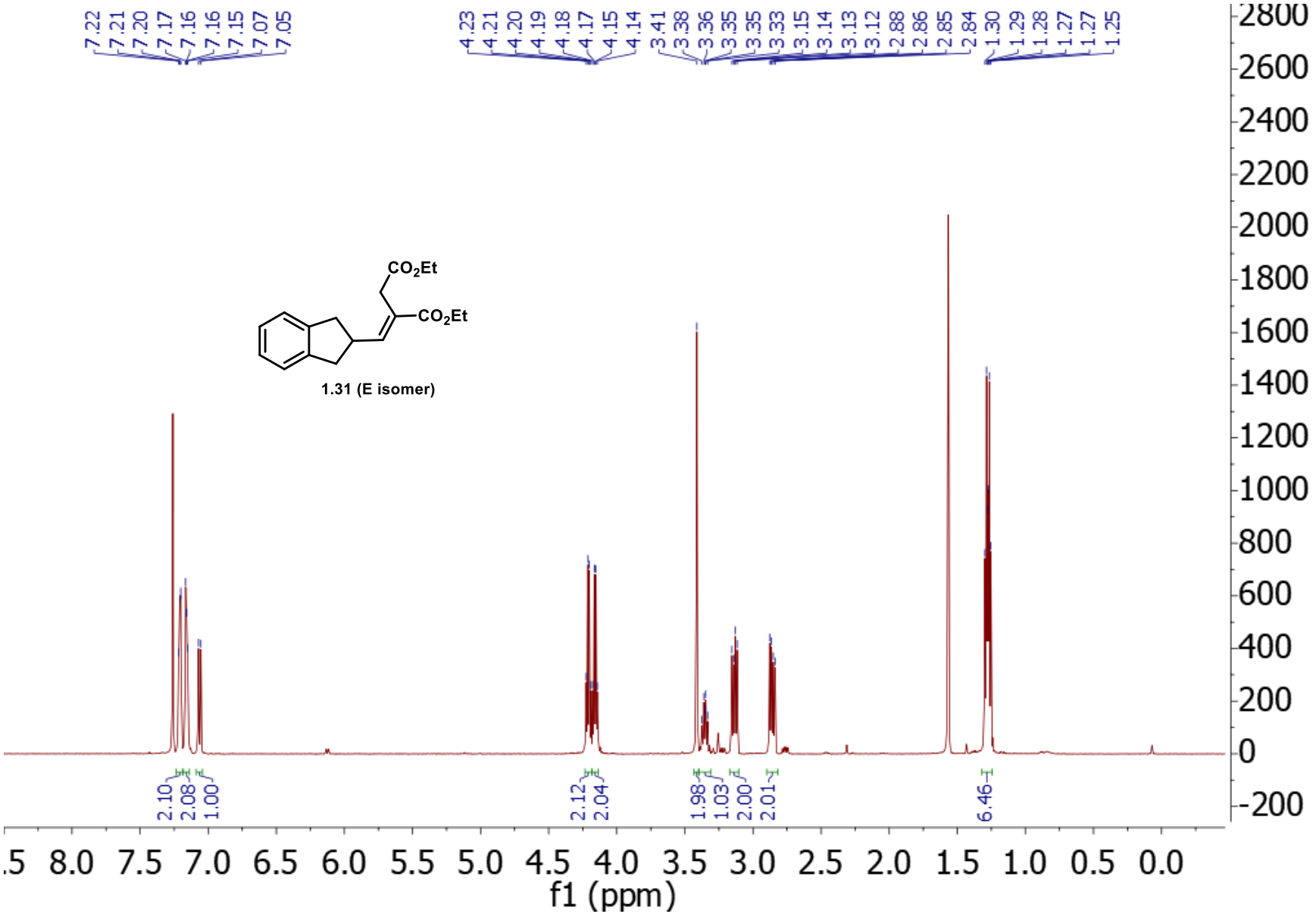
7.22
7.21
7.20
7.17
7.16
7.16
7.15
7.07
7.05
4.23
4.21
4.20
4.19
4.18
4.17
4.15
4.14
3.41
3.38
3.36
3.35
3.35
3.33
3.15
3.14
3.13
3.12
2.88
2.86
2.85
2.84
1.30
1.29
1.28
1.27
1.27
1.25
CO2Et
CO2Et
1.31 (E isomer)
2.10
2.08
1.00
2.12
2.04
1.98
1.03
2.00
2.01
6.46
f1 (ppm)

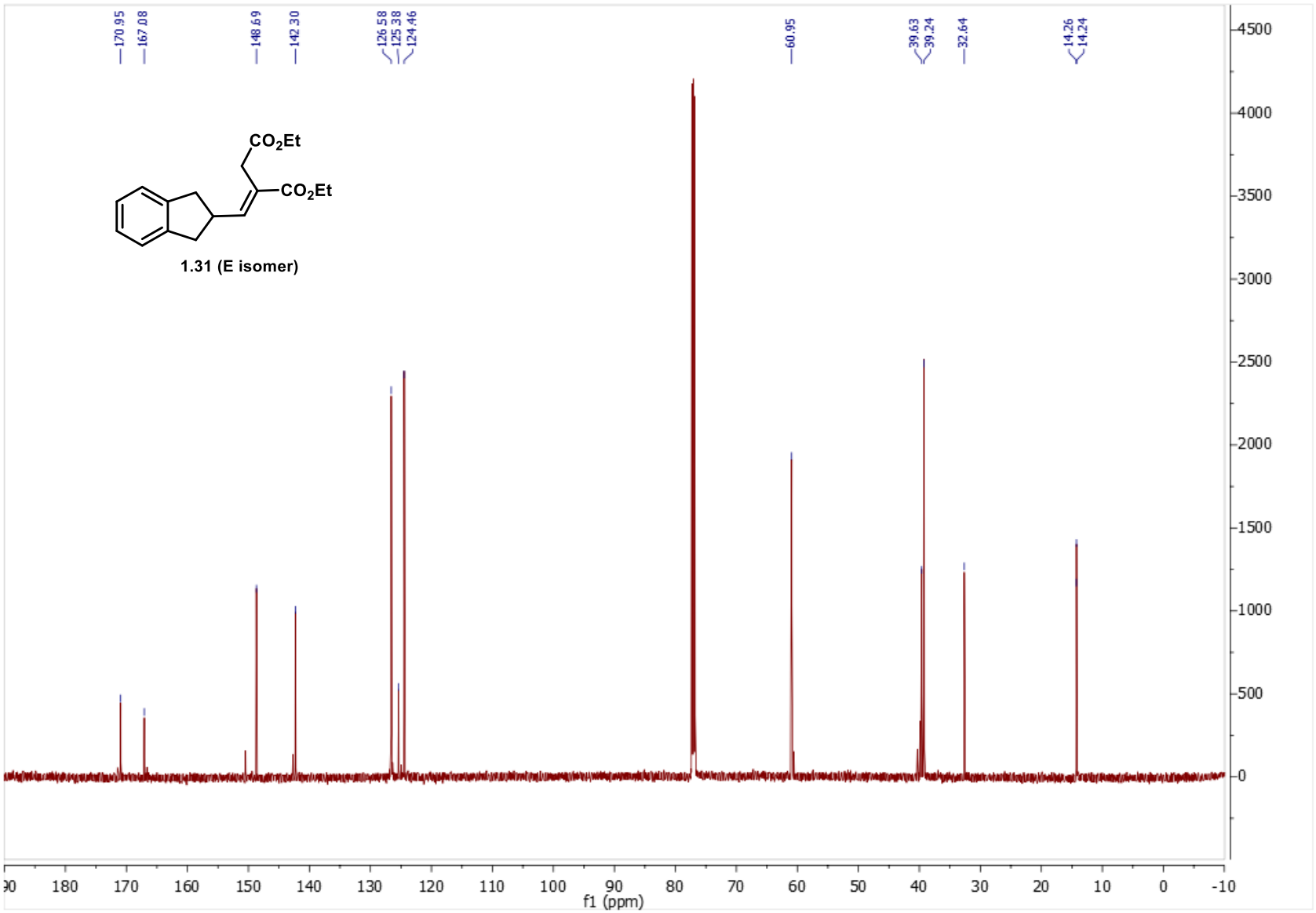
170.95
167.08
148.69
142.30
126.58
125.38
124.46
60.95
39.63
39.24
32.64
14.26
14.24
CO2Et
CO2Et
1.31 (E isomer)
f1 (ppm)

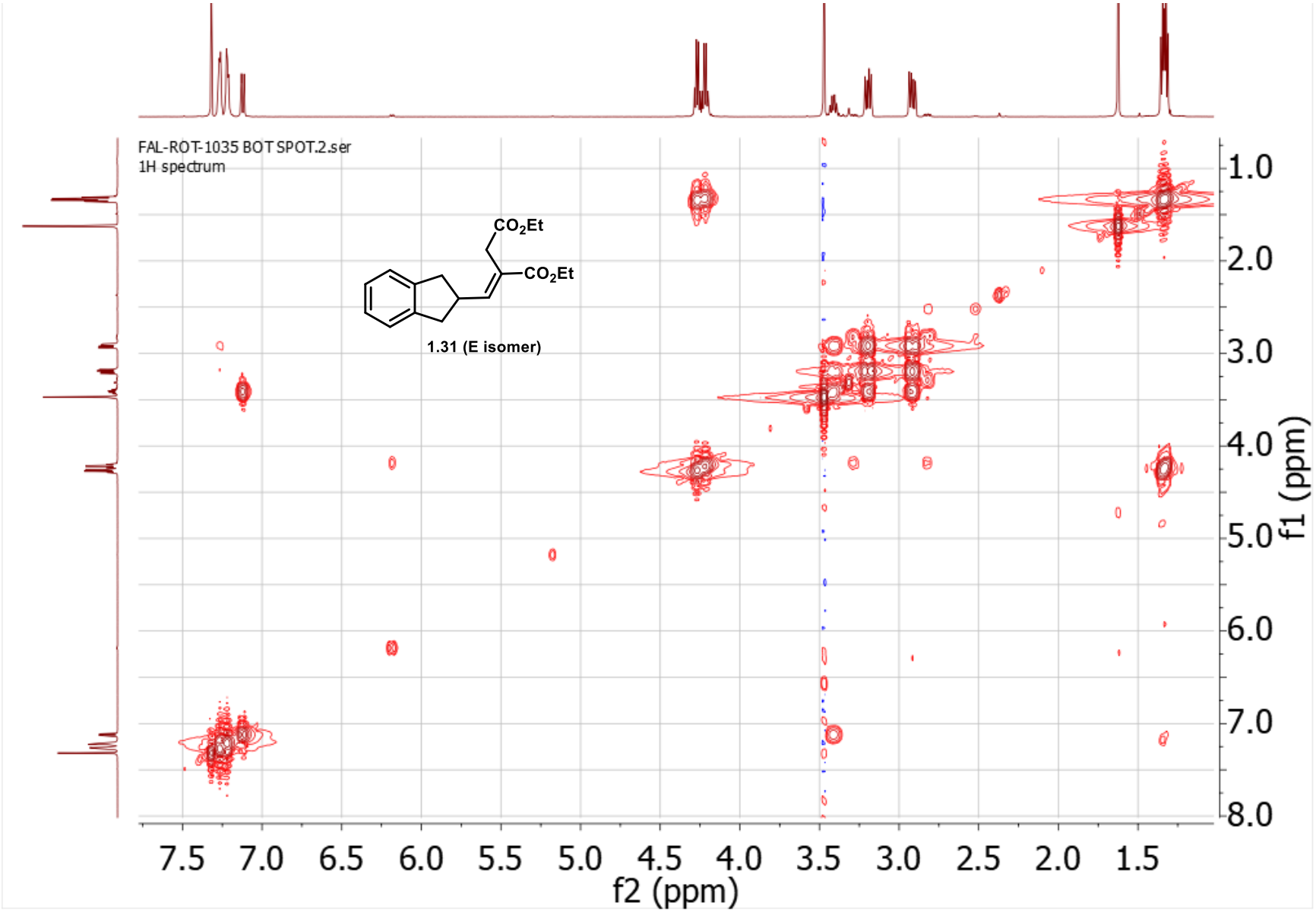
FAL-ROT-1035 BOT SPOT.2.ser
1H spectrum
CO2Et
CO2Et
1.31 (E isomer)
f2 (ppm)
f1 (ppm)

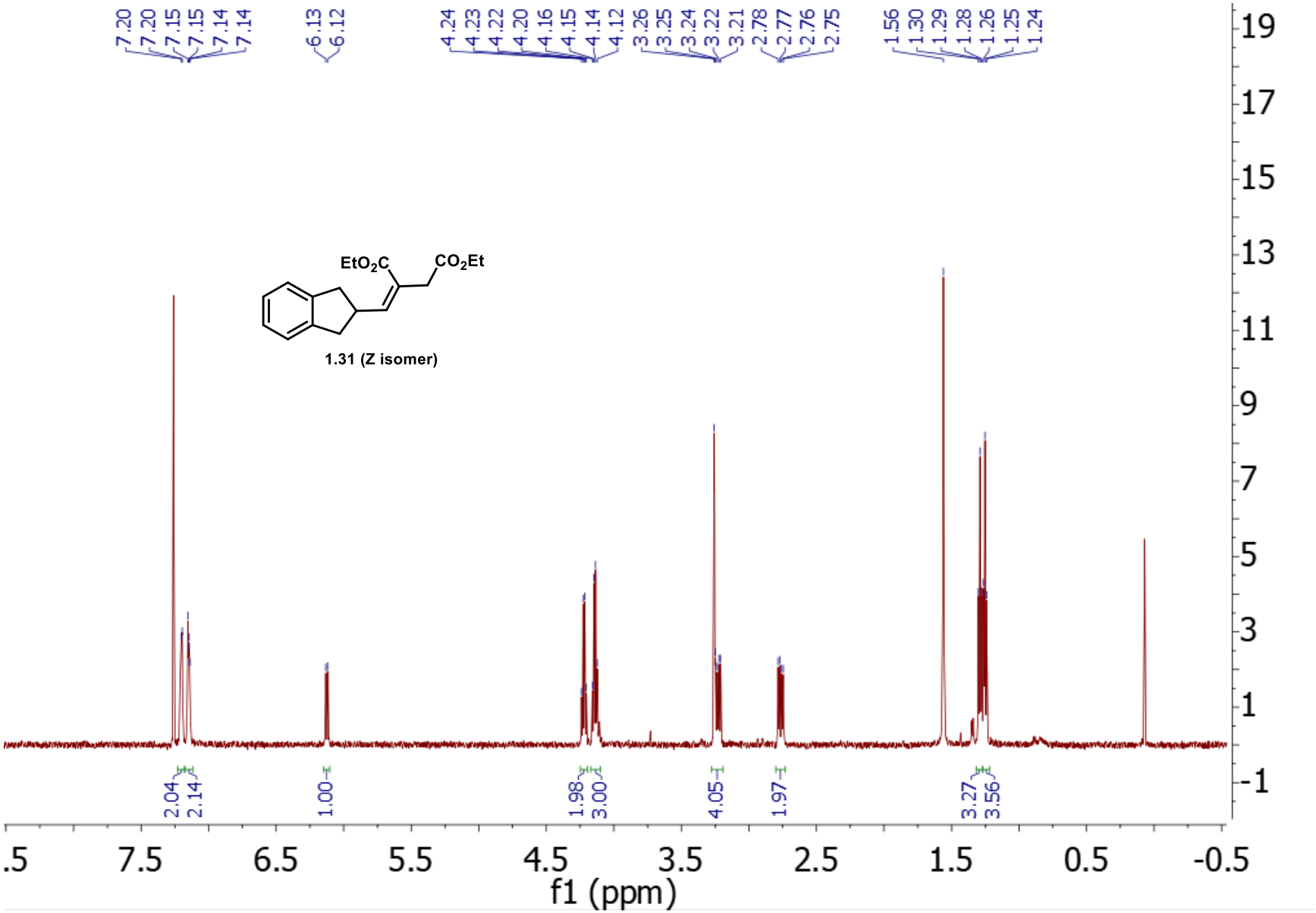
7.20
7.20
7.15
7.15
7.14
7.14
6.13
6.12
4.24
4.23
4.22
4.20
4.16
4.15
4.14
4.12
3.26
3.25
3.24
3.22
3.21
2.78
2.77
2.76
2.75
1.56
1.30
1.29
1.28
1.26
1.25
1.24
EtO2C
CO2Et
1.31 (Z isomer)
2.04
2.14
1.00
1.98
3.00
4.05
1.97
3.27
3.56
19
17
15
13
11
9
7
5
3
1
-1
.5
7.5
6.5
5.5
4.5
3.5
2.5
1.5
0.5
-0.5
f1 (ppm)

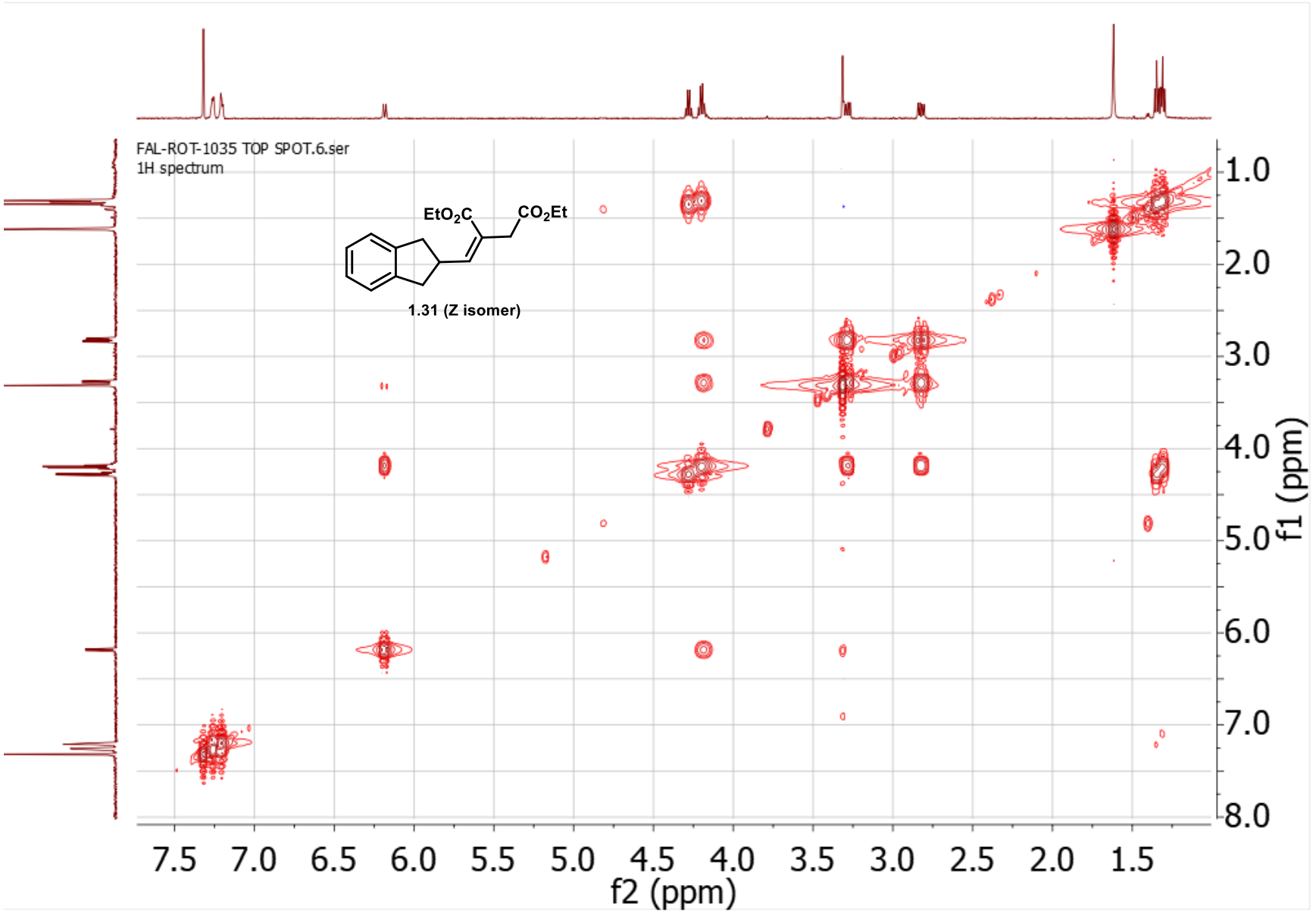
FAL-ROT-1035 TOP SPOT.6.ser
1H spectrum
EtO2C
CO2Et
1.31 (Z isomer)
7.5
7.0
6.5
6.0
5.5
5.0
4.5
4.0
3.5
3.0
2.5
2.0
1.5
f2 (ppm)
1.0
2.0
3.0
4.0
5.0
6.0
7.0
8.0
f1 (ppm)

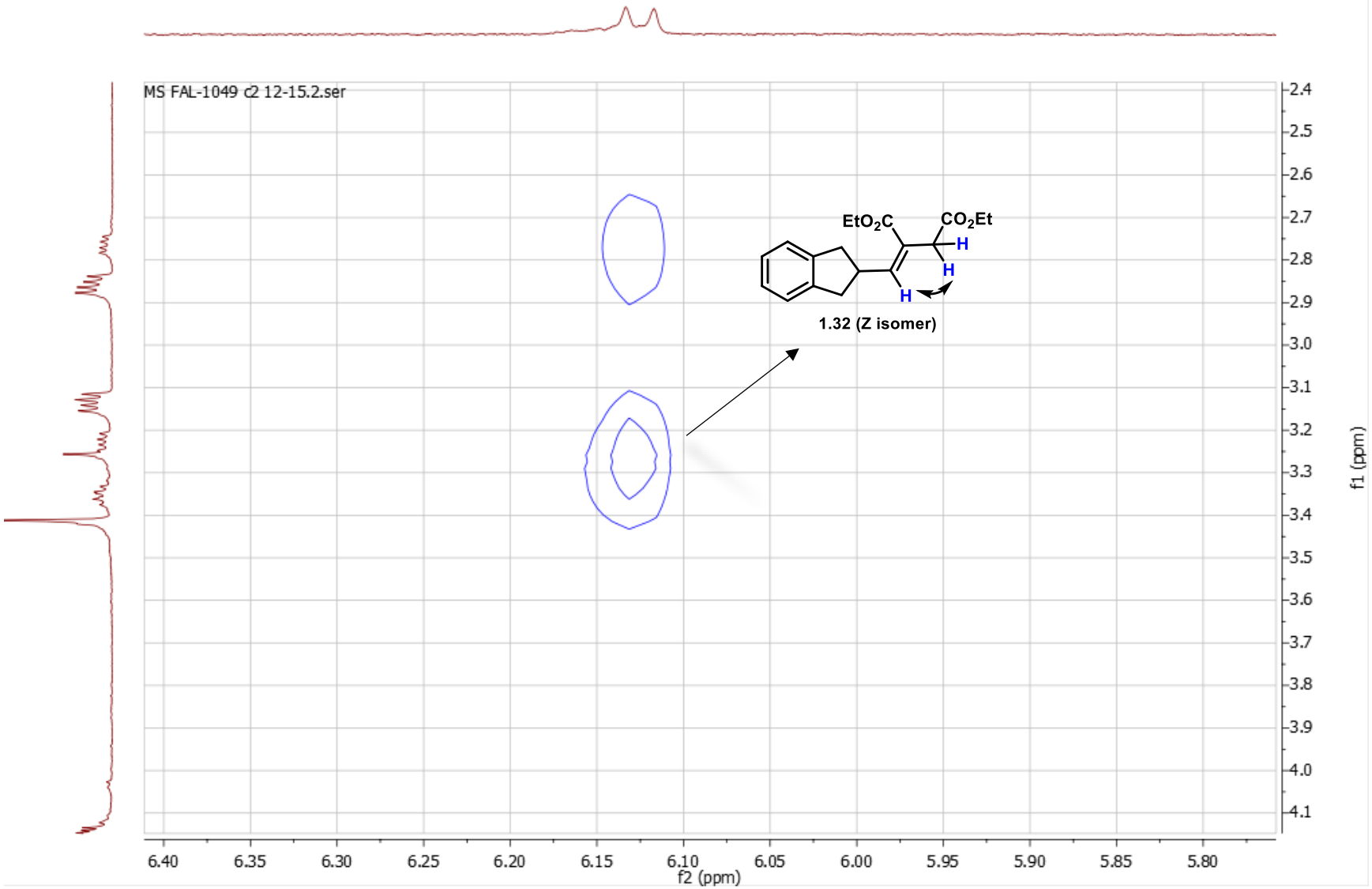
MS FAL-1049 c2 12-15.2.ser
EtO2C
CO2Et
H
H
H
1.32 (Z isomer)
f1 (ppm)
f2 (ppm)
6.40
6.35
6.30
6.25
6.20
6.15
6.10
6.05
6.00
5.95
5.90
5.85
5.80
2.4
2.5
2.6
2.7
2.8
2.9
3.0
3.1
3.2
3.3
3.4
3.5
3.6
3.7
3.8
3.9
4.0
4.1

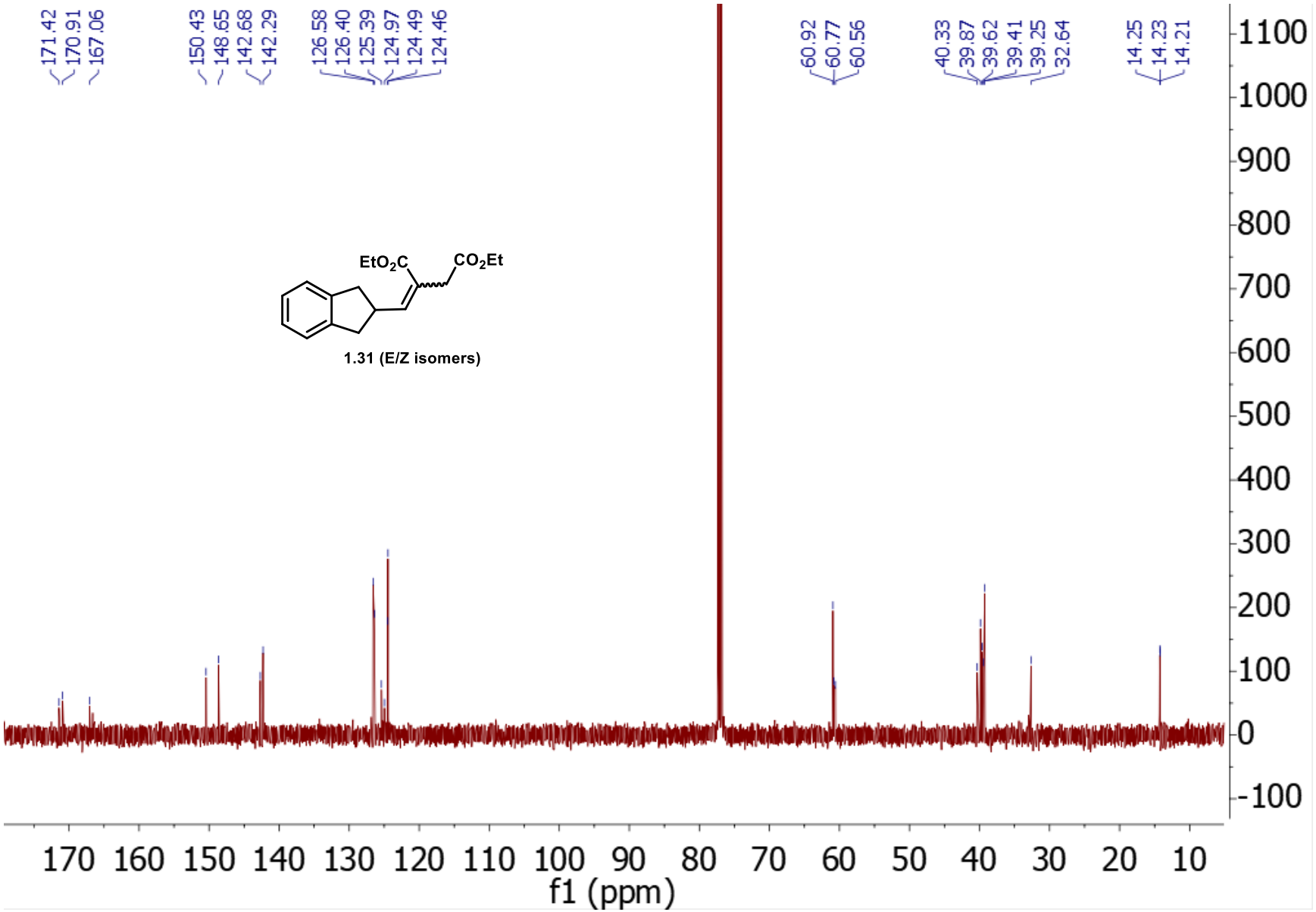
171.42
170.91
167.06
150.43
148.65
142.68
142.29
126.58
126.40
125.39
124.97
124.49
124.46
60.92
60.77
60.56
40.33
39.87
39.62
39.41
39.25
32.64
14.25
14.23
14.21
EtO2C
CO2Et
1.31 (E/Z isomers)
1100
1000
900
800
700
600
500
400
300
200
100
0
-100
170 160 150 140 130 120 110 100 90 80 70 60 50 40 30 20 10
f1 (ppm)

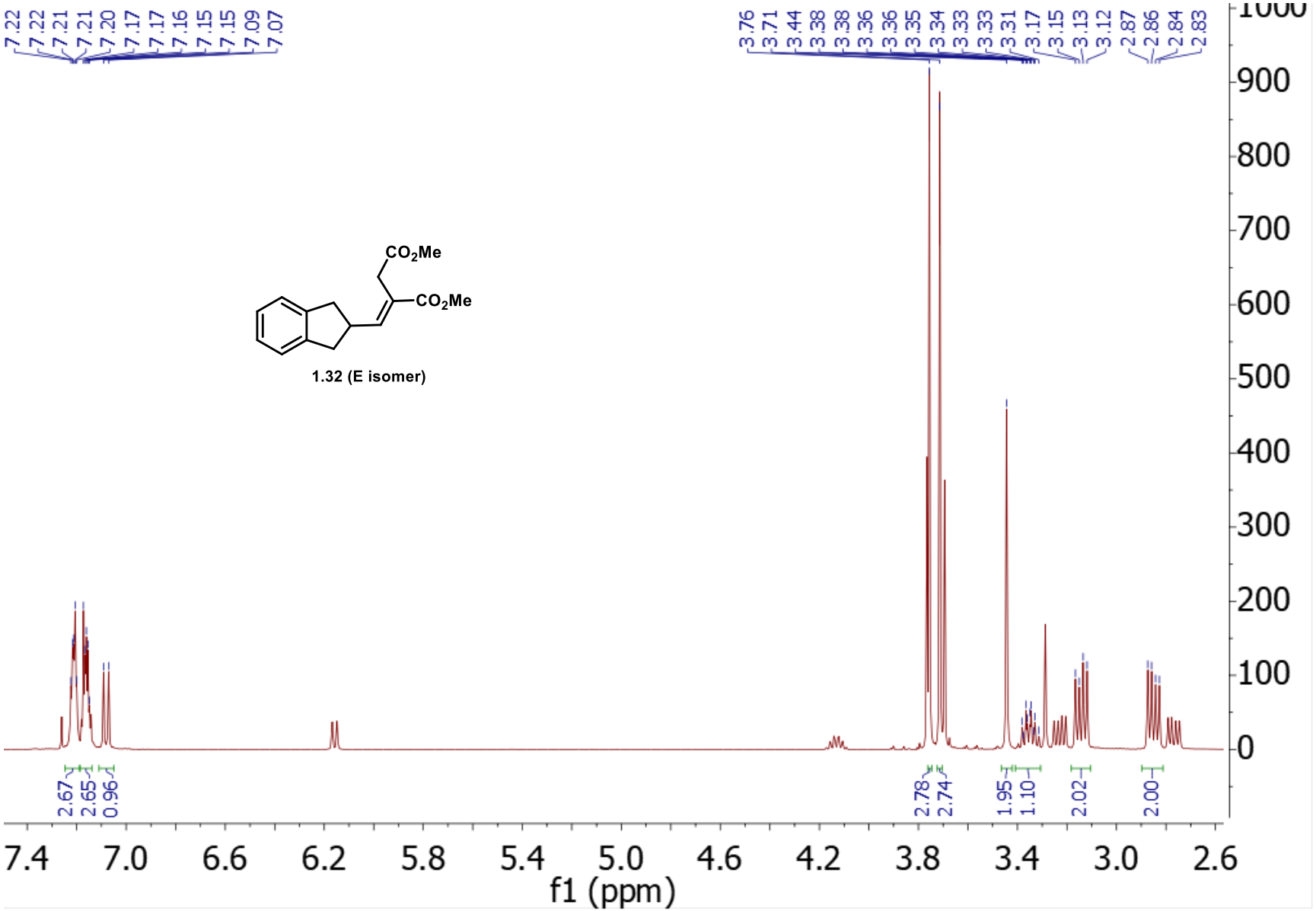
7.22
7.22
7.21
7.21
7.20
7.17
7.17
7.16
7.15
7.15
7.09
7.07
3.76
3.71
3.44
3.38
3.38
3.36
3.36
3.35
3.34
3.33
3.33
3.31
3.17
3.15
3.13
3.12
2.87
2.86
2.84
2.83
CO2Me
CO2Me
1.32 (E isomer)
2.67
2.65
0.96
2.78
2.74
1.95
1.10
2.02
2.00
f1 (ppm)

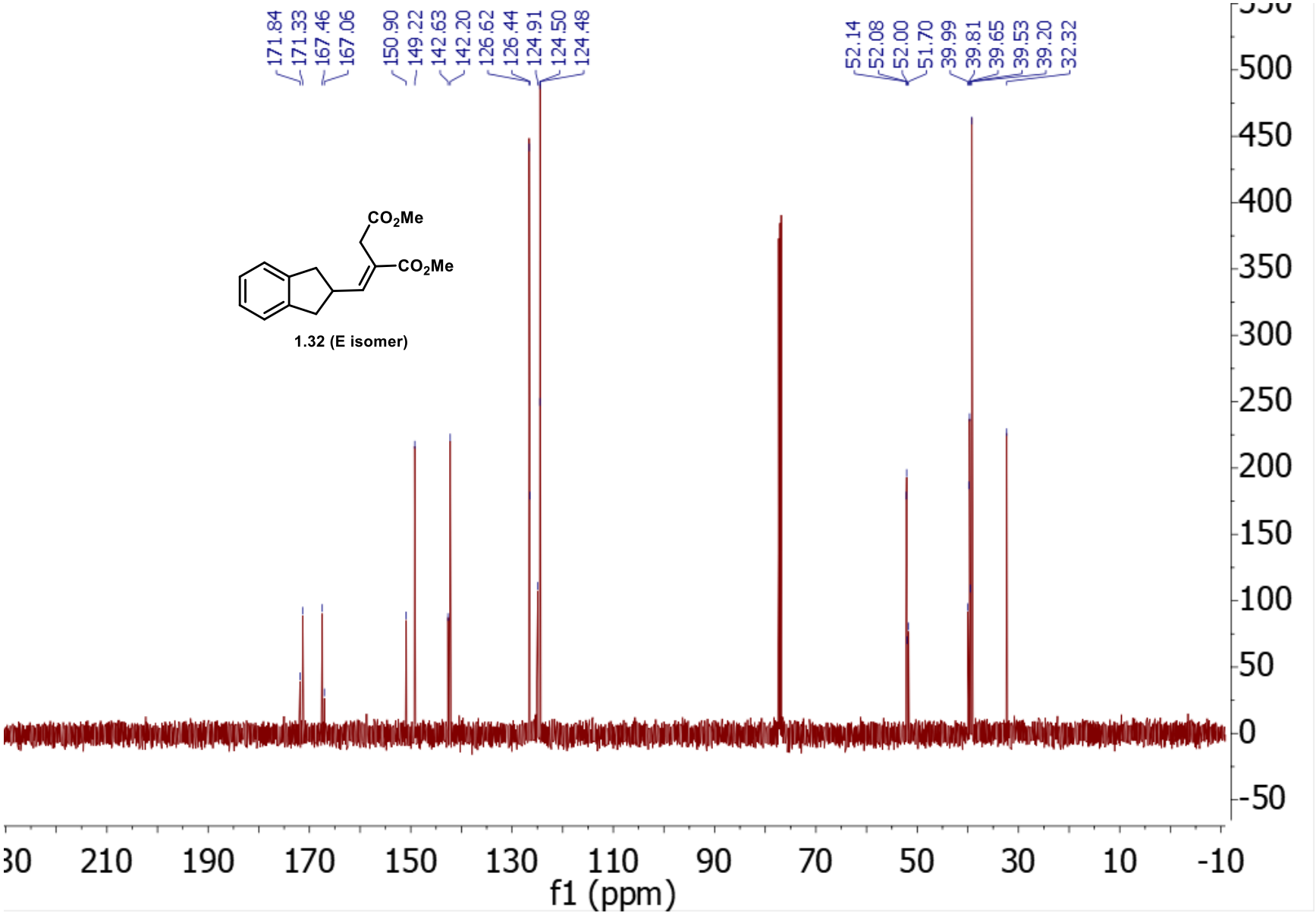
171.84
171.33
167.46
167.06
150.90
149.22
142.63
142.20
126.62
126.44
124.91
124.50
124.48
52.14
52.08
52.00
51.70
39.99
39.81
39.65
39.53
39.20
32.32
CO2Me
CO2Me
1.32 (E isomer)
500
450
400
350
300
250
200
150
100
50
0
-50
210
190
170
150
130
110
90
70
50
30
10
-10
f1 (ppm)

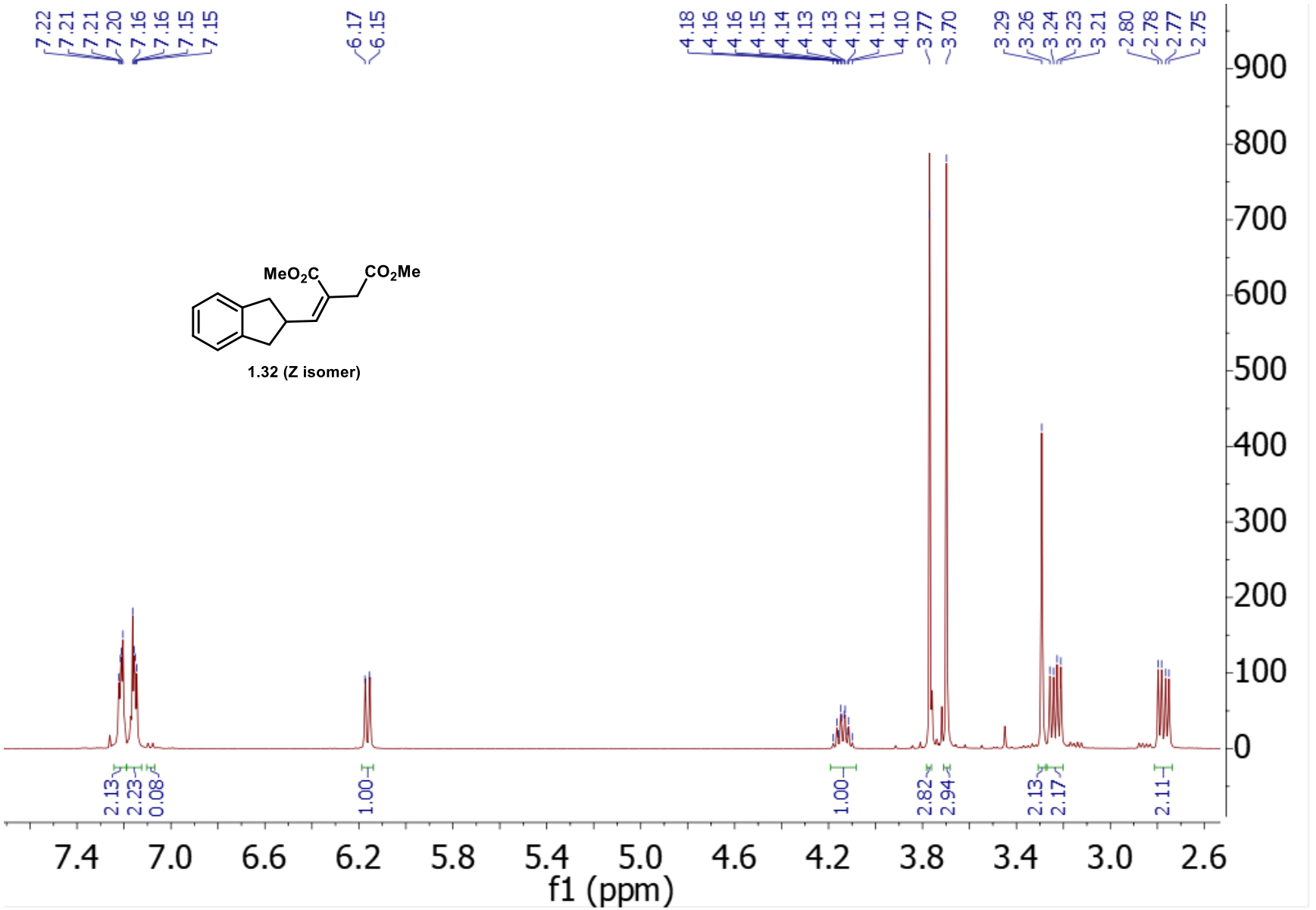
7.22
7.21
7.21
7.20
7.16
7.16
7.15
7.15
6.17
6.15
4.18
4.16
4.16
4.15
4.14
4.13
4.13
4.12
4.11
4.10
3.77
3.70
3.29
3.26
3.24
3.23
3.21
2.80
2.78
2.77
2.75
MeO2C
CO2Me
1.32 (Z isomer)
2.13
2.23
0.08
1.00
1.00
2.82
2.94
2.13
2.17
2.11
900
800
700
600
500
400
300
200
100
0
7.4
7.0
6.6
6.2
5.8
5.4
5.0
4.6
4.2
3.8
3.4
3.0
2.6
f1 (ppm)

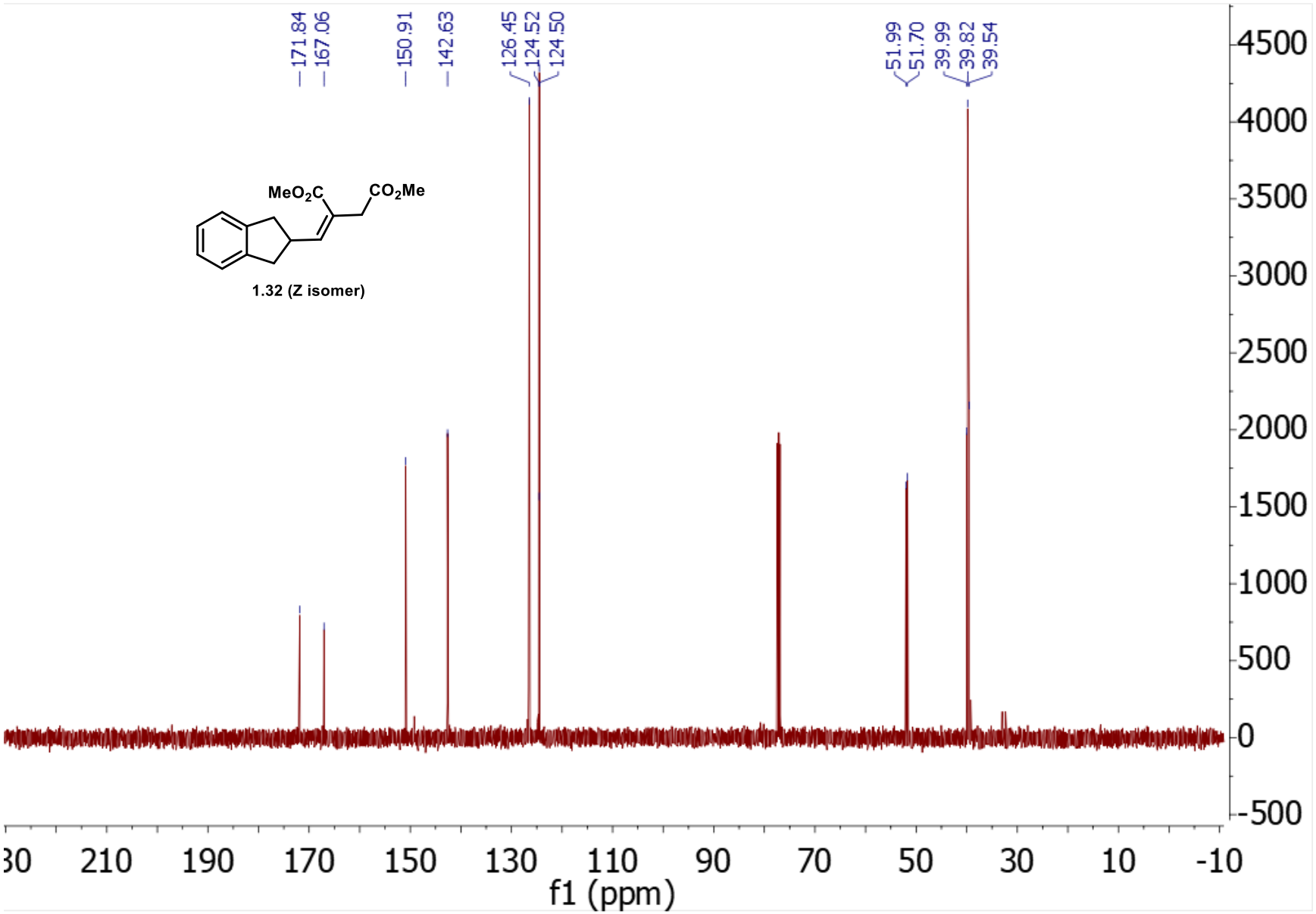
171.84
167.06
150.91
142.63
126.45
124.52
124.50
51.99
51.70
39.99
39.82
39.54
MeO2C
CO2Me
1.32 (Z isomer)
4500
4000
3500
3000
2500
2000
1500
1000
500
0
-500
210
190
170
150
130
110
90
70
50
30
10
-10
f1 (ppm)

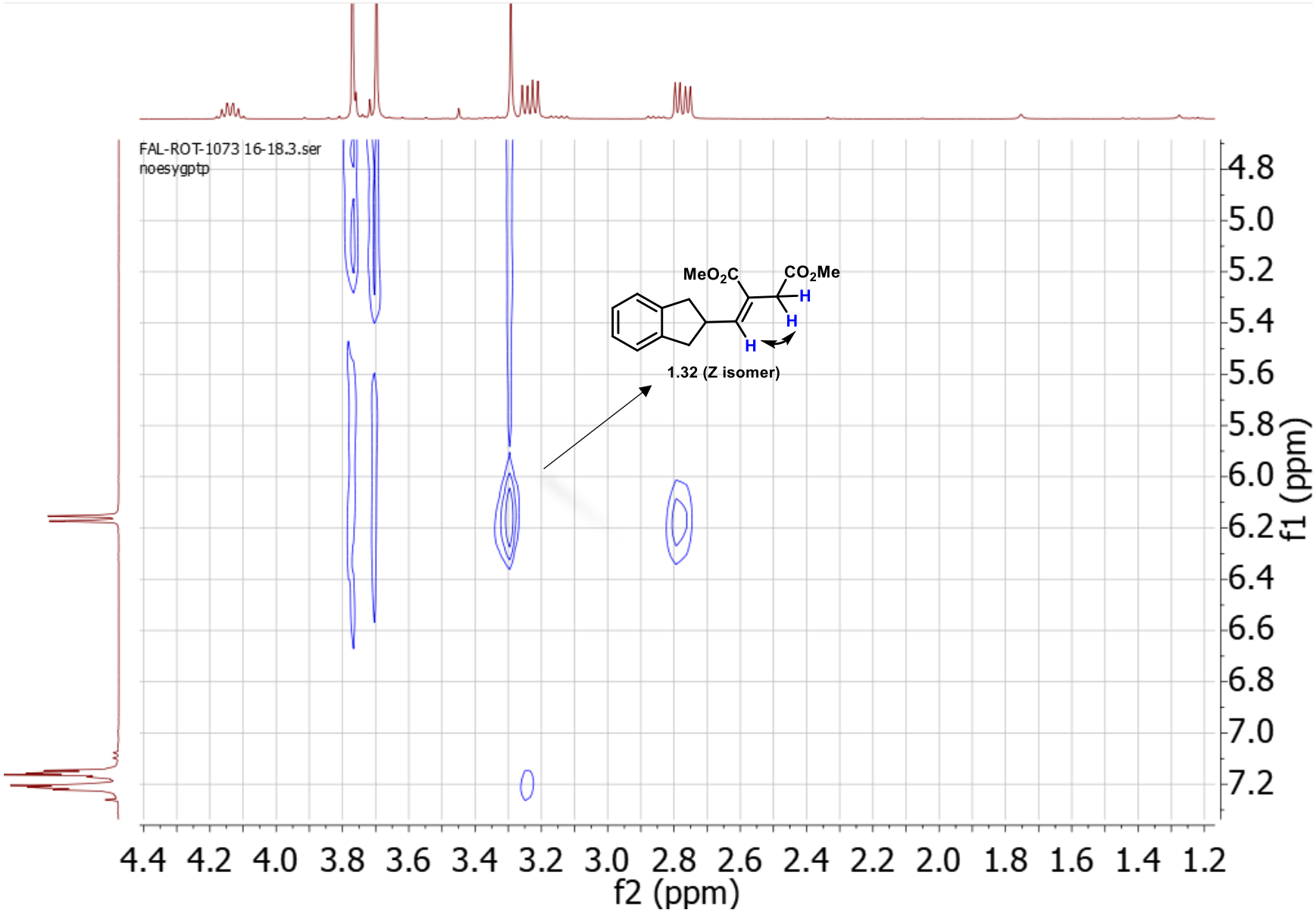
FAL-ROT-1073 16-18.3.ser
noesygptp
MeO2C
CO2Me
H
H
H
1.32 (Z isomer)
4.8
5.0
5.2
5.4
5.6
5.8
6.0
6.2
6.4
6.6
6.8
7.0
7.2
f1 (ppm)
4.4 4.2 4.0 3.8 3.6 3.4 3.2 3.0 2.8 2.6 2.4 2.2 2.0 1.8 1.6 1.4 1.2
f2 (ppm)

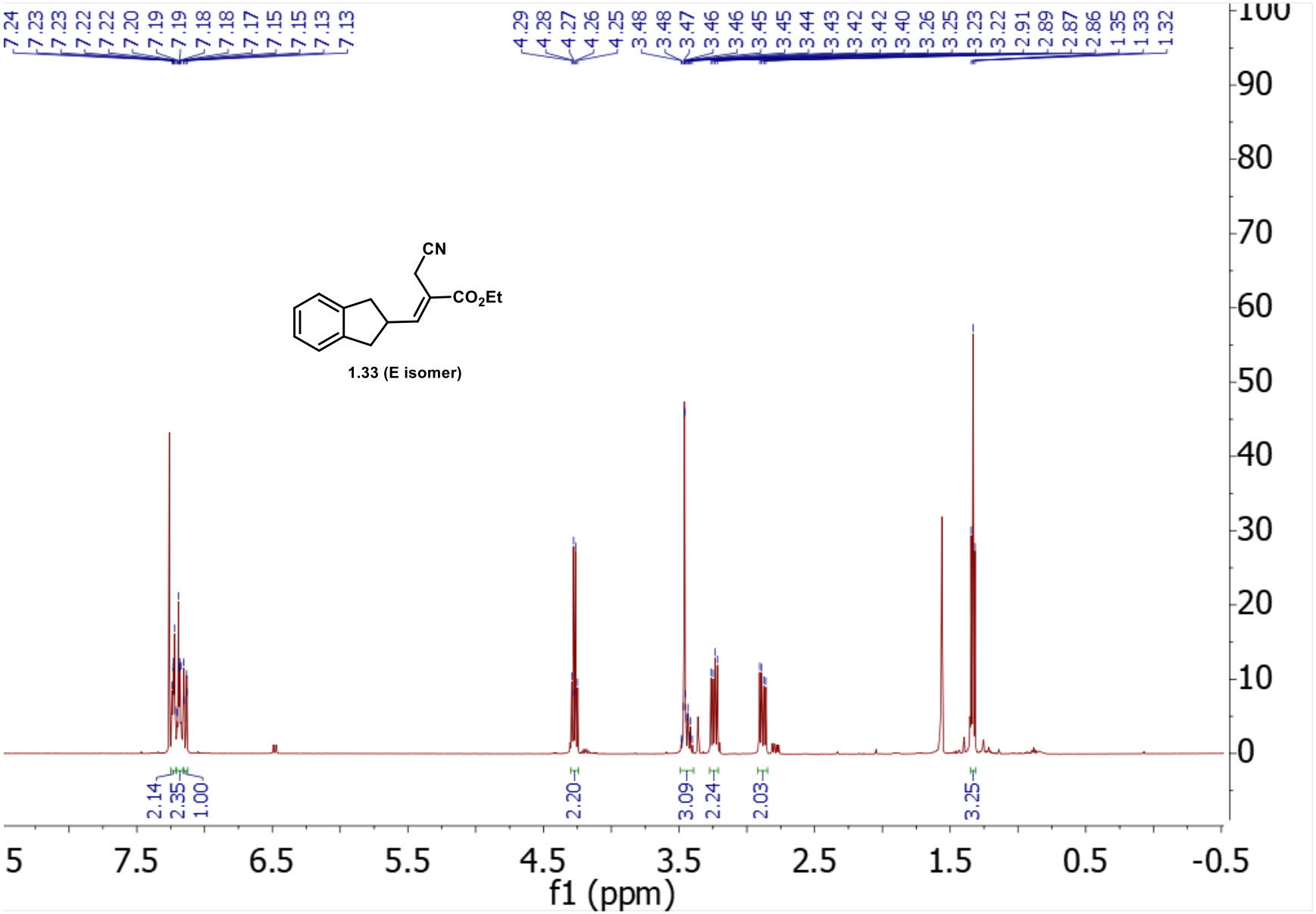
7.24
7.23
7.23
7.22
7.22
7.20
7.19
7.19
7.18
7.18
7.17
7.15
7.15
7.13
7.13
4.29
4.28
4.27
4.26
4.25
3.48
3.48
3.47
3.46
3.46
3.45
3.45
3.44
3.43
3.42
3.42
3.40
3.26
3.25
3.23
3.22
2.91
2.89
2.87
2.86
1.35
1.33
1.32
CN
CO2Et
1.33 (E isomer)
2.14
2.35
1.00
2.20
3.09
2.24
2.03
3.25
100
90
80
70
60
50
40
30
20
10
0
5
7.5
6.5
5.5
4.5
3.5
2.5
1.5
0.5
-0.5
f1 (ppm)

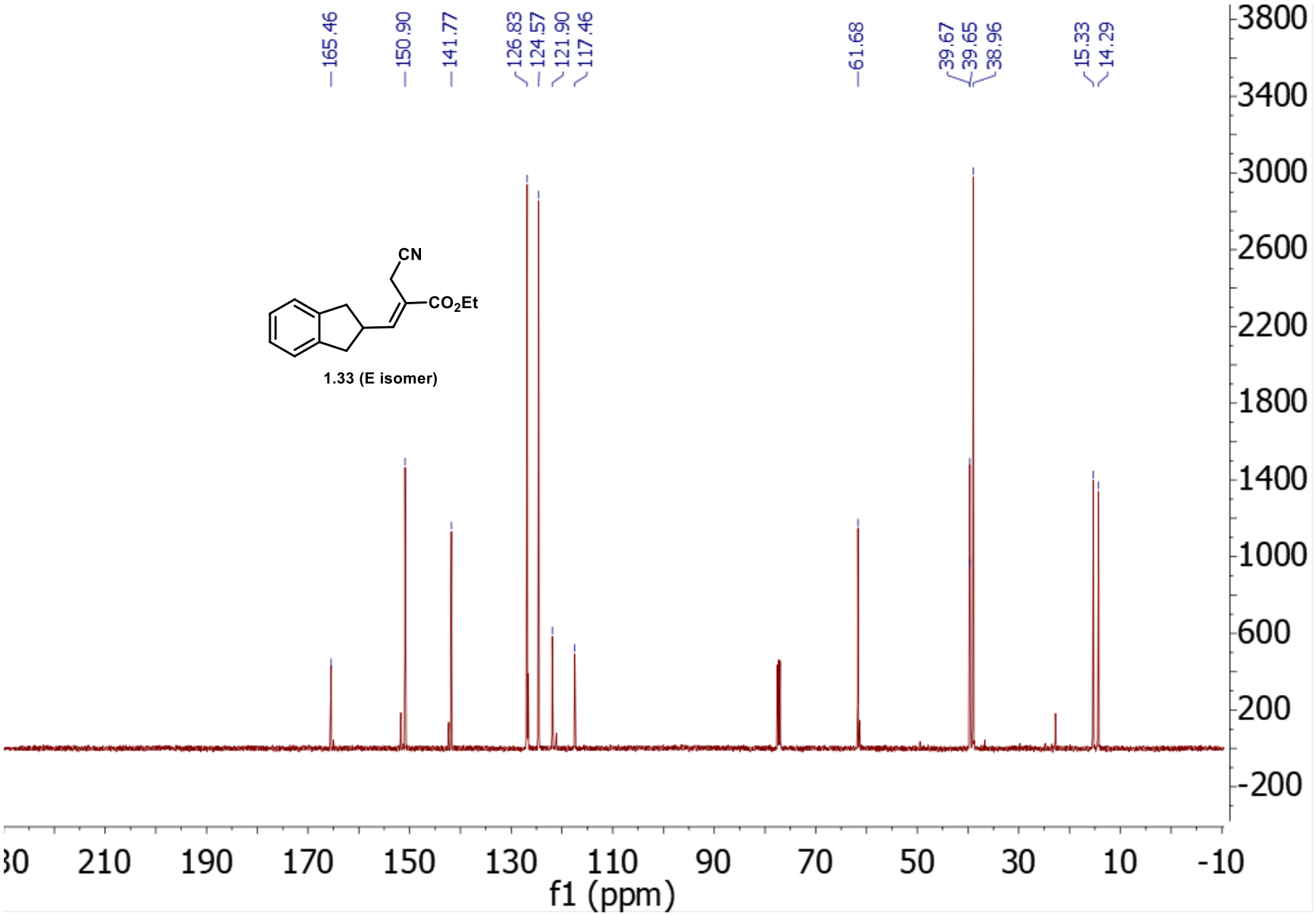
165.46
150.90
141.77
126.83
124.57
121.90
117.46
61.68
39.67
39.65
38.96
15.33
14.29
CN
CO2Et
1.33 (E isomer)
3800
3400
3000
2600
2200
1800
1400
1000
600
200
-200
210
190
170
150
130
110
90
70
50
30
10
-10
f1 (ppm)

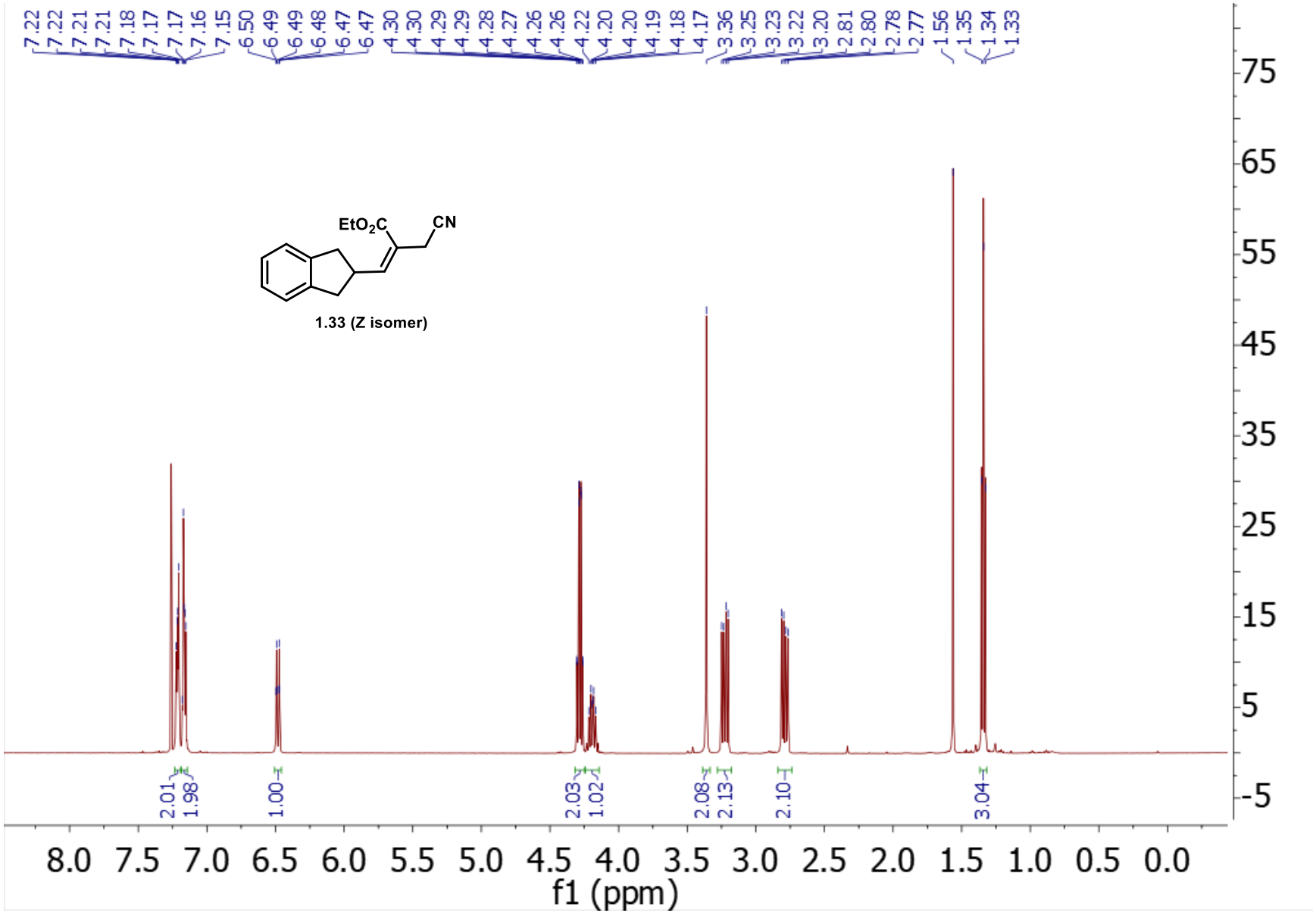
7.22
7.22
7.21
7.21
7.18
7.17
7.17
7.16
7.15
6.50
6.49
6.49
6.48
6.47
6.47
4.30
4.30
4.29
4.29
4.28
4.27
4.26
4.26
4.22
4.20
4.20
4.19
4.18
4.17
3.36
3.25
3.23
3.22
3.20
2.81
2.80
2.78
2.77
1.56
1.35
1.34
1.33
EtO2C
CN
1.33 (Z isomer)
2.01
1.98
1.00
2.03
1.02
2.08
2.13
2.10
3.04
75
65
55
45
35
25
15
5
-5
8.0 7.5 7.0 6.5 6.0 5.5 5.0 4.5 4.0 3.5 3.0 2.5 2.0 1.5 1.0 0.5 0.0
f1 (ppm)

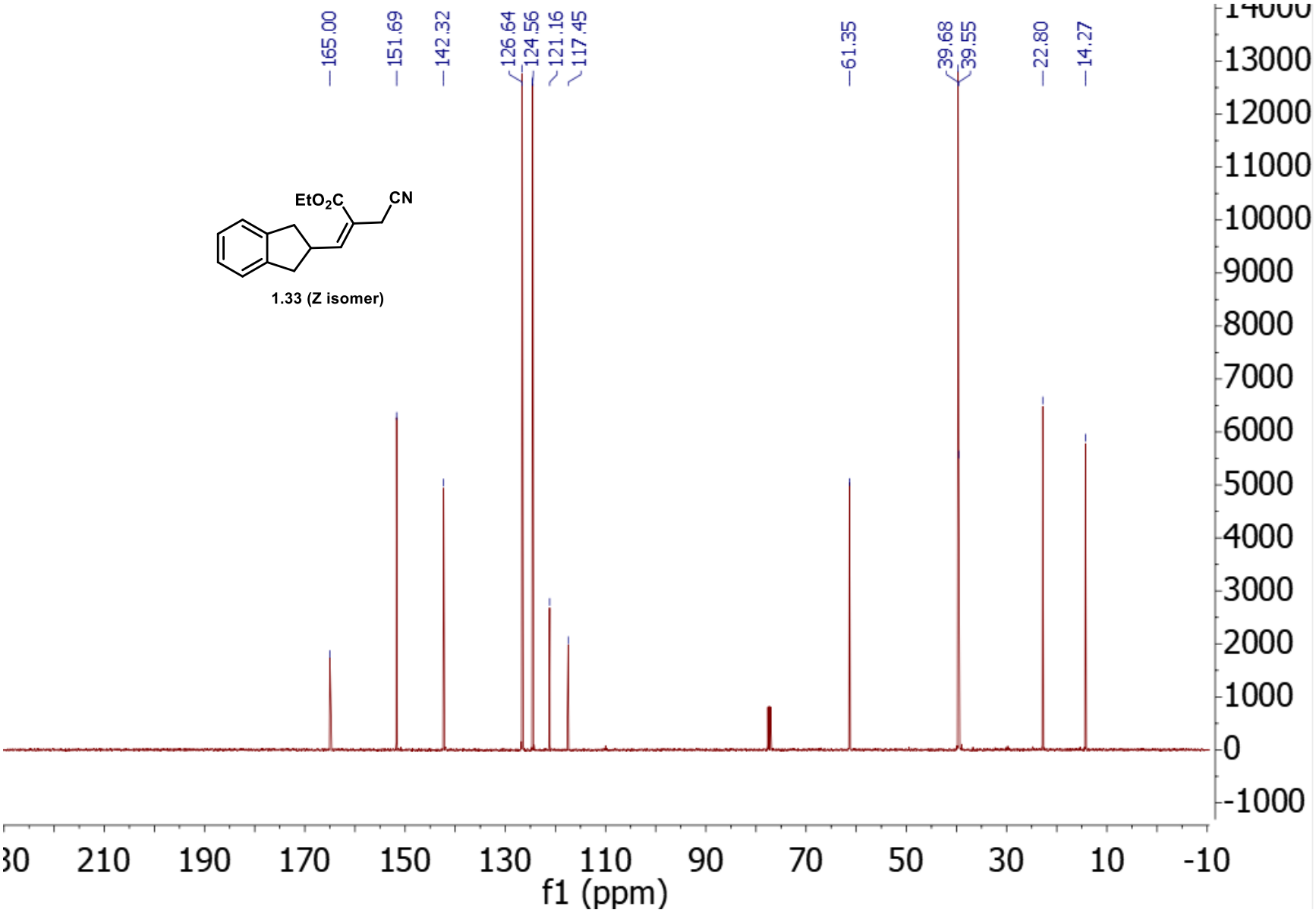
165.00
151.69
142.32
126.64
124.56
121.16
117.45
61.35
39.68
39.55
22.80
14.27
EtO2C
CN
1.33 (Z isomer)
14000
13000
12000
11000
10000
9000
8000
7000
6000
5000
4000
3000
2000
1000
0
-1000
30
210
190
170
150
130
110
90
70
50
30
10
-10
f1 (ppm)

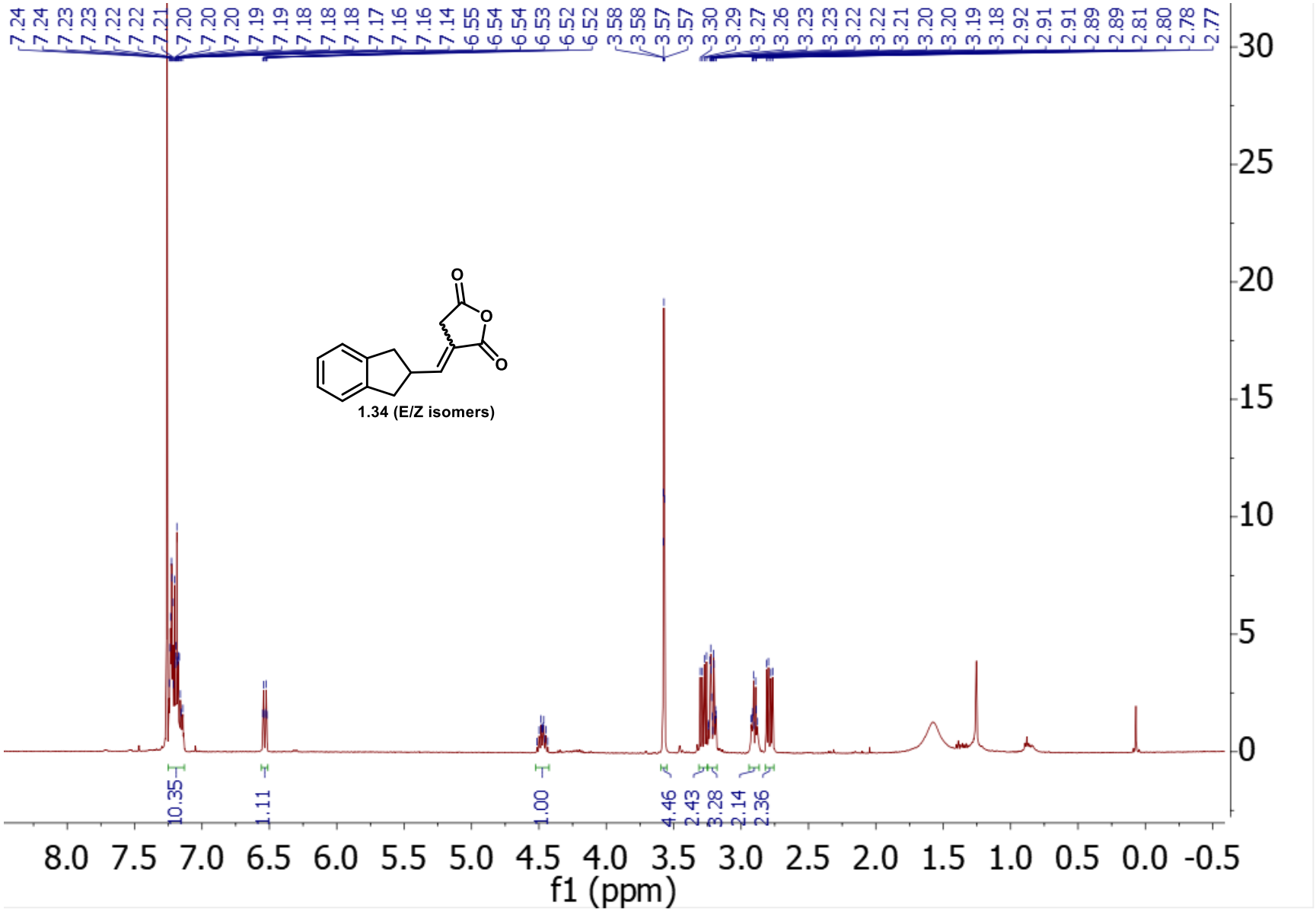
7.24 7.24 7.23 7.23 7.22 7.22 7.21 7.20 7.20 7.20 7.19 7.19 7.18 7.18 7.18 7.17 7.16 7.16 7.14 6.55 6.54 6.54 6.53 6.52 6.52 3.58 3.58 3.57 3.57 3.30 3.29 3.27 3.26 3.23 3.23 3.22 3.22 3.21 3.20 3.20 3.19 3.18 2.92 2.91 2.91 2.89 2.89 2.81 2.80 2.78 2.77
O
O
O
1.34 (E/Z isomers)
10.35
1.11
1.00
4.46
2.43
3.28
2.14
2.36
30
25
20
15
10
5
0
8.0 7.5 7.0 6.5 6.0 5.5 5.0 4.5 4.0 3.5 3.0 2.5 2.0 1.5 1.0 0.5 0.0 -0.5
f1 (ppm)

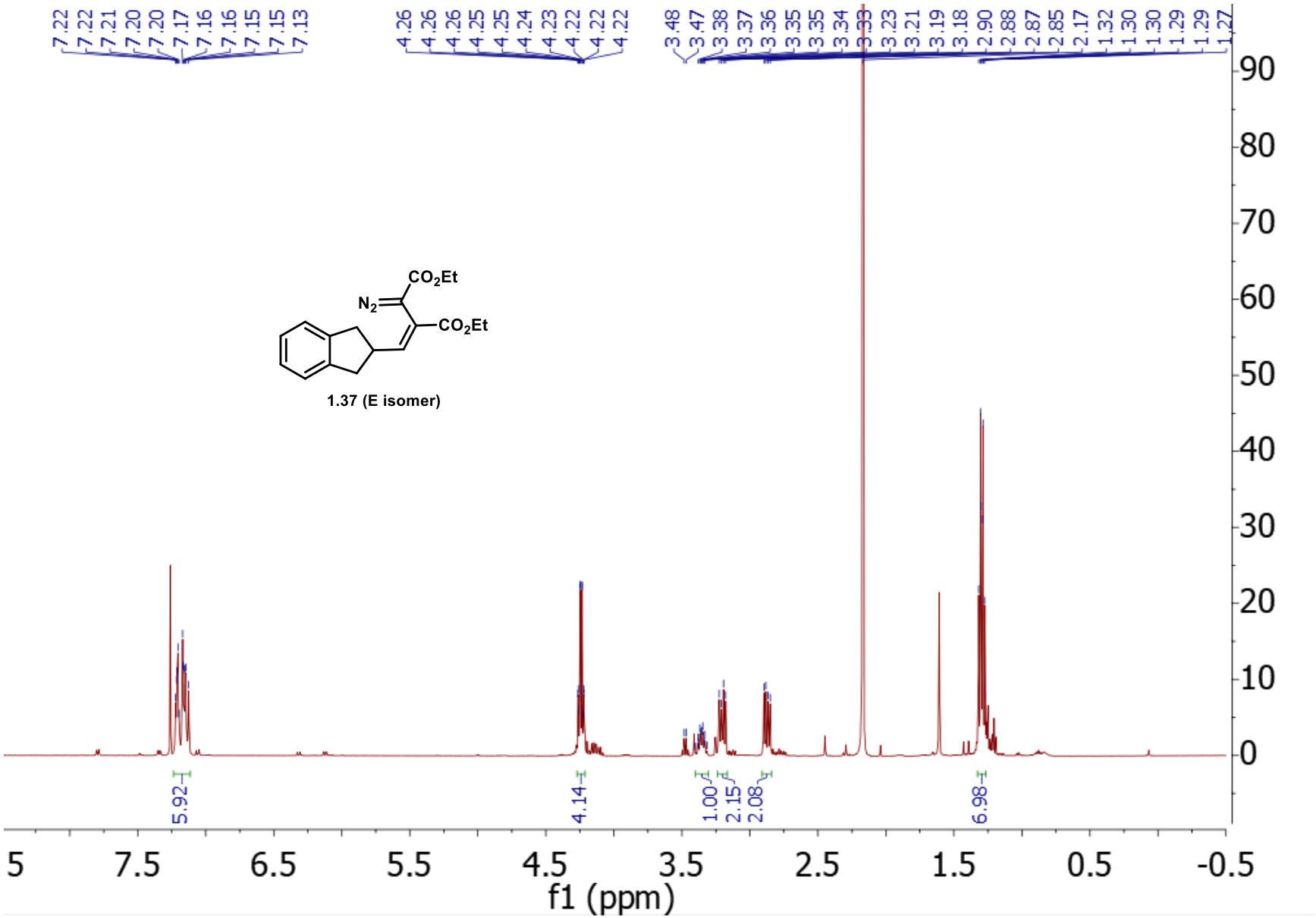
7.22 7.22 7.21 7.20 7.20 7.17 7.16 7.16 7.15 7.15 7.13
4.26 4.26 4.26 4.25 4.25 4.24 4.23 4.22 4.22 4.22
3.48 3.47 3.38 3.37 3.36 3.35 3.35 3.34 3.33 3.23 3.21 3.19 3.18 2.90 2.88 2.87 2.85 2.17 1.32 1.30 1.30 1.29 1.29 1.27
CO2Et
N2
CO2Et
1.37 (E isomer)
5.92
4.14
1.00
2.15
2.08
6.98
90
80
70
60
50
40
30
20
10
0
5
7.5
6.5
5.5
4.5
3.5
2.5
1.5
0.5
-0.5
f1 (ppm)

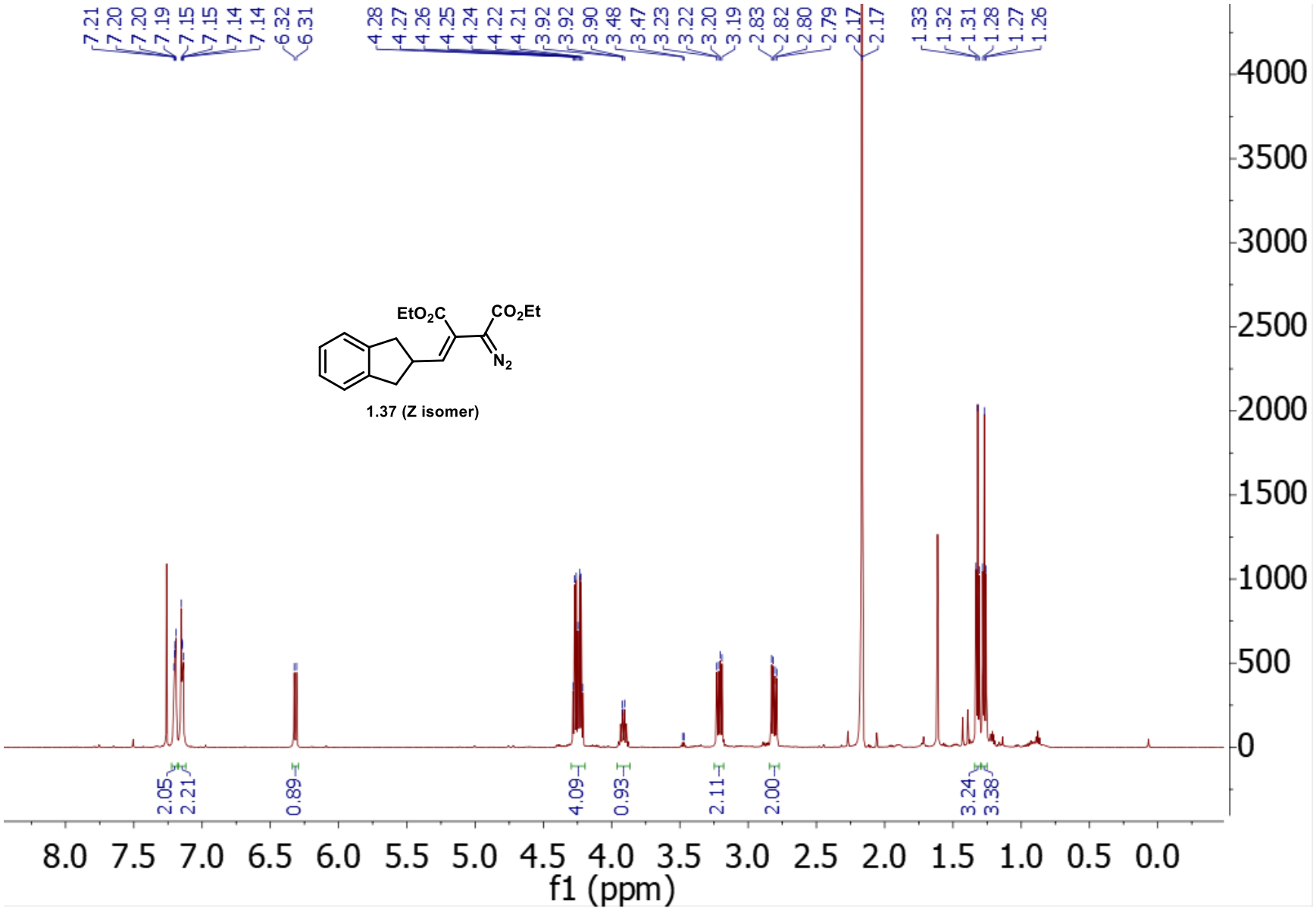
7.21
7.20
7.20
7.19
7.15
7.15
7.14
7.14
6.32
6.31
4.28
4.27
4.26
4.25
4.24
4.22
4.21
3.92
3.92
3.90
3.48
3.47
3.23
3.22
3.20
3.19
2.83
2.82
2.80
2.79
2.17
2.17
1.33
1.32
1.31
1.28
1.27
1.26
EtO2C
CO2Et
N2
1.37 (Z isomer)
2.05
2.21
0.89
4.09
0.93
2.11
2.00
3.24
3.38
4000
3500
3000
2500
2000
1500
1000
500
0
8.0 7.5 7.0 6.5 6.0 5.5 5.0 4.5 4.0 3.5 3.0 2.5 2.0 1.5 1.0 0.5 0.0
f1 (ppm)

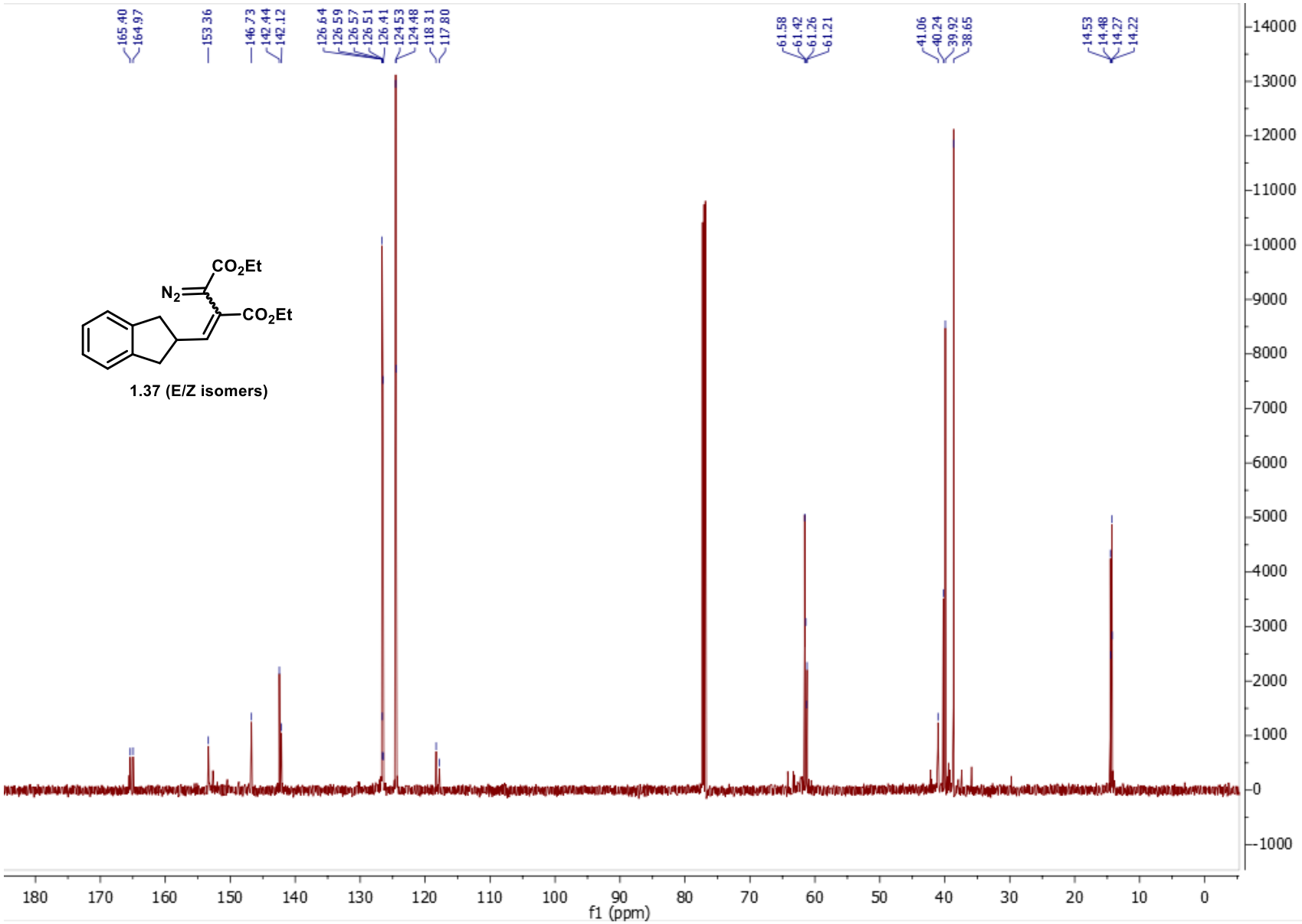
165.40
164.97
153.36
146.73
142.44
142.12
126.64
126.59
126.57
126.51
126.41
124.53
124.48
118.31
117.80
61.58
61.42
61.26
61.21
41.06
40.24
39.92
38.65
14.53
14.48
14.27
14.22
CO2Et
N2
CO2Et
1.37 (E/Z isomers)
f1 (ppm)

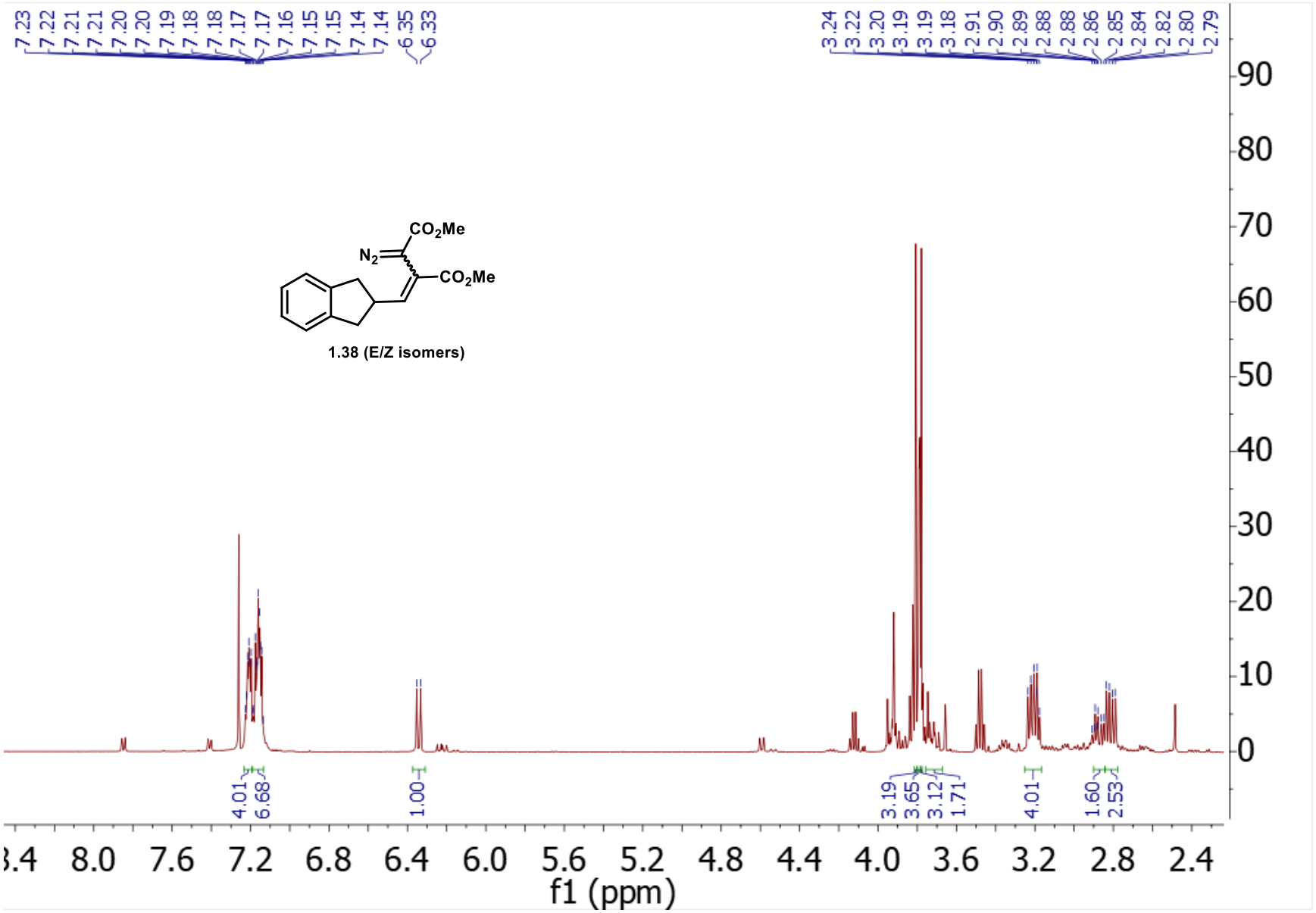
7.23
7.22
7.21
7.21
7.20
7.20
7.19
7.18
7.18
7.17
7.17
7.16
7.15
7.15
7.14
7.14
6.35
6.33
3.24
3.22
3.20
3.19
3.19
3.18
2.91
2.90
2.89
2.88
2.88
2.86
2.85
2.84
2.82
2.80
2.79
CO2Me
N2
CO2Me
1.38 (E/Z isomers)
4.01
6.68
1.00
3.19
3.65
3.12
1.71
4.01
1.60
2.53
f1 (ppm)

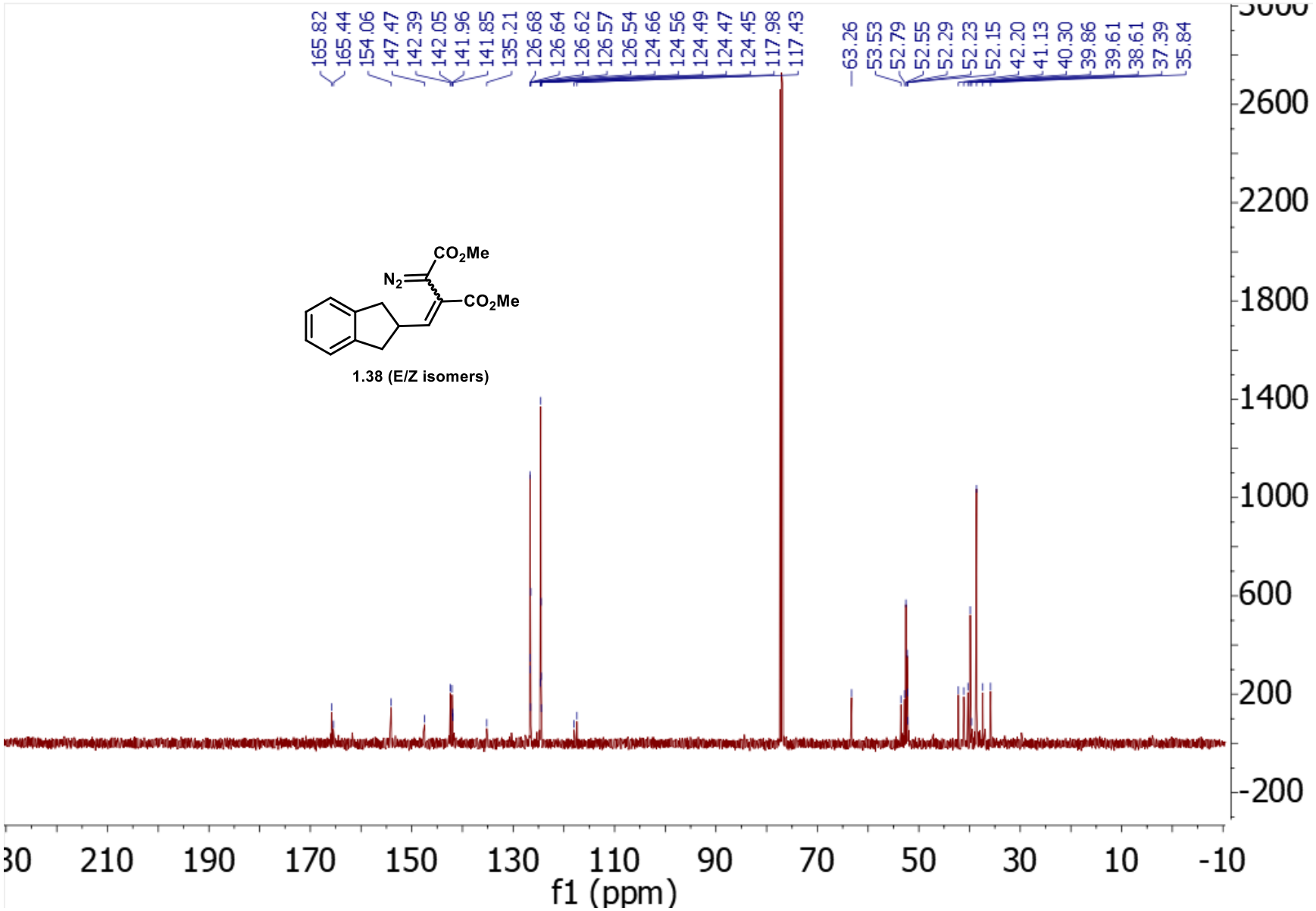
165.82
165.44
154.06
147.47
142.39
142.05
141.96
141.85
135.21
126.68
126.64
126.62
126.57
126.54
124.66
124.56
124.49
124.47
124.45
117.98
117.43
63.26
53.53
52.79
52.55
52.29
52.23
52.15
42.20
41.13
40.30
39.86
39.61
38.61
37.39
35.84
CO2Me
N2
CO2Me
1.38 (E/Z isomers)
2600
2200
1800
1400
1000
600
200
-200
210
190
170
150
130
110
90
70
50
30
10
-10
f1 (ppm)

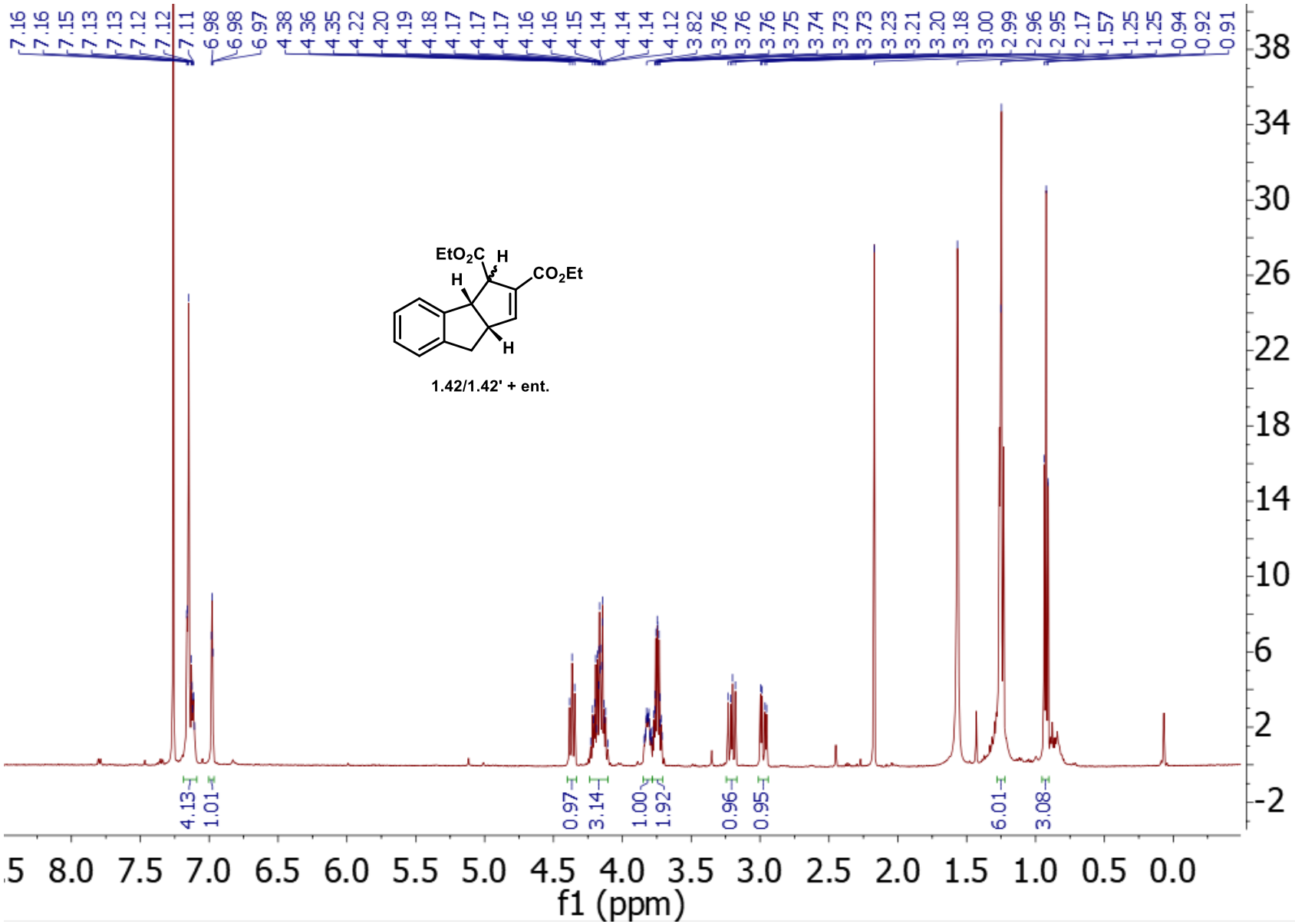
7.16 7.16 7.15 7.13 7.13 7.12 7.12 7.11 6.98 6.98 6.97 4.38 4.36 4.35 4.22 4.20 4.19 4.18 4.17 4.17 4.17 4.16 4.16 4.15 4.14 4.14 4.14 4.12 3.82 3.76 3.76 3.76 3.75 3.74 3.73 3.73 3.23 3.21 3.20 3.18 3.00 2.99 2.96 2.95 2.17 1.57 1.25 1.25 0.94 0.92 0.91
EtO2C H
H
CO2Et
H
1.42/1.42' + ent.
4.13 1.01 0.97 3.14 1.00 1.92 0.96 0.95 6.01 3.08
38 34 30 26 22 18 14 10 6 2 -2
5 8.0 7.5 7.0 6.5 6.0 5.5 5.0 4.5 4.0 3.5 3.0 2.5 2.0 1.5 1.0 0.5 0.0
f1 (ppm)

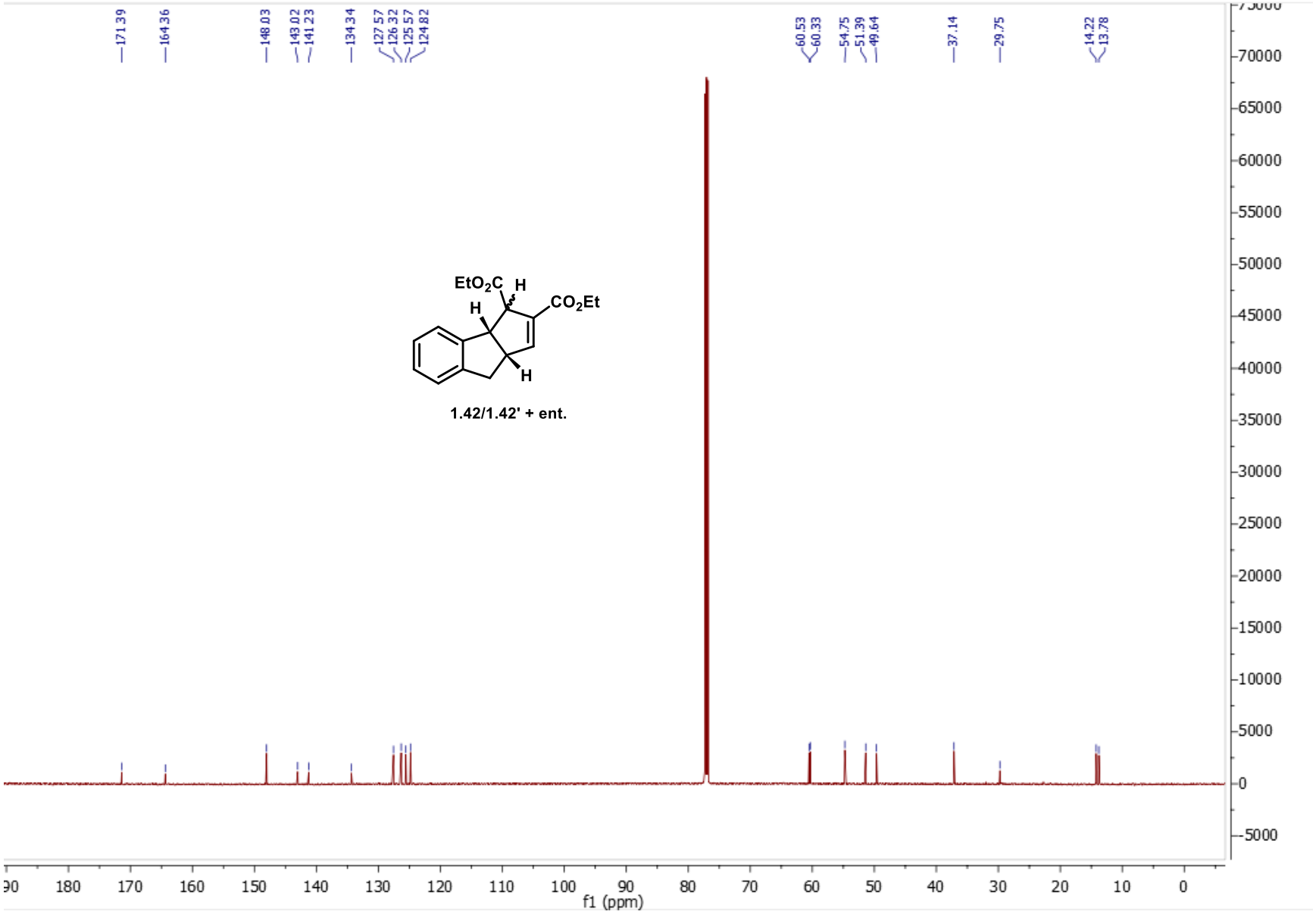
171.39
164.36
148.03
143.02
141.23
134.34
127.57
126.32
125.57
124.82
60.53
60.33
54.75
51.39
49.64
37.14
29.75
14.22
13.78
EtO2C
H
H
CO2Et
H
1.42/1.42' + ent.
f1 (ppm)

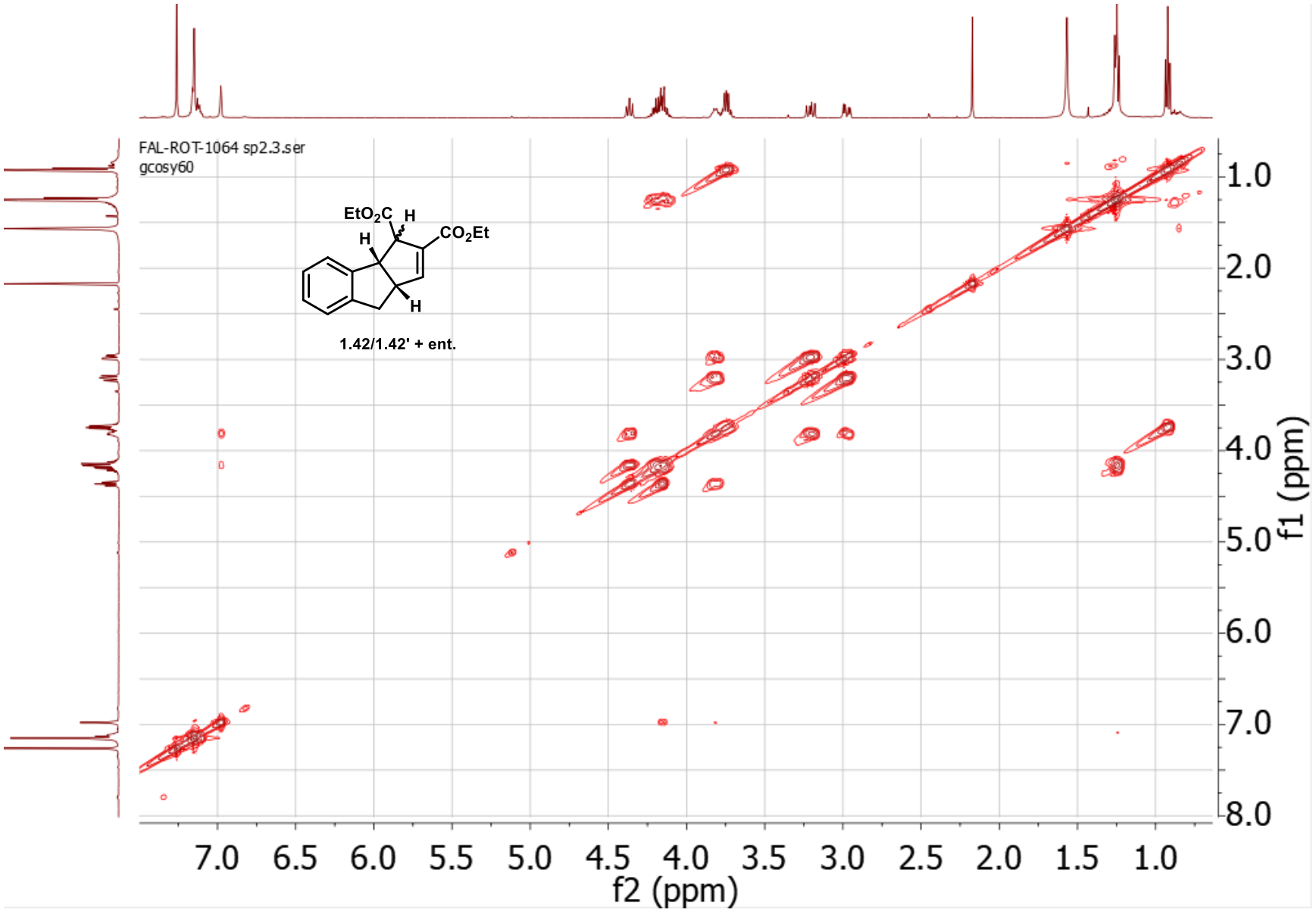
FAL-ROT-1064 sp2.3.ser
gcosy60
EtO2C H
H
CO2Et
H
1.42/1.42' + ent.
f1 (ppm)
f2 (ppm)
1.0
2.0
3.0
4.0
5.0
6.0
7.0
8.0
7.0 6.5 6.0 5.5 5.0 4.5 4.0 3.5 3.0 2.5 2.0 1.5 1.0

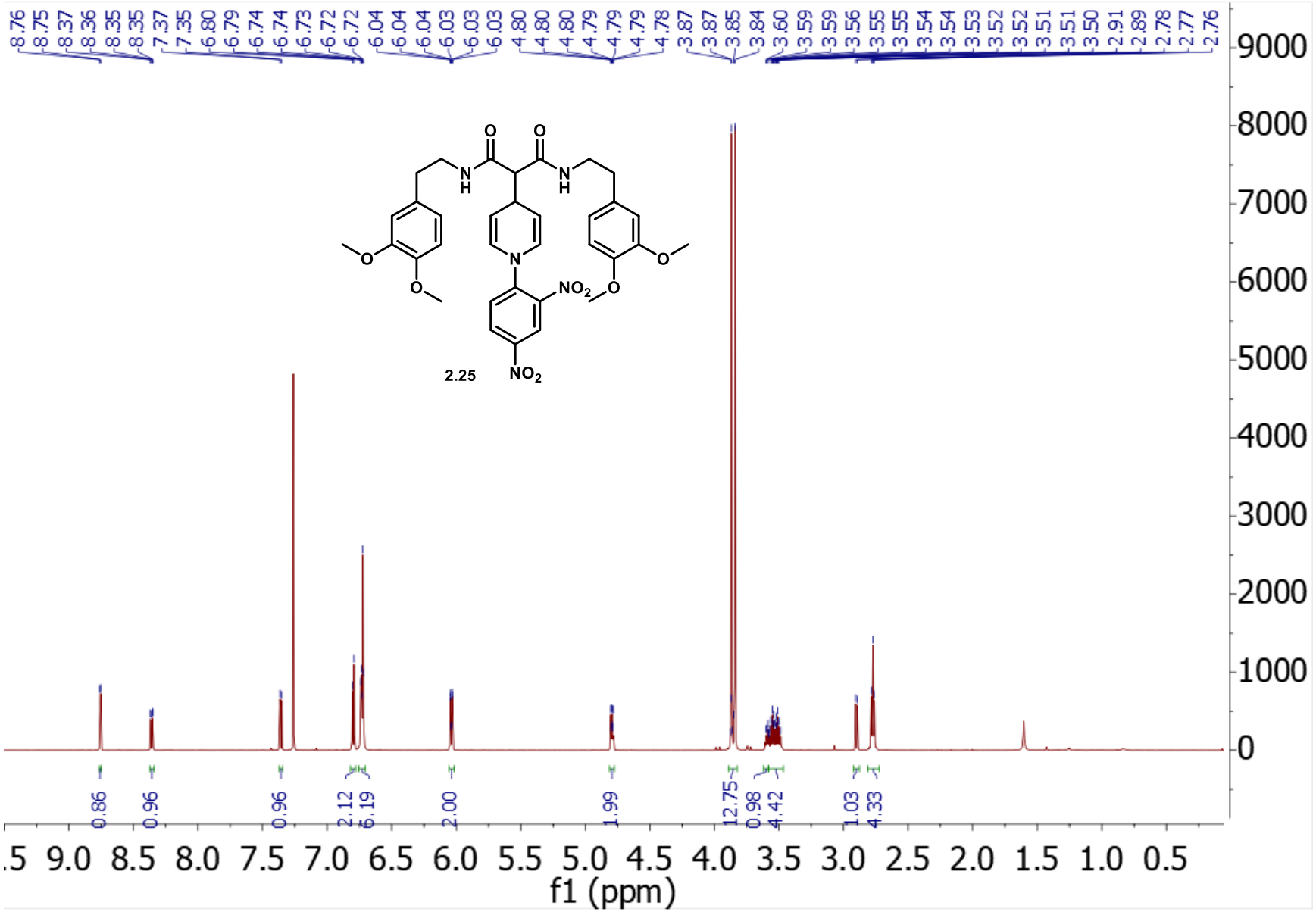
8.76 8.75 8.37 8.36 8.35 8.35 7.37 7.35 6.80 6.79 6.74 6.74 6.73 6.72 6.72 6.04 6.04 6.04 6.03 6.03 6.03 4.80 4.80 4.80 4.79 4.79 4.79 4.78 3.87 3.87 3.85 3.84 3.60 3.59 3.59 3.56 3.55 3.55 3.54 3.54 3.53 3.52 3.52 3.51 3.51 3.50 2.91 2.89 2.78 2.77 2.76
O
O
N
H
N
H
O
O
N
O
O
NO2
O
2.25
NO2
9000
8000
7000
6000
5000
4000
3000
2000
1000
0
0.86
0.96
0.96
2.12
6.19
2.00
1.99
12.75
0.98
4.42
1.03
4.33
.5 9.0 8.5 8.0 7.5 7.0 6.5 6.0 5.5 5.0 4.5 4.0 3.5 3.0 2.5 2.0 1.5 1.0 0.5
f1 (ppm)

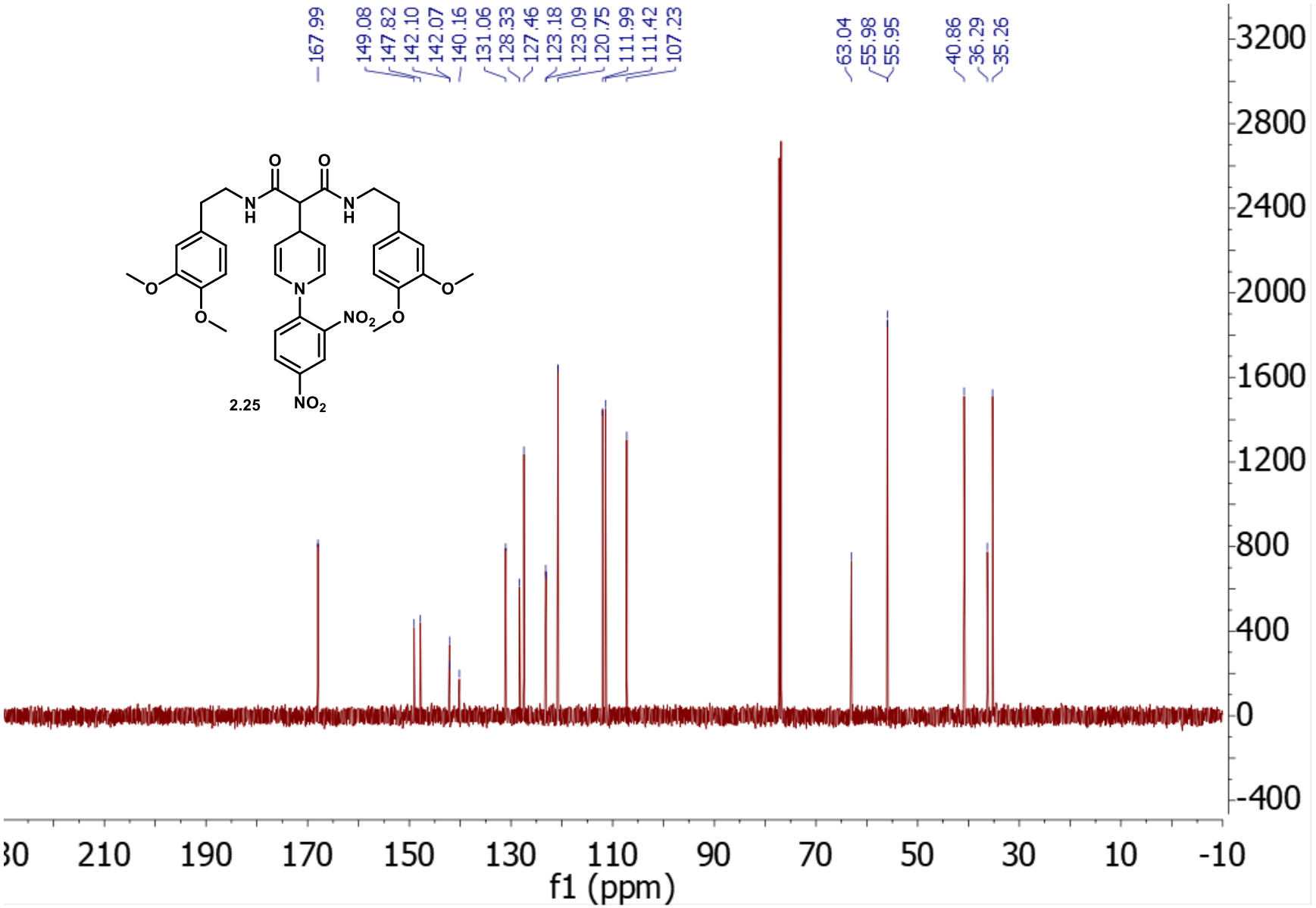
167.99
149.08
147.82
142.10
142.07
140.16
131.06
128.33
127.46
123.18
123.09
120.75
111.99
111.42
107.23
63.04
55.98
55.95
40.86
36.29
35.26
2.25
NO2
NO2
3200
2800
2400
2000
1600
1200
800
400
0
-400
210
190
170
150
130
110
90
70
50
30
10
-10
f1 (ppm)

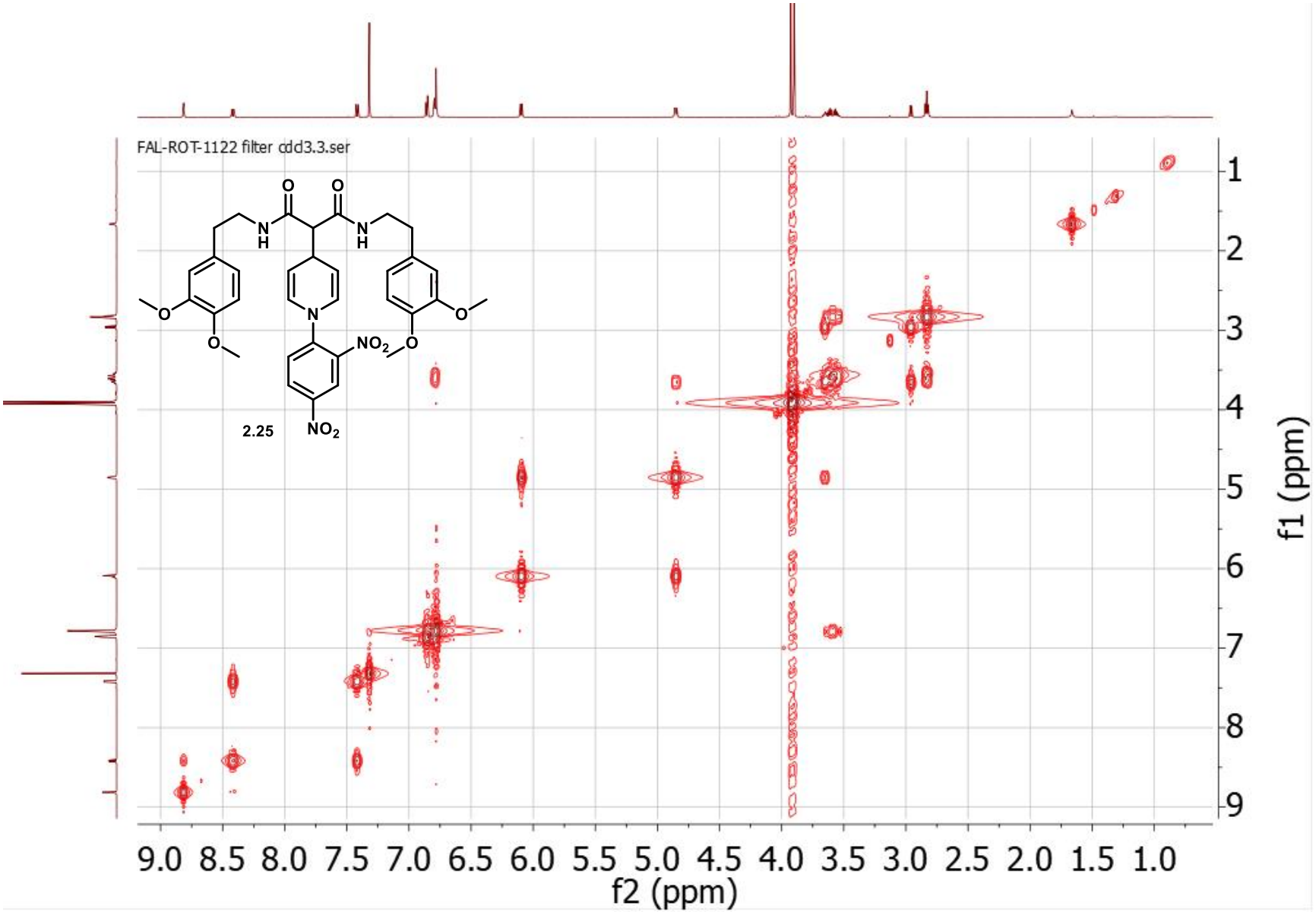
FAL-ROT-1122 filter cdd3.3.ser
2.25
f2 (ppm)
f1 (ppm)

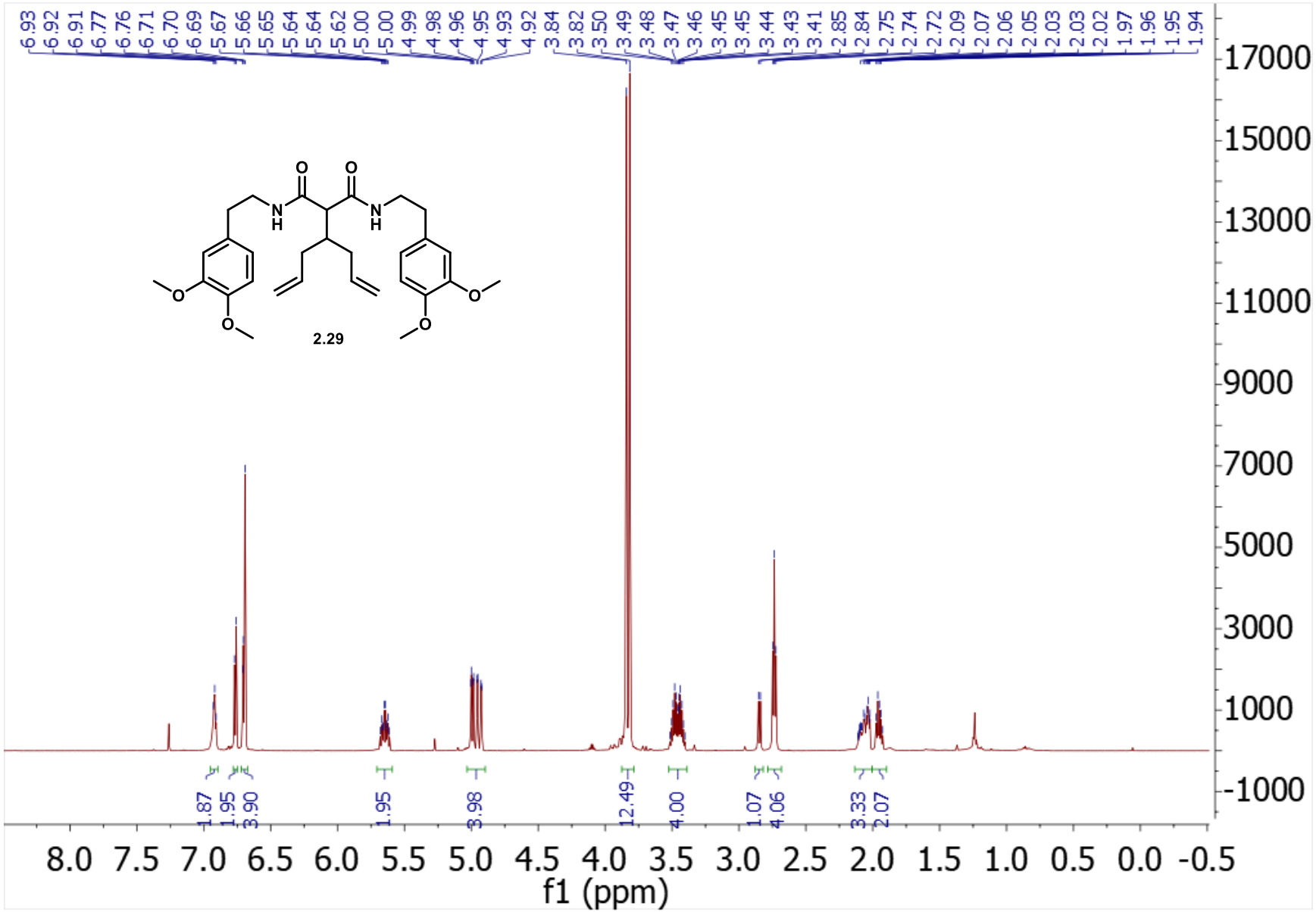
6.93 6.92 6.91 6.77 6.76 6.71 6.70 6.69 6.67 5.66 5.65 5.64 5.64 5.62 5.00 5.00 4.99 4.98 4.96 4.95 4.93 4.92 3.84 3.82 3.50 3.49 3.48 3.47 3.46 3.45 3.45 3.44 3.43 3.41 2.85 2.84 2.75 2.74 2.72 2.09 2.07 2.06 2.05 2.03 2.03 2.02 1.97 1.96 1.95 1.94
O
O
N
H
N
H
O
O
O
O
2.29
17000
15000
13000
11000
9000
7000
5000
3000
1000
-1000
1.87
1.95
3.90
1.95
3.98
12.49
4.00
1.07
4.06
3.33
2.07
8.0 7.5 7.0 6.5 6.0 5.5 5.0 4.5 4.0 3.5 3.0 2.5 2.0 1.5 1.0 0.5 0.0 -0.5
f1 (ppm)

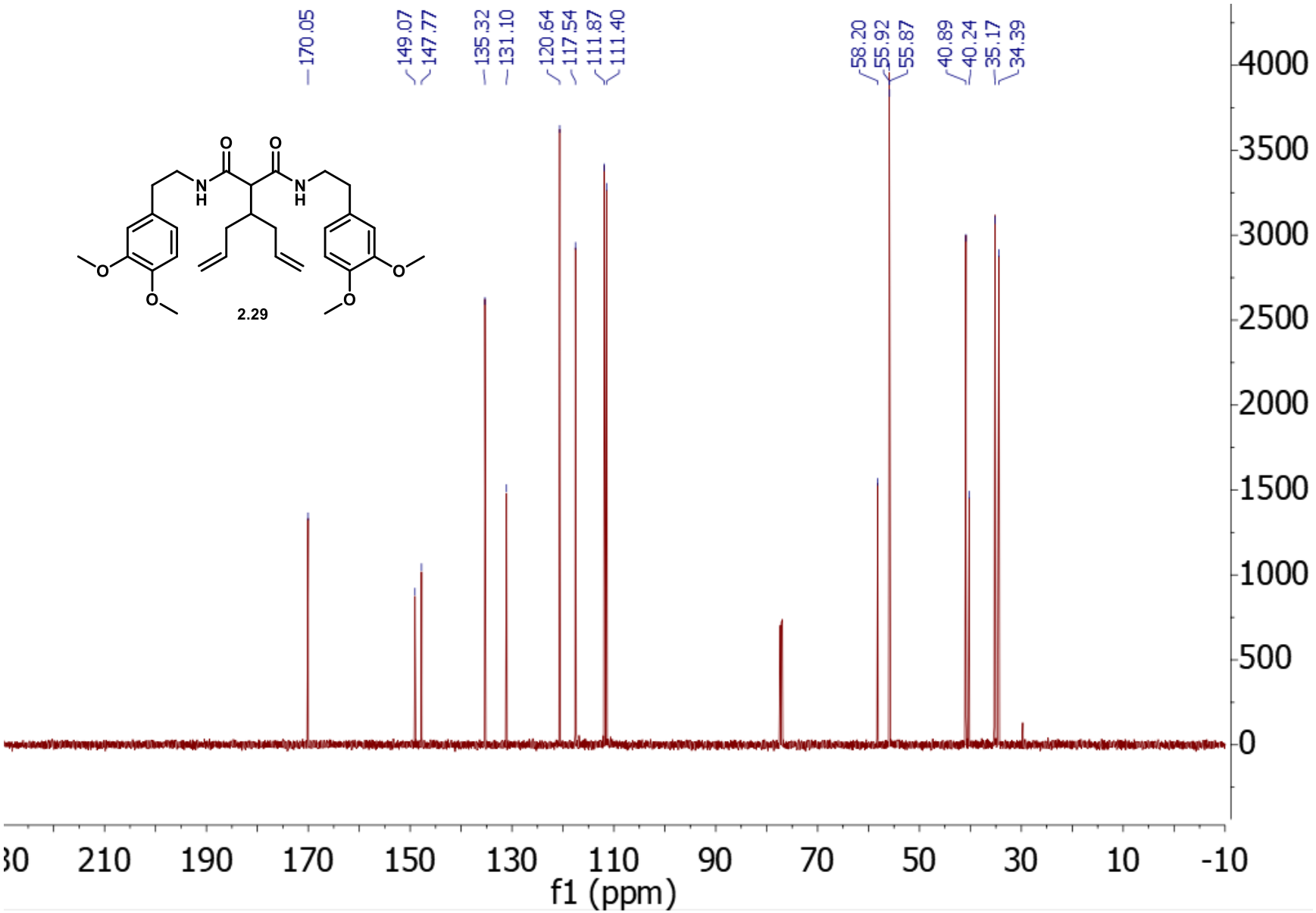
170.05
149.07
147.77
135.32
131.10
120.64
117.54
111.87
111.40
58.20
55.92
55.87
40.89
40.24
35.17
34.39
2.29
4000
3500
3000
2500
2000
1500
1000
500
0
210
190
170
150
130
110
90
70
50
30
10
-10
f1 (ppm)

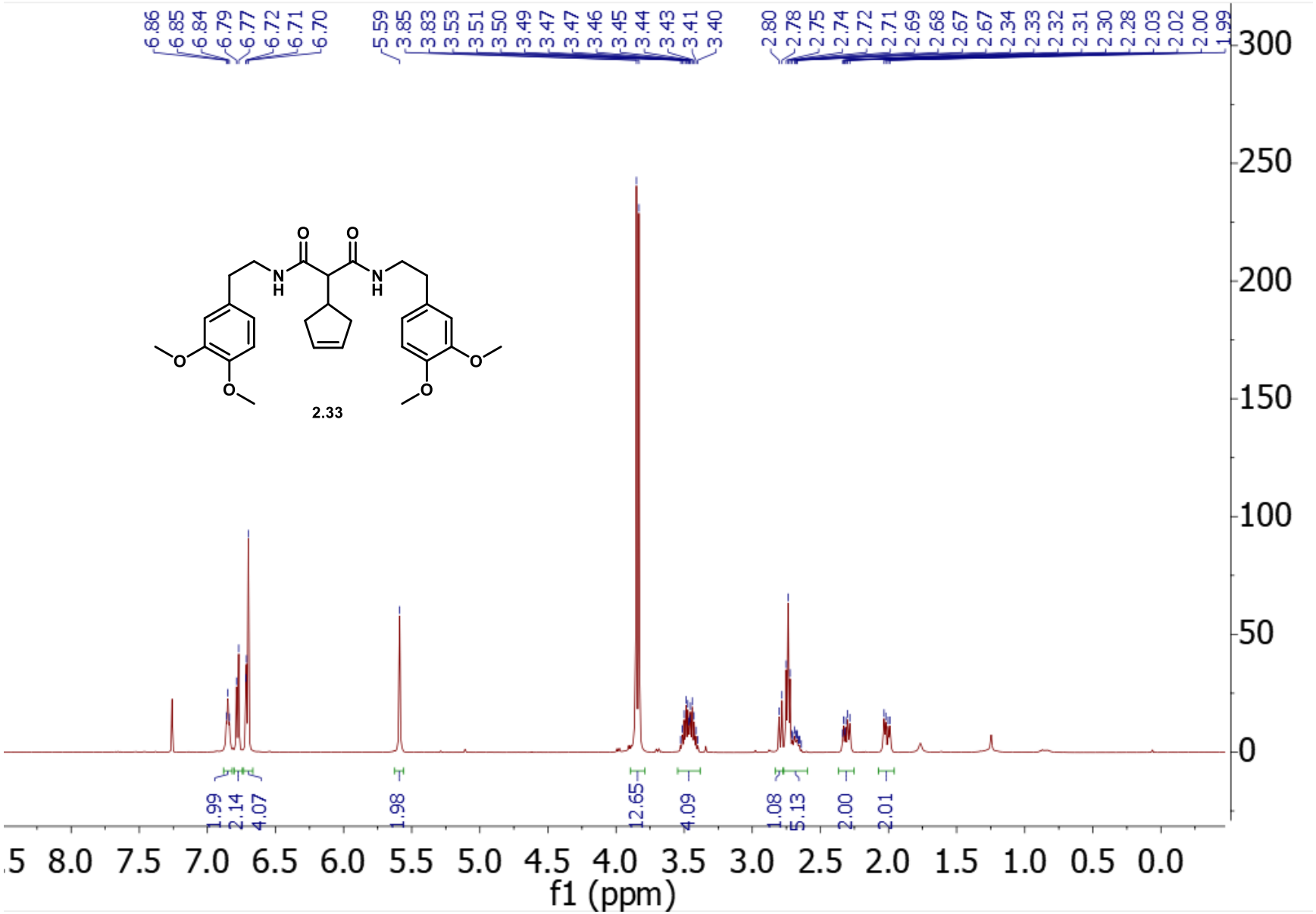
6.86 6.85 6.84 6.79 6.77 6.72 6.71 6.70
5.59 3.85 3.83 3.53 3.51 3.50 3.49 3.47 3.47 3.46 3.45 3.44 3.43 3.41 3.40
2.80 2.78 2.75 2.74 2.72 2.71 2.69 2.68 2.67 2.67 2.34 2.33 2.32 2.31 2.30 2.28 2.03 2.02 2.00 1.99
O
O
N
H
N
H
O
O
O
O
2.33
300
250
200
150
100
50
0
1.99 2.14 4.07 1.98 12.65 4.09 1.08 5.13 2.00 2.01
.5 8.0 7.5 7.0 6.5 6.0 5.5 5.0 4.5 4.0 3.5 3.0 2.5 2.0 1.5 1.0 0.5 0.0
f1 (ppm)

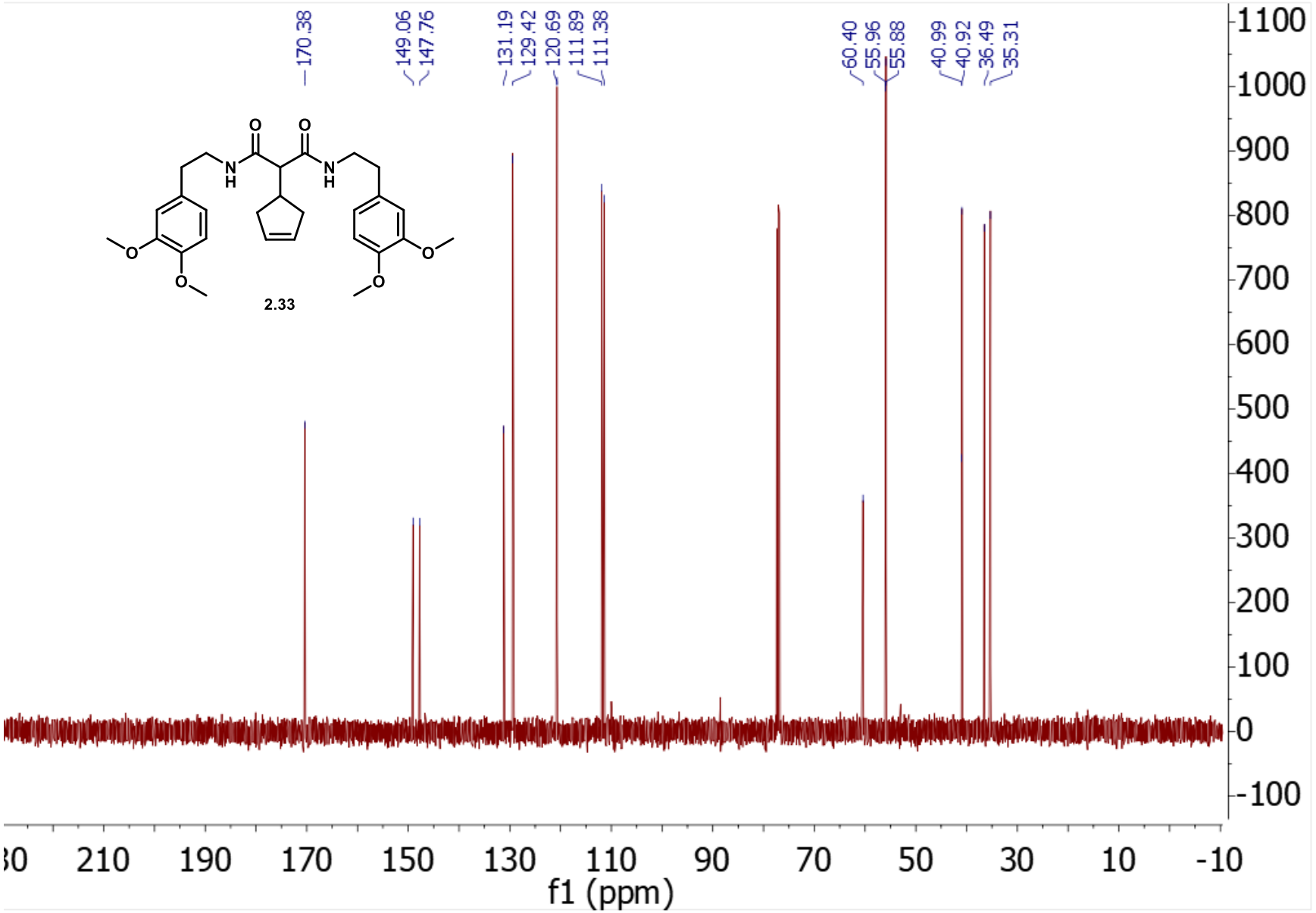
170.38
149.06
147.76
131.19
129.42
120.69
111.89
111.38
60.40
55.96
55.88
40.99
40.92
36.49
35.31
2.33
1100
1000
900
800
700
600
500
400
300
200
100
0
-100
210
190
170
150
130
110
90
70
50
30
10
-10
f1 (ppm)

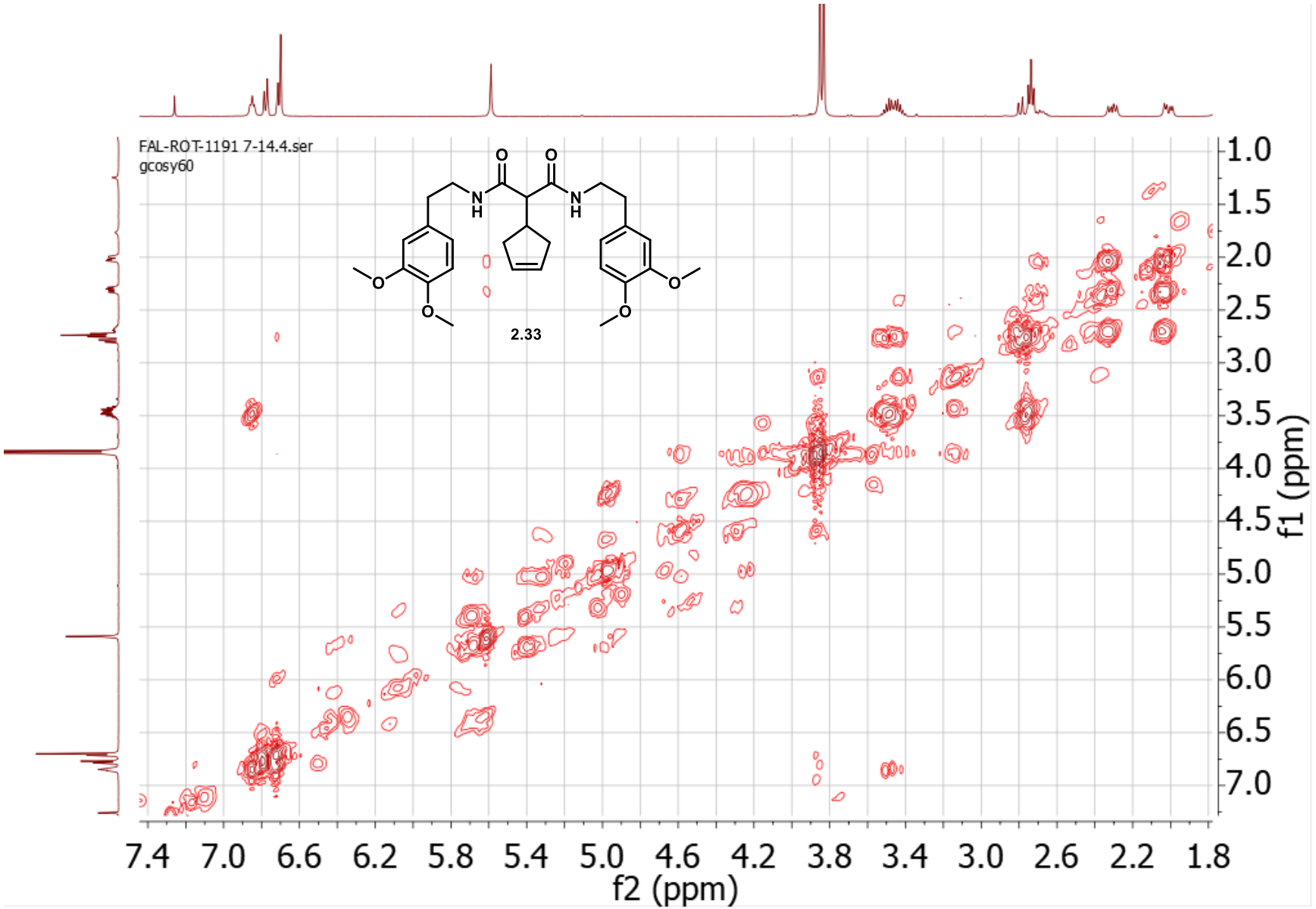
FAL-ROT-1191 7-14.4.ser
gcosy60
2.33
7.4 7.0 6.6 6.2 5.8 5.4 5.0 4.6 4.2 3.8 3.4 3.0 2.6 2.2 1.8
f2 (ppm)
1.0 1.5 2.0 2.5 3.0 3.5 4.0 4.5 5.0 5.5 6.0 6.5 7.0
f1 (ppm)

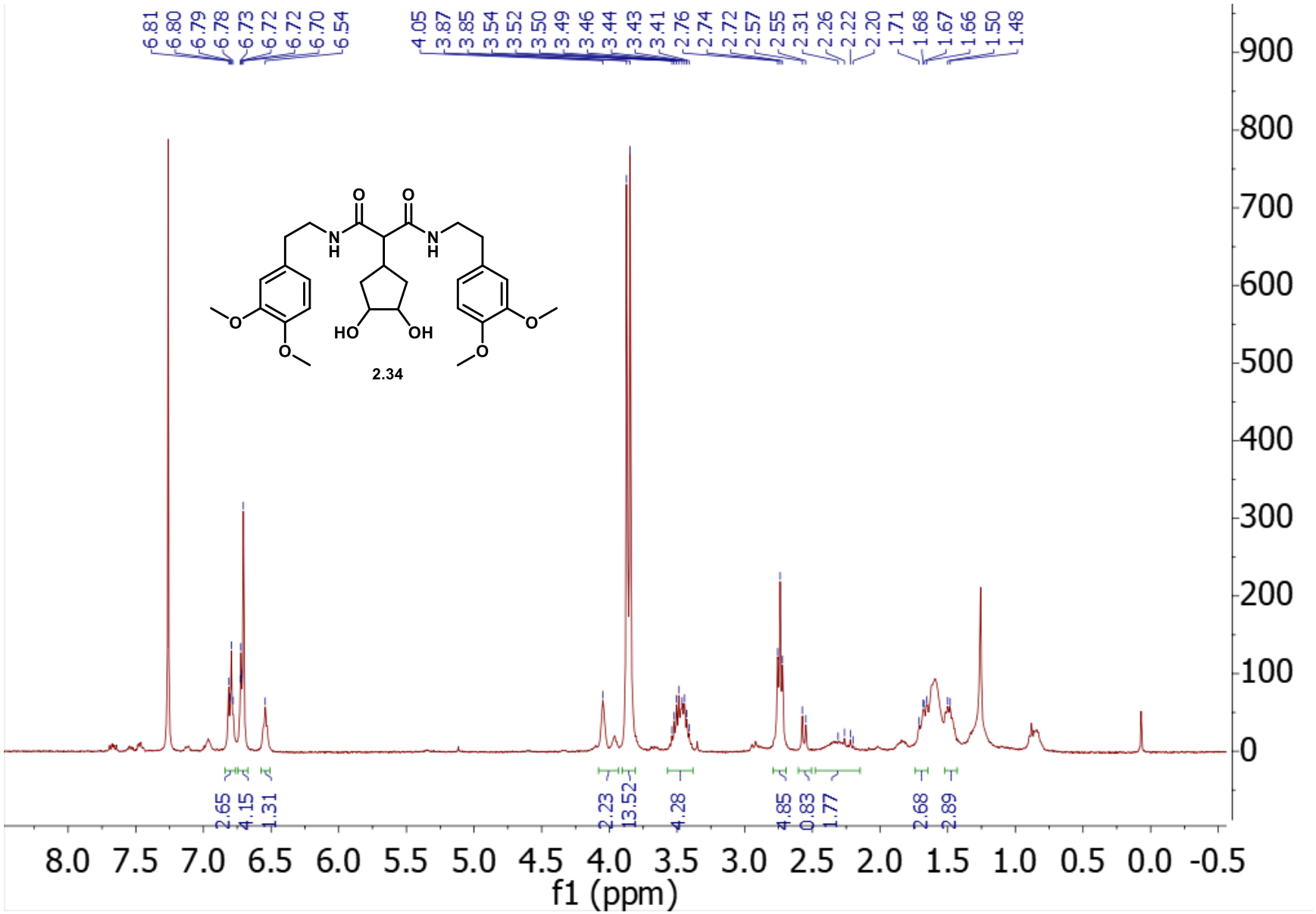
6.81
6.80
6.79
6.78
6.73
6.72
6.72
6.70
6.54
4.05
3.87
3.85
3.54
3.52
3.50
3.49
3.46
3.44
3.43
3.41
2.76
2.74
2.72
2.57
2.55
2.31
2.26
2.22
2.20
1.71
1.68
1.67
1.66
1.50
1.48
HO
OH
2.34
2.65
4.15
1.31
2.23
13.52
4.28
4.85
0.83
1.77
2.68
2.89
f1 (ppm)

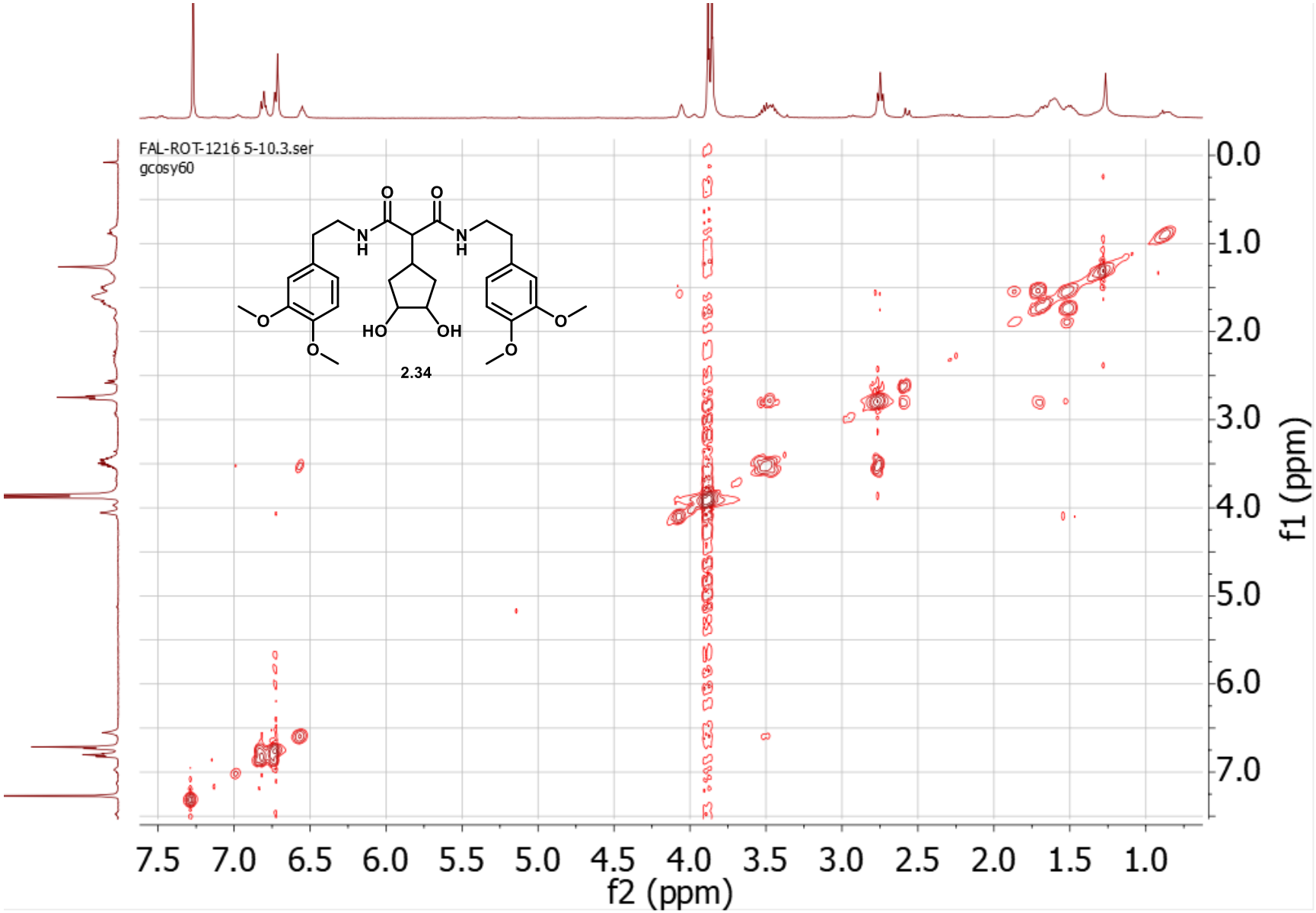
FAL-ROT-1216 5-10.3.ser
gcosy60
2.34
f2 (ppm)
f1 (ppm)

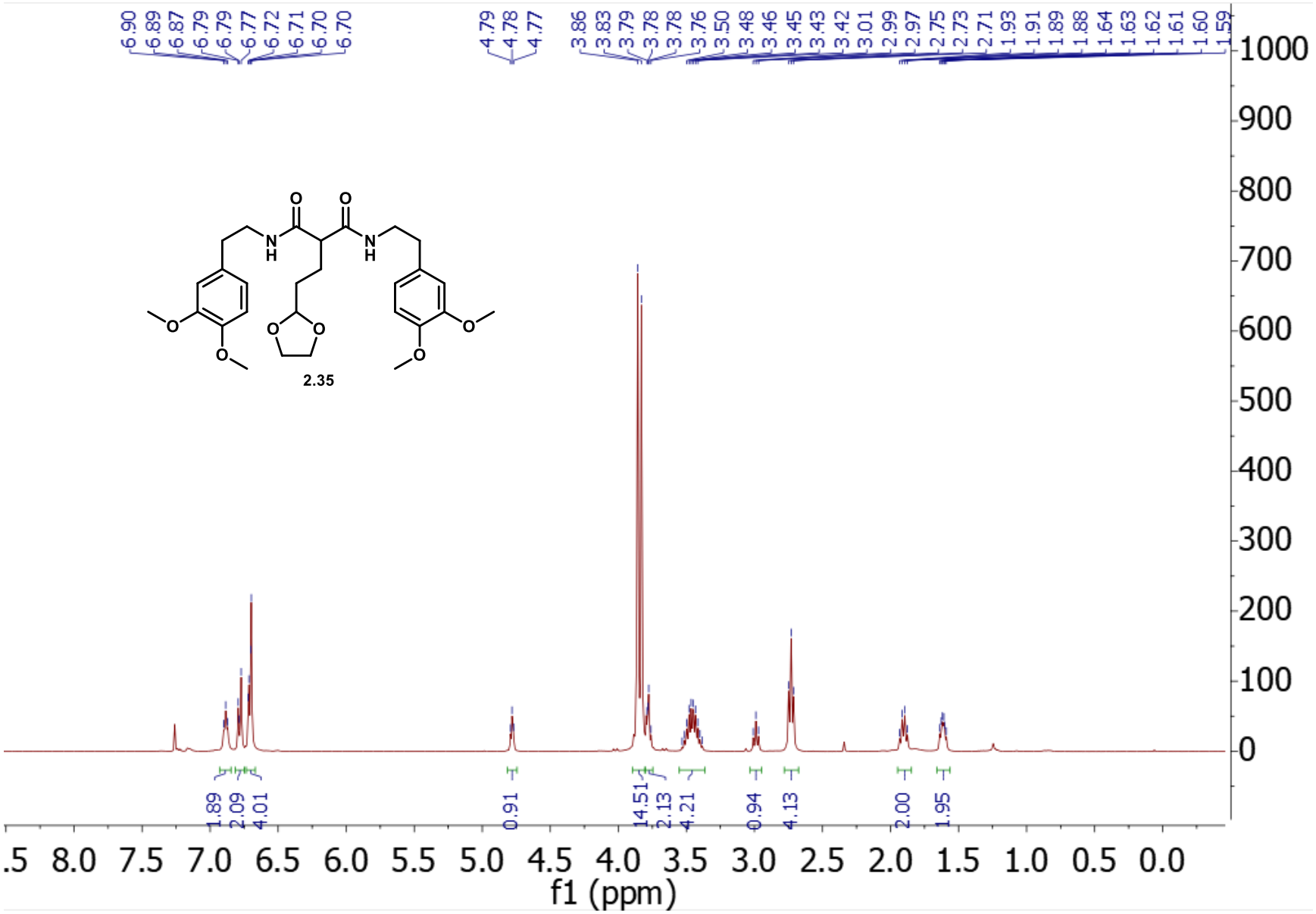
6.90
6.89
6.87
6.79
6.79
6.77
6.72
6.71
6.70
6.70
4.79
4.78
4.77
3.86
3.83
3.79
3.78
3.78
3.76
3.50
3.48
3.46
3.45
3.43
3.42
3.01
2.99
2.97
2.75
2.73
2.71
1.93
1.91
1.89
1.88
1.64
1.63
1.62
1.61
1.60
1.59
2.35
1000
900
800
700
600
500
400
300
200
100
0
1.89
2.09
4.01
0.91
14.51
2.13
4.21
0.94
4.13
2.00
1.95
.5 8.0 7.5 7.0 6.5 6.0 5.5 5.0 4.5 4.0 3.5 3.0 2.5 2.0 1.5 1.0 0.5 0.0
f1 (ppm)

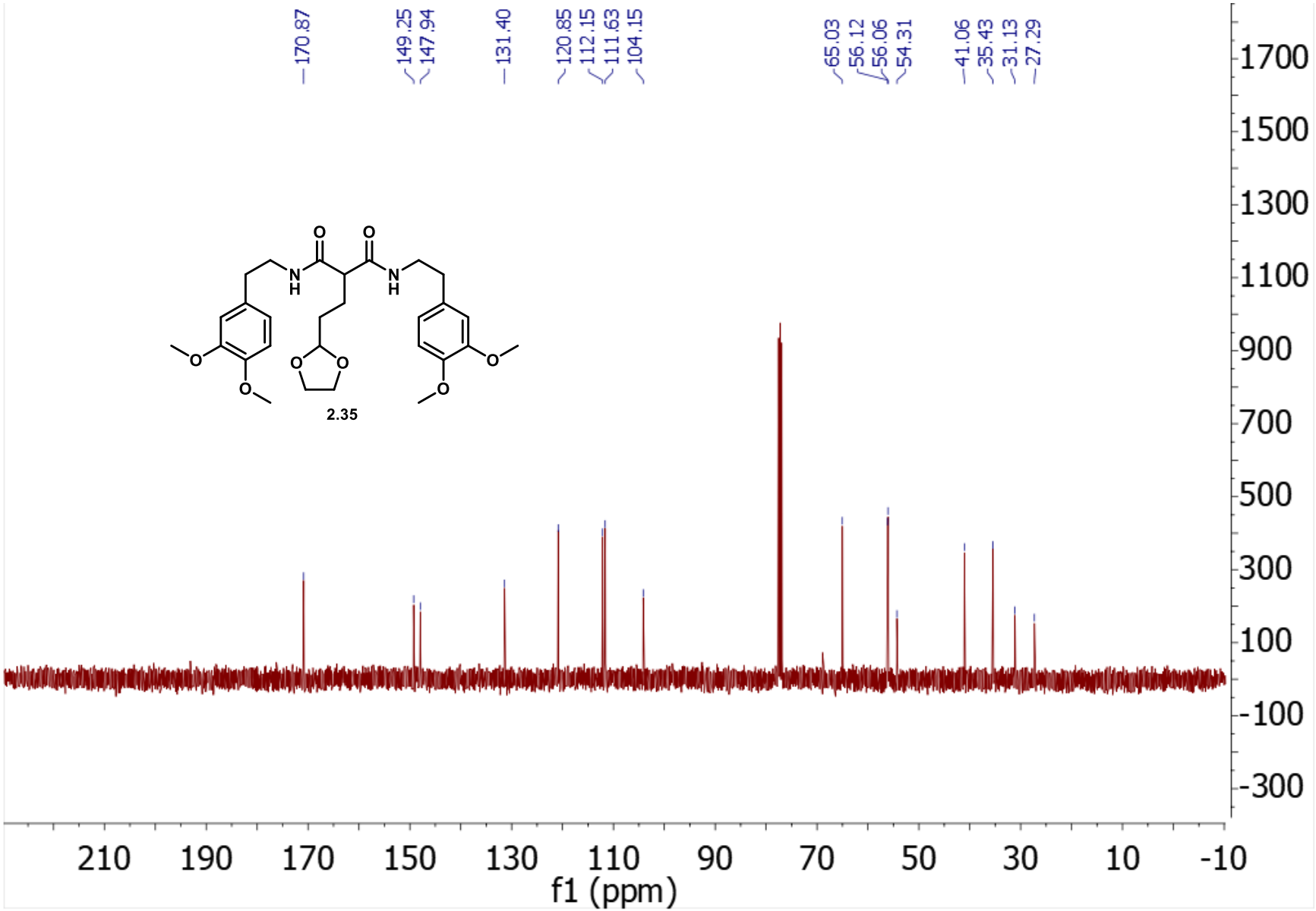
170.87
149.25
147.94
131.40
120.85
112.15
111.63
104.15
65.03
56.12
56.06
54.31
41.06
35.43
31.13
27.29
2.35
1700
1500
1300
1100
900
700
500
300
100
-100
-300
210
190
170
150
130
110
90
70
50
30
10
-10
f1 (ppm)

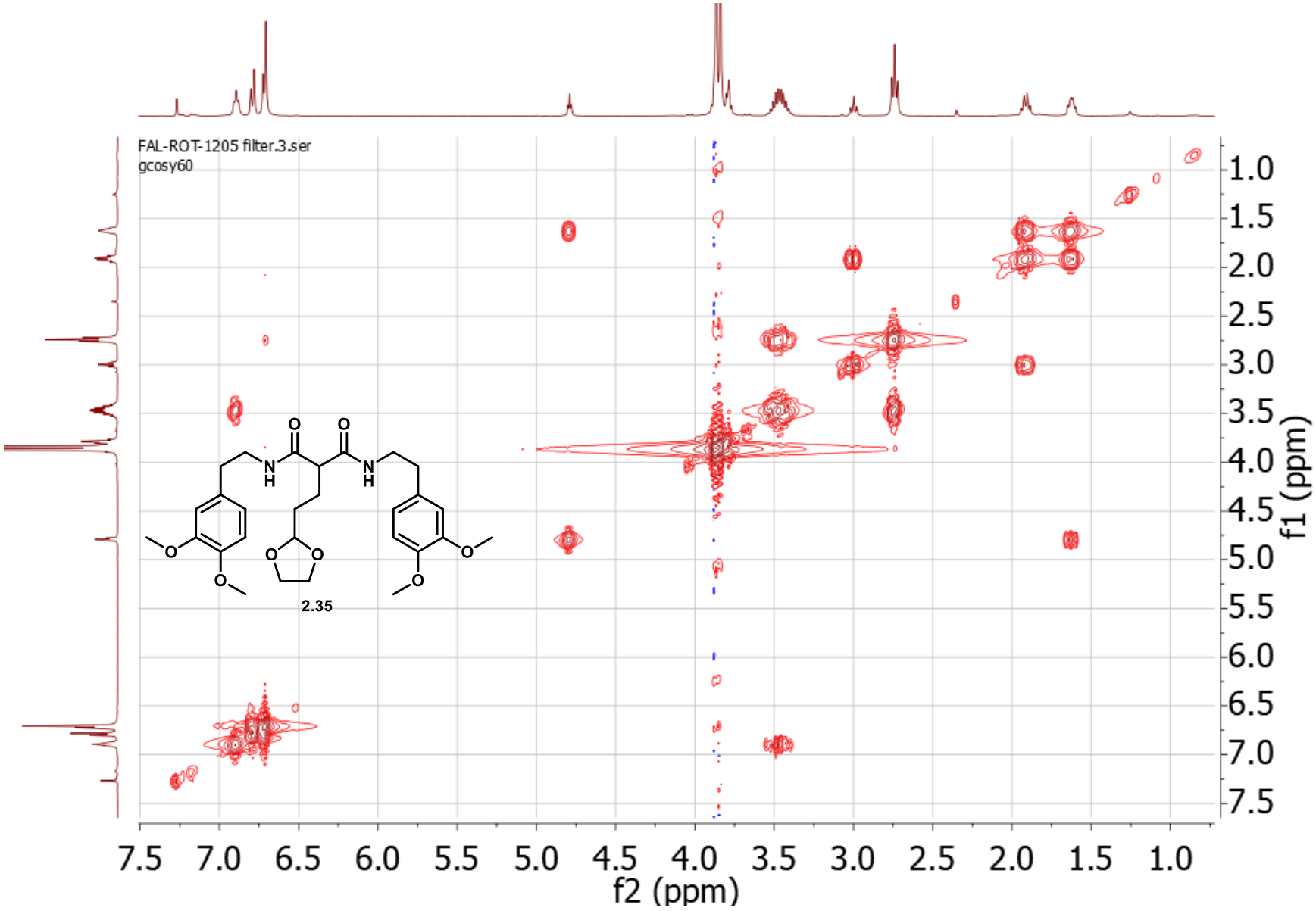
FAL-ROT-1205 filter.3.ser
gcosy60
2.35
f2 (ppm)
f1 (ppm)

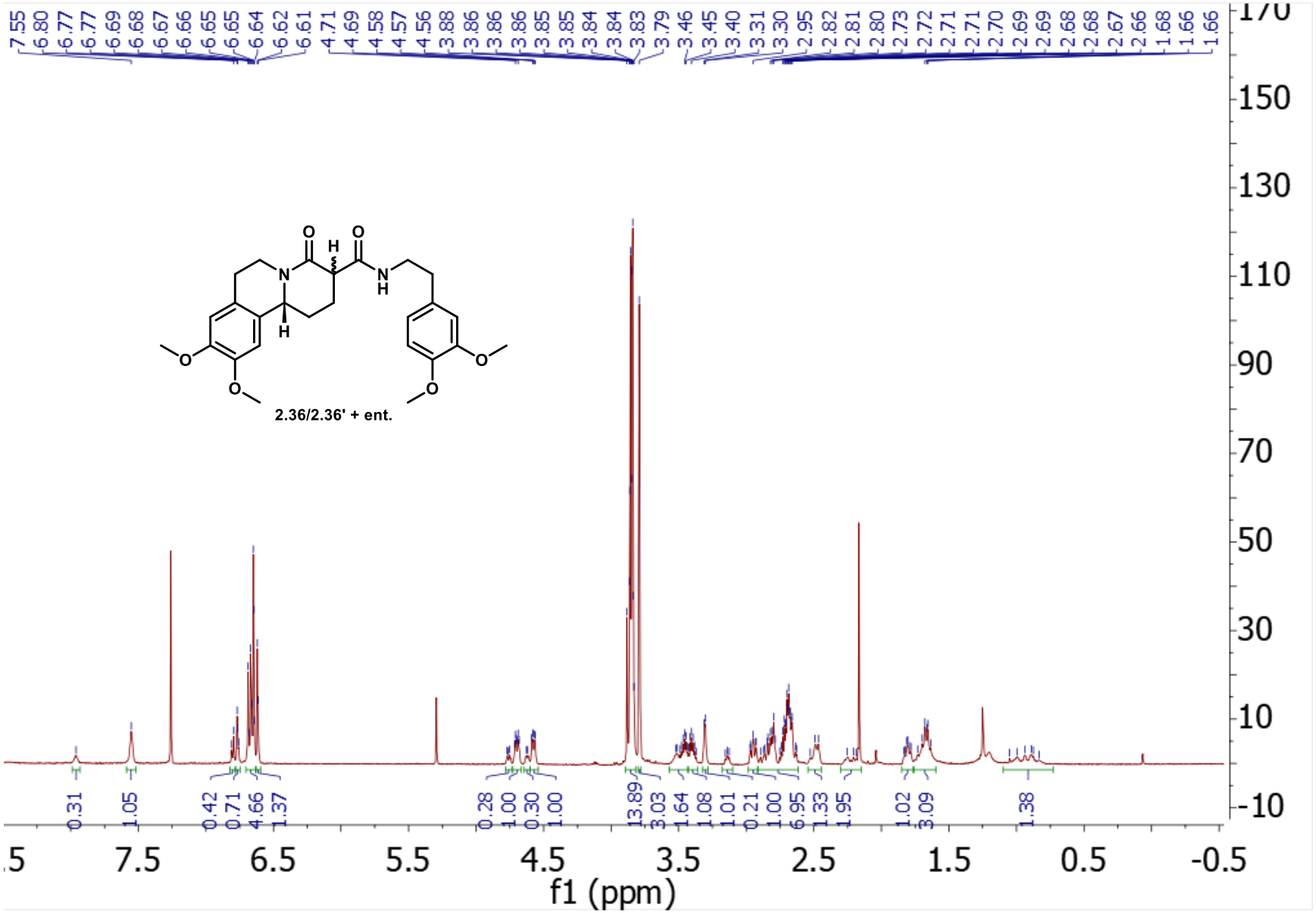
7.55 6.80 6.77 6.77 6.69 6.68 6.67 6.66 6.65 6.65 6.64 6.62 6.61 4.71 4.69 4.58 4.57 4.56 3.88 3.86 3.86 3.86 3.85 3.85 3.84 3.84 3.83 3.79 3.46 3.45 3.40 3.31 3.30 2.95 2.82 2.81 2.80 2.73 2.72 2.71 2.71 2.70 2.69 2.69 2.68 2.68 2.67 2.66 1.68 1.66 1.66
2.36/2.36' + ent.
0.31 1.05 0.42 0.71 4.66 1.37 0.28 1.00 0.30 1.00 13.89 3.03 1.64 1.08 1.01 0.21 1.00 6.95 1.33 1.95 1.02 3.09 1.38
f1 (ppm)

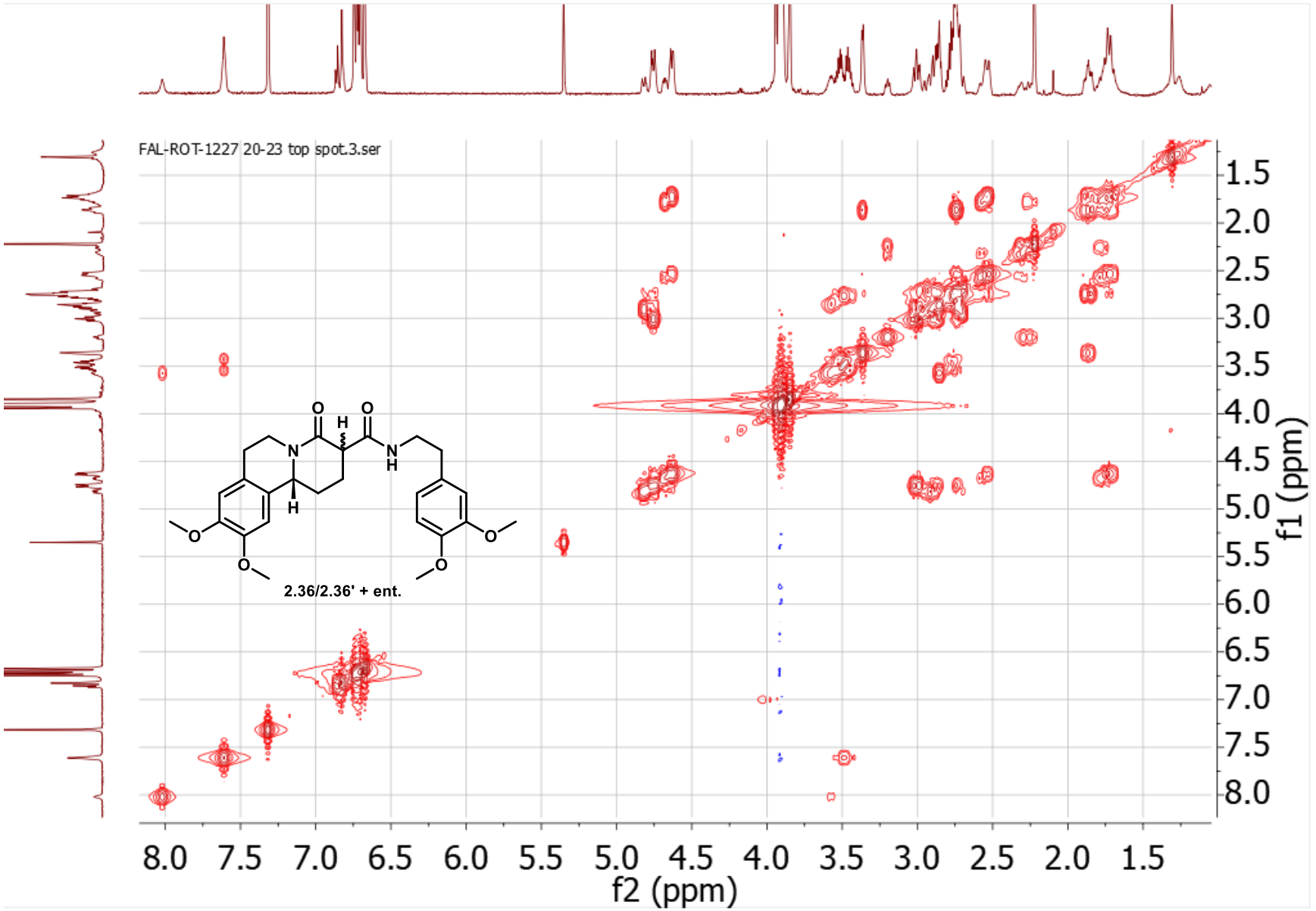
FAL-ROT-1227 20-23 top spot.3.ser
2.36/2.36' + ent.
f2 (ppm)
f1 (ppm)